

https://dspace.org/

Characterization of respirable crystalline silica dust around the abandoned mines situated in Roodepoort, West Rand, Johannesburg

Madzivhandila, Thingahangwi

2017

https://hdl.handle.net/10539/25820

Downloaded from a DSpace repository. https://dspace.org/

CHARACTERIZATION OF RESPIRABLE CRYSTALLINE SILICA DUST AROUND THE ABANDONED MINES SITUATED IN ROODEPOORT, WEST RAND, JOHANNESBURG

A Dissertation submitted to the Faculty of Science, University of the Witwatersrand, in fulfilment of the requirements of Master of Science

BY

Thingahangwi Madzivhandila

Student no: 914004

DECLARATION

I hereby declare the ownership of this report and it is not being submitted before for any degree in any university. It is being submitted for the Masters of Science degree at the University of the Witwatersrand, Johannesburg.

Candidate Signature 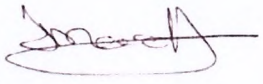

03 November 2017.

DEDICATION

I dedicated this project wholeheartedly to the creator Almighty God for guiding and encouraging me to complete this program.

ACKNOWLEDGEMENTS

I would never have been able to finish my dissertation without the guidance of my colleagues, help from friends, and support from my family.

I would like to thank everyone who contributed to this dissertation.

I would especially like to thank Prof. Ivo Petr and Prof James Larkin who reviewed and commented on the entire manuscript with good faith, incredible patience and guidance as my supervisors.

Special thanks go to Mr. Gopolang Sekobe and Dr. Boitumelo Kgarebe for their technical supervision throughout the research.

This project wouldn't have gone this far if not for the financial support of NHLS. Particularly I want to thank NHLS finance department for awarding the bursary for this study.

ABSTRACT

There are many abandoned mines in South Africa, so it is important to determine whether or not they cause a potential health risk. The mines in the West Rand are mostly gold mines and are associated with silica dust. Inhalation of crystalline silica dust may cause Silicosis (IARC, 2002). The current study aims to characterize the respirable crystalline silica in the dust collected from abandoned mines around Roodepoort and to evaluate the seasonal exposure risks to the community staying near abandoned mines.

Air and soil samples have been collected at the source (0 m from of the abandoned mine), 500m away from the source, 1000m away from the source and 1500m away from the source targeting downwind from the source in all six selected abandoned mines (Durban deep, Bantjies dump, Princess, East camp D'Or, Crown mines and Randfontein estates-Doornkop section. Sampling was done in all four seasons (summer, winter, spring and autumn). 96 air samples were collected on a PVC filters using air sampling pumps calibrated at 2.2 litres per minute and 48 soil samples were gathered and sent to a laboratory for analysis. For quality purposes, 24 blank samples were collected.

Respirable samples were analysed to establish the crystalline phases using X-ray powder diffraction (XRD) based on (MDHS101); gravimetric analysis was done using RADWAG weighing balance following (MDHS14/3). X-ray fluorescence was used to identify the element composition in the soil with guidance of EPA 6200. Air samples had a detectable level of respirable crystalline silica. Soil samples determine crystalline minerals and clay minerals. IN-SITU XRF determines the heavy metal including the trace elements.

TABLE OF CONTENTS

CONTENTS **PAGE**

DECLARATION i

DEDICATION ii

ACKNOWLEDGEMENTS iii

ABSTRACT iv

TABLE OF CONTENTS v

TABLE OF FIGURES viii

TABLE OF TABLES x

LIST OF ABBREVIATIONS xi

TERMS AND DEFINITIONS xiiiiv

CHAPTER ONE 1

1. **INTRODUCTION** 1

1.1 Problem statement 1

1.2 Motivation of the study 2

1.3 Purpose of the study 2

1.4 Hypothesis 2

1.5 Study objectives 2

CHAPTER TWO 3

2. LITERATURE REVIEW 3

2.1. Health effects caused by Respirable Crystalline Silica dust 3

2.1.1. Silicosis 3

2.2. The deposition of dust particles in the respiratory tract 4

2.3. Legislation, Guidelines, Policy, and Standards governs environmental exposure to respirable crystalline silica 6

2.3.1 Current legislative framework for abandoned mine closure 6

2.3.2 National Environmental Management Act, 1998 (Act No 107 of 1998) 6

2.3.3. National Environmental Management Air quality Act 2004 6

2.6. Recommended control measures 7

CHAPTER THREE 8
3. METHODS AND MATERIALS 8
3.1 Introduction 8
3.2. Selection of study areas 8
3.3. Location of the study areas 8
3.4. Description of the study areas 8
3.4.1. Geology of the study areas 13
3.4.2. Soil Cover 13
3.4.3. Condition of Mine dumps 16
3.5. Sample collection 16
3.6. Material used for the study 18
3.7. Calibration of sampling pumps 18
3.8. Assembling the sampling equipment in the sterile area 19
3.10. Sampling strategy 23
3.10. Transportation of the samples into the laboratory 24
3.10.1. Air samples 24
3.10.2. Soil samples 25
3.11. Overview of the laboratory which was respinsible for analysis 28
3.12. Equipments used in the laboratory for analysis 29
3.12.1. RADWAG Balance 29
3.12.2. X-ray Fluorescence 32
3.12.3. X-ray diffraction 33
CHAPTER FOUR 37
4. RESULTS 37
4.2.1. Temperature 37
4.2.2. Wind speed 39
4.2.3. Wind direction 41
4.2.4. Humidity 43
4.3. Air sample results 45

4.4. Mineral identification using XRD.....53
4.5. Geochemical analysis.....54
CHAPTER FIVE.....79
5. INTERPRETATION AND DISCUSSION.....56
5.1 Introduction.....56
5.2. Crystalline silica concentration.....56

CHAPTER SIX.....68
6. CONCLUSION.....68
CHAPTER SEVEN.....68
7. REFERENCES.....68
CHAPTER EIGHT.....70
APENDICES.....70

TABLE OF FIGURES

Figure	Description	Page
Figure 2-1	Lung structure and air sac (OSHA, 1989)	7
Figure 2-2	The particle deposition in a respiratory tract (OSHA, 1989)	9
Figure 2-3	Graphic showing how deeply particles can be inhaled into the human respiratory tract (Moore et al., 2011).	10
Figure 3-1	The satellite image showing location of Durban deep mine dump study area (www. Google Earth)	23
Figure 3-2	The satellite image showing location of Bentjies mine dump study area (www. Google Earth)	24
Figure 3-3	The satellite image showing location of Crown mines study area (www. Google Earth)	24
Figure 3-4	The satellite image showing location of East camp D'Or study area (www. Google Earth)	25
Figure 3-5	The satellite image showing location of Princess mine dump study area (www. Google Earth)	25
Figure 3-6	The satellite image showing location of Randfontein Estates study area (www. Google Earth)	26
Figure 3-7	Durban deep un-rehabilitated mine with old trees and located near a community	28
Figure 3-8	Crown mines un-rehabilitated mine, solidified slimes dam, which has developed cracks, and surrounded by trees	28
Figure 3-9	Bantjies dump mine, re-mining is taking place (brick making)	29
Figure 3-10	Princess un-rehabilitated abandoned mine	31
Figure 3-11	Calibration setup	32
Figure 3-12	Setting up the air sampling train	33
Figure 3-13	Sampling plan for Durban deep mine	34
Figure 3-14	Sampling plan for Bentjies mine	34
Figure 3-15	Sampling plan for Bentjies mine	34
Figure 3-16	Sampling plan for Crown mines	35
Figure 3-17	Sampling plan for Princess mine	36

Figure	Description	Page
Figure 3-18	Sampling plan for Randfontein estates mine	36
Figure 3-19	Sampling strategy	37
Figure 3-20	Air samples inside the sample transportation box	38
Figure 3-21	Air samples analysis preparation	38
Figure 3-22	Measuring soil depth A & B= Soil samples collected in the study areas; C=Soil samples being prepared for analysis	39
Figure 3-23	Mettle Toledo weighing balance	40
Figure 3-24	Drying out the soil samples for 120 hours	41
Figure 3-25	Soil sample preparation for XRD analysis	41
Figure 3-26	**A=** RADWAG weighing balance to weigh the air samples **B=** Mettle Toledo weighing balance to weigh the soil samples; green represents weighing dish and red represents display screen.	42
Figure 3-27	Position of a weighing balance workstation	43
Figure 3-28	Acclimatization of air samples in a stable environmental condition at weighing balance room where temperature range is 20°c-25°c and Humidity range of 45%-75%.	44
Figure 3-29	IN-SITU analysis of soil in the abandoned mines by X-rays Fluorescence	45
Figure 3-30	(Bohr, 2003)	46
Figure 3-31	Atomic structure after George Siegbahn, 1924	46
Figure 3-32	How does light affect molecules and atoms (D.C Harris, 2007)	46
Figure 3-33	XRD equipment	47
Figure3-34	XRD equipment	47
Figure 4-1	Average hourly autumn temperature	50
Figure 4-2	Average hourly winter temperature	50
Figure 4-3	Average hourly spring temperature	51

Figure	Description	Page

Figure 4-4 Average hourly summer temperature 51

Figure 4-5 Average daily autumn wind speed 60

Figure 4-6 Average daily winter wind speed 60

Figure 4-7 Average daily spring wind speed 61

Figure 4-8 Average daily summer wind speed 61

Figure 4-13 Average hourly autumn humidity 62

Figure 4-13 Average hourly winter humidity 62

Figure 4-15 Average hourly spring humidity 63

Figure 4-16 Average hourly summer humidity 63

ABLE OF TABLES

TABLE	DESCRIPTION
Table 2-1	Reference exposure levels (OEHHA, 2005)
Table 3-1	Names and Locations of the study areas
Table 3-2	Season calendar for the measurement taken at the study areas
Table 4-1	Environmental conditions
Table 4-2	Analysis results for the air samples collected in Durban deep
Table 4-3	Analysis results for the air samples collected in East Champ D'Or
Table 4-2	Analysis results for the air samples collected in Bantjies Dump
Table 4-2	Analysis results for the air samples collected in Crown mines
Table 4-2	Analysis results for the air samples collected in Princess
Table 4-2	Analysis results for the air samples collected in Randfontein estates
Table 4-8	Mineral identification results for the samples taken in all study areas
Table 4-9	Geochemical analysis results in Durban deep
Table 4-10	Geochemical analysis results in East Champ D'Or
Table 4-11	Geochemical analysis results in Bantjies Dump
Table 4-12	Geochemical analysis results in Crown mines
Table 4-13	Geochemical analysis results in Princess
Table 4-14	Geochemical analysis results in Randfontein estates
Table 5-1	Overall statistical interpretation of the results obtained from all sites

LIST OF ABBREVIATIONS

ABBREVIATION	DESCRIPTION
CGS	Council for Geosciences
COPD	Chronic Obstructive Pulmonary Disease
DNA	Deoxyribonucleic acid
EEC	Environmental Equivalent Concentration
HSL	Health and Safety Laboratory
IARC	International Agency for Research on Cancer
ILO	International Labour Organization
LIDAR	Light Detection and Ranging
LoD	Limit of detection
MPRD	Mineral and Petroleum Resource Development
MDHS	Method for the Determination of Hazardous Substances
MRC	Medical Research Council
NIOH	National Institute for Occupational Health
NIOSH	National Institute for Occupational Safety and Health
NIST-SRM	National Institute of Standards and Technology
NBS-SRM	National Bureau of Standard Reference Material
NAAQS	National ambient air quality standard
NCRP	National Council on Radiation Protection
NEMA	National Environmental Management Act
NEMAQA	National Environmental Management: Air Quality Act
NEMWA	National Environmental Management: Waste Act
NWMS	National Waste Management Strategy
OSHA	Occupational Safety and Health Administration
OEHHA	Office of Environmental Health Hazard Assessment
PVC	Polyvinyl chloride
PSD	Particle size distribution
PPM	Parts per million
RCS	Respirable Crystalline Silica

| ABBREVIATION | DESCRIPTION |

RSA	Republic of South Africa
RHPU	Radiation and Health Physics Unit
REL	Relative scale
STDEV	Standard deviation
USA	United State of America
EPA	Environmental Protection Agency's
UFh	Infrahuman uncertainty factor to protect the sensitive individual within the general population
WRDM	West Rand District Municipality
WITS	Witwatersrand
WHO	World Health Organization
XRD	X-ray Diffraction
XRF	X-ray fluorescence

TERMS AND DEFINITIONS

Calibration- is a operations set to establish the condition of adjustment in related to the values demonstrated by a measuring system.

Calibrator- a flow metering device used to calibrate a sampling pump.

Calibration Standard- this is the reference material that are used to used to quantify the relationship between the output of an instrument and the property to be measured.

Crystalline silica- is the second most common mineral on the earth's surface which in every type of the rock.

Electromagnetic Field- Is a field created by electrically charged objects and affects the behaviour of charged objects nearby.

Endogenic- Taking place beneath the surface of the Earth, and includes geological processes, such as for example, melting, metamorphism.

$PM_{2.5}$ – this is the particles that correspond to the high-risk respirable convention.

PM_{10} – this is the particles that correspond to the thoracic convention.

Respirable dust fraction- referred to the airborne particles that penetrate to the pulmonary alveolar region of the lungs.

Sampling Pump- a device used to draw air through specific collection air sampling media to collect a representative sample of airborne contaminant(s) in the mine environment.

Silicon dioxide (silica)- is a chemical compound that is an oxide of silicon with the chemical formula SiO_2 . found in nature as well as in living organisms and a major

constituent of sand and produced in synthetic forms such as fused quartz, crystal, fumed silica, silica gel, and aerogels.

Silicosis is incurable, irreversible disease caused by breathing dust containing quartz particles that are tiny, less tha10 microns (μ) in diameter, as illustrated in figure 1 below. Silicosis progresses after removal from exposure (Stanton et al., 2006).

Topography - Both the transport and the diffusion of air pollutants are complicated by topographical features. Minor topographical features may exert small influences; major features, such as deep river valleys or mountain ranges, may affect large areas. Before final site selection, review the topography of the area to ensure that the purpose of monitoring at that site will not be adversely affected.

X-ray powder diffraction (XRD) - a rapid analytical technique primarily used for phase identification of a crystalline material and can provide information on unit cell dimensions. The analyzed material is finely ground, homogenized, and average bulk composition is determined.

X-ray fluorescence (**XRF**) the emission of characteristic "secondary" (or fluorescent) X-rays from a material that has been excited by bombarding with high-energy X-rays or gamma rays.

CHAPTER ONE

1. INTRODUCTION

Abandoned mines are places where exploration, mining or mine production stopped without the rehabilitation done. They occurred in regions that have a mining history (MMSD, 2002). They could also contain low and ultra-low grade ores from uneconomic mineral horizons thus resulting in slimes dams and stockpiles (CGS, 2006). The problem of abandoned mines started when the mine owners left their operations either without having rehabilitated them or their rehabilitation was not completed. When such operations are not rehabilitated, the illegal miners can take advantage of re-mining without permission.

These kinds of operations result in environmental and human health problems. If a mine ceases to operate and the closure certificate has not been issued in terms of section 43 of Mineral and Petroleum Resources Development Act., 2002 the particular mine is not regarded as closed by the Department of Mineral Resources South Africa (MMSD, 2002). Officially, the owner of a mine remains responsible for all liabilities related to the mine until a closure has been issued. The mines in the West Rand are mostly gold mines and are associated with crystalline silica dust (IARC, 1987a). Breathing dust contained crystalline silica can cause Silicosis (IARC, 1987b).

1.1. PROBLEM STATEMENT

The risks associated with abandoned mines include air pollution by dust, combustion products from burning mine workings dumps, as well as physical hazards posed by sites with open shafts and unstable stopes (Bowen G.G. Dussek C. Hamilton R.M. Mather J, 1998). Although there have been a few attempts at the quantification of non-occupational exposure to silica, the issue abandoned mines is unresolved and it is still a concern to most of communities living nearby or around abandoned mines. (Nevada, 2003)

1.2. MOTIVATION OF THE STUDY

Despite a number of investigations undertaken and reports issued by Department of Mineral Resources in 2009, there is a need of researches to be conducted to quantify the nature associated with abandoned mines problems. (MMSD, 2002) conducted an environmental study around mine dumps where he identified contaminated areas (the community situated near the mine dumps) and recommended that there is a need for comprehensive air monitoring, toxicological and epidemiological studies in affected communities.

1.3. PURPOSE OF THE STUDY

The intention of this project is to characterize the respirable crystalline silica dust and quantify the air from concentration of crystalline silica around selected abandoned mines and prioritize the risk regarding the identified hazard and thereafter provide the recommendation.

1.4. STUDY OBJECTIVES

- To evaluate, quantify and characterize the seasonal exposure risks to the community staying next to and around abandoned mines
- To determine the chemical composition of a sample

1.5. HYPOTHESIS

Environmental exposure to crystalline silica around abandoned mines in Roodepoort is greater than a concentration of 3µg/m^3 (OEHHA, 2005)

CHAPTER TWO

2. LITERATURE REVIEW

This chapter covered the following topics: health effects caused by respirable crystalline silica dust, the deposition of dust particles in the respiratory tract, the Legislation, Guidelines, Policy, and Standards governs environmental exposure to respirable crystalline silica.

2.1. HEALTH EFFECTS CAUSED BY RESPIRABLE CRYSTALLINE SILICA DUST

Dust is a chemical hazard that found in many mining industries (Fubini, 1998)).There is a evidence for association between exposure to crystalline silica and disease (Hardy, 1995). ILO, 1991 confirms that inhalation of dust contain crystalline silica may cause silicosis, lung cancer, renal disease, kidney cancer, chronic obstructive pulmonary disease, scleroderma, rheumatoid arthritis, and polyarthritis, mixed connective tissue diseases, systematic lupus erythematosus, polymyositis, fibrosis, leukaemia, lymphomas, stomach and gastrointestinal malignancies, dermatomyosistis.

2.1.1. Silicosis

Silicosis is a incurable disease caused by damaging an area of the lung called alveoli after breathing in tiny bits of silica dust (Hnizdo and Cremer, 1991) (**Fig. 2.1)**. The presence of silica dust in the alveoli of the lungs causes a body defence reaction that results in the formation of black nodules of scar tissue in the lungs. This scar tissue limits the ability of the lungs to stretch, thereby limiting the amount of air that can be inhaled in (Hnizdo and Cremer, 1993).

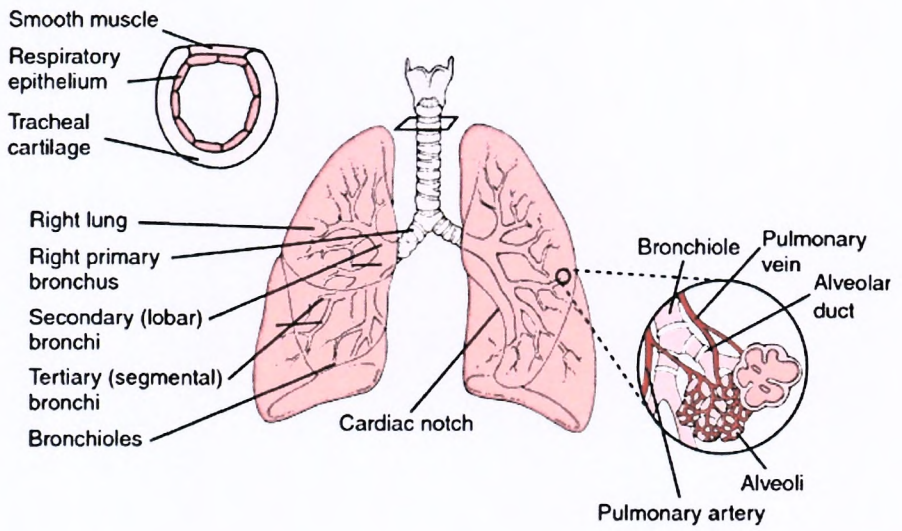

Figure 2-2-1: Lung Structure and air sac (Hnizdo and Murray, 1998)

The risk of silicosis depends on the cumulative dose of silica dust, although the latency period between exposure and diagnosis appears to be independent of the dose.

Silica is classified as a carcinogen by the International Agency for Research on Cancer (IARC 1987). Three types of silicosis are classified below:

- Acute silicosis can occur in only weeks or months of exposure to crystalline silica levels of above health limit and be fatal within months.
- Accelerated silicosis occurs in 5 to 10 years after exposure of high level of crystalline silica dust.
- Chronic silicosis dominated at low level of crystalline silica exposure for more than 10 years.

2.2. THE DEPOSITION OF DUST PARTICLES IN THE RESPIRATORY TRACT

The size of the dust particle is one of the more significant factors in the development of silicosis (Castranova V, 1997). In reviewing the characteristics of dusts, the respirable fraction (particle size of between 2-7μm) is the most harmful one, as it reaches the alveoli (Giles and Cee, 1987) (**Fig. 2-2)**.

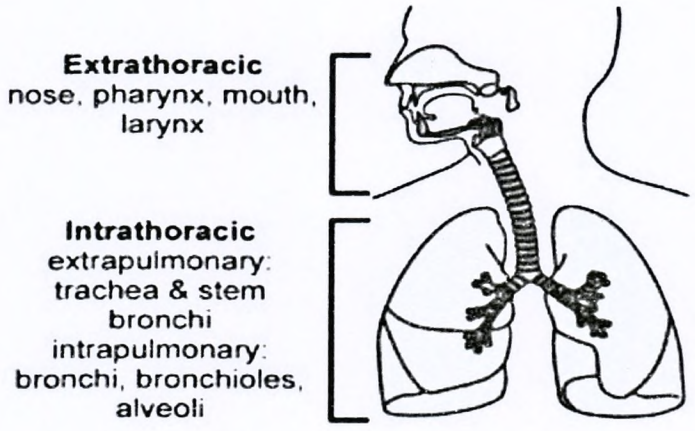

Figure 2-2-2: The respiratory track for a normal male adult (Little, 1976)

Dust particles less than 2 µm can pass into the lungs and be phagocytised by alveolar macrophages (Moore, 2011).

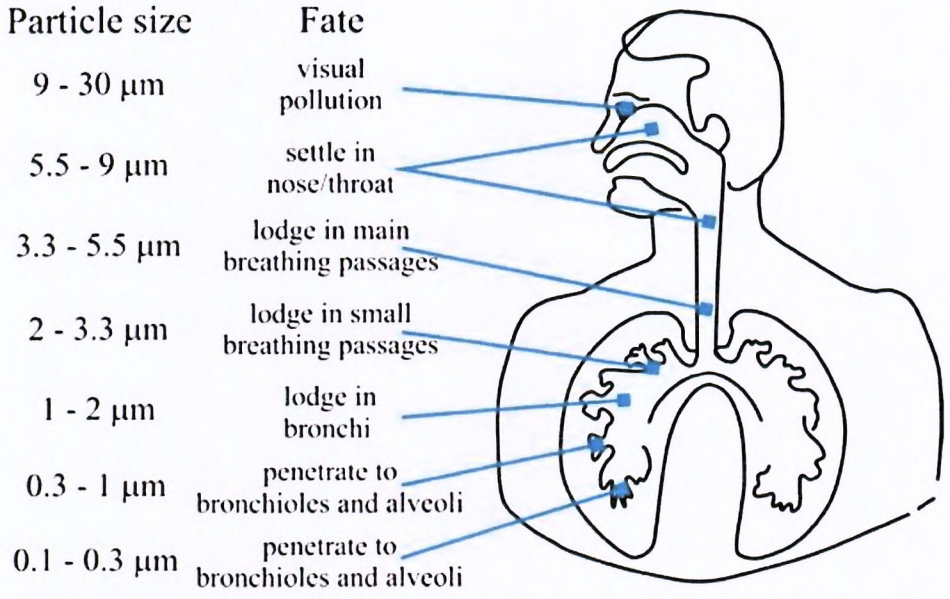

Figure 2-2-3: Showing how deeply particles can be inhaled into human respiratory track (Muhle H., 1989)

The dust particle ranges from 0.1 µm to 0.001 µm can enter the brain and be distributed around the whole body through blood stream resulting in ill-health (Abell M. T., 1984)

2.3. LEGISLATION, GUIDELINES, POLICY, AND STANDARDS THAT GOVERNS CRYSTALLINE SILICA EXPOSURE IN SOUTH AFRICA

The standard of crystalline silica, guidelines, policy and legislations are taken seriously in South Africa to minimize the health risk exposure of respirable crystalline silica so far as reasonably practicable (Freeman and Grossman, 1995).

2.3.1 Current legislative framework for abandoned mine closure

An abandoned mine is defined as a mine that ceased to operate without rehabilitation being done. The abandoned closure certificate must be enforced to ensure that the person who holds the mine permit must not abandon mine before being rehabilitated (Bowen G.G. Dussek C. Hamilton R.M. Mather J, 1998).

2.3.2 National Environmental Management Act, 1998 (Act No 107 of 1998) and Minerals Act, 1991 (Act 50 of 1991) of South Africa

> "*Section 28 of this Act also imposes a duty of care and remediation of environmental damage on any person who causes, has caused or may cause significant pollution or degradation of the environment. Furthermore, sections 32 and 33 of the Act provides for legal standing to enforce environmental laws and private prosecution respectively. The most important requirement concerning the environment and the rehabilitation thereof is that an Environmental Management Programme (EMP), based on an environmental impact assessment, must be submitted and officially approved*".

2.3.3. National Environmental Management Air Quality Act, 2004 (act no. 39 of 2004) Minerals Act, 1991 (act 50 of 1991) of South Africa

The environmental exposures to quartz occurs when quartz dust is released into the atmosphere as a constituent of particulate emissions formed by activities such as construction and demolition, quarrying and abandoned mines (EPA, 1996b).

2.4. RECOMMENDED CONTROL MEASURES

In 2005, Office of Environmental Health Hazard Assessment (OEHHA) reviewed different studies in line with recommended control measures of respirable crystalline silica and the study resulted in the recommendation of 3µg/m^3 as an inhalation reference level for ambient environmental exposure to respirable crystalline silica. This is broadly consistent with a recent protocol developed by the United State of America Environmental Protection Agency for a $PM_{2.5}$ (Vic EPA, 2008).**Table 2.1.**

Table 2-1: Reference Environmental exposure levels (OEHHA, 2005)

Study	BMC_{01} (mg/m^3)	Exposure duration (yrs)	Environmental equivalent concentration (mg/m^3)	Cumulative Uncertainty factor (UFh)	Reference exposure level (µg/m^3)
Hnzido and Sluis Cremer (1993)	0.636	24	908	3	3
Steenland and Brown (1995)	0.34	9	12.4	3	4
Hughes *et al.* 2001	N/A	11.5	29	10	3
Chen *et al.* 2001	0.132	2.2	18	3	6
Churchyard *et al.* 2004	21.8	11.4	3	4	

Fine particulate matter are particulate matter with aerodynamic diameter of 2.5 microns derived from volatilization and condensation of combustion material such as Sulphur dioxide, nitrogen oxides and volatile organic compound (Zunckei, 2008), heterogeneous or homogeneous nucleation of vapor phase material and atmospheric reactions of gases to form vapors that homogenously and heterogeneously nucleate to form particles(Zunckei, 2008). (Perrino, 2011) described them as respirable, since they can

be inhaled deep into the lungs. Despite their ability to enter the alveoli in the lungs $PM_{2.5}$ tend to stay suspended in the atmosphere for long periods of time and can be transported over large distances (Zunckei, 2008).

As noted by (Perrino, 2011) as scientific evidence that bring out the effects of finer particles has emerged, regulatory attention has subsequently focused on respirable fine particles with diameter less than 2.5 micrometer. According to (Matooane, 2008) noted that $PM_{2.5}$ pose the greatest health effects as they can penetrate deep into the lung and cause more damage.

The effects of air pollutants on human health occur in a number of ways with short-term, or acute effects, and chronic, or long-term, effects (Affairs, 2009). The size and surface of particles, their number and their composition are of paramount importance in bringing about health effects (Kampa, 2008). (Zunckei, 2008) noted the short and long term exposure to $PM_{2.5}$ effects which include increase in risk for cardiovascular and respiratory disease among people over 65 years of age and chronic effects on children's health, such as impaired development of lung function.

CHAPTER THREE

3. METHODS AND MATERIALS

3.1. INTRODUCTION

This chapter provides a description of the research design and methodology selected for the study and adoption of a blended research design, with both qualitative and quantitative features.

3.2. SELECTION OF STUDY AREAS

The selections of study areas (abandoned mines) were determined by means of a survey. Six abandoned mines were selected and the selection criteria were based on un-rehabilitated abandoned mines situated near or around the communities.

3.3. LOCATION OF THE STUDY AREAS

The study areas are located around Roodepoort west of Johannesburg at 26°05" latitude and 27°50" longitude 24km west of the Johannesburg city centre. This area forms part of the northern margin of the Witwatersrand Basin and is bounded in the east by the East Rand Goldfield and on the west by the West Rand Goldfield. Names, locations and coordinates of abandoned mines are listed below in the **Table 3-1**.

Table 3-1: Names and Locations of the study areas

Name of Abandoned mine	Area	Coordinates of the mine Location
Durban Deep(SS1)	Roodepoort	26°10'10"S & 27°52'34"E
Bantjies dump (SS2)	Roodepoort	26°11'08"S & 27°54'34"E
Princess (SS3)	Bramficherville	26°09'37"S & 27°51'21"E
East camp D'Or (SS4)	Kagiso	26°07'56"S & 27°49'18"E
Crown mines (SS5)	Soweto	26°14'30"S & 27°58'11"E
Randfontein Estates (SS6)	Doornkop -Soweto	26°12'48"S & 27°46'45"E



Figure 3-1: The satellite image showing location of Durban deep mine dump study area (www. Google Earth)



Figure 3-2: The satellite image showing location of Bentjies mine dump study area (www. Google Earth)



Figure 3-3: The satellite image showing location of Crown mines study area (www. Google Earth)



Figure 3-4: The satellite image showing location of East camp D'Or study area (www. Google Earth)



Figure 3-5: The satellite image showing location of Princess mine dump study area (www. Google Earth)



Figure 3-6: The satellite image showing location of Randfontein Estates study area (www. Google Earth)

3.4. DESCRIPTION OF THE STUDY AREAS

The Gauteng province was chosen as the study area due to the rapid rate of urbanization and the rise in population, and to determine the possible impact of dust pollution on these populations. As stated earlier, the study was conducted in Roodepoort. The environmental characteristics of each study area are summarized below, respectively.

3.4.1. Geology of the study areas

The study area is unconformably overlies the Dominion Group and composed of oldest crystalline rocks of Archean age namely granitic rocks, meta-sedimentary rocks and meta-volcanic rocks (Kositcin, 2004). These rocks were resulted from thermal subsidence basins (DA, 1975) and tectonically stable environment of the volcano-sedimentary succession of the Dominion Group (Beach, 2007); (Frimmel, 2002.). The basement rocks of the Kaapvaal craton aged between 3 074 Ma and 2 714 Ma (H. Z. Massoud, 1985, DA, 1982). Exposure of these rocks also occurs on the southern edge

of Johannesburg dome and underlies the Witwatersrand Super group (Frimmel, 2002., Brandl and De Wit, 1997).The study area has structurally elongated basin underlain the Northern Orange Free State and Southern Transvaal within Vredefort area (Minter, 1982). These structures resulted to the development of the large faults between Roodepoort and witpoortjie(Schmitz, 2004).

3.4.2. Soil Cover

The study area is comprised of a fine clay soil, intermediate silt soil and coarse sandy soil. These soil types are products of weathering and decomposition of quartzite, conglomerate, and shale (Seta J.A, 1988). Witwatersrand soils confirms the human effort due to the extraction of gold and nutrient supply of sandy soils developed on fluvial sediments. Such soils have a thin, very light to brown, inorganic-rich surface horizon formed by long-continued decomposition of organic matter that may produce CO_2 due to microbial activity (Blume and Leinweber, 2004).

The formation of Witwatersrand soil has been influenced by physical factors such as heat and cold, wind, rain, and solid rock is shattered into smaller pieces (mechanical weathering) (White R.E., 1987) and human impact

3.4.3. Condition of abandoned mines

All the abandoned mine tailing dumps were un-rehabilitated, and characterized by heaps of soil and sediments, laminated sediments, grasses at the bottom of the mine dump, living and dead trees, polycrystalline crushed rock particles and mineral wastes (**Fig. 3-2).**



Figure 3-7: Durban deep un-rehabilitated mine with old trees and located near a community



Figure 3-8: Crown mines un-rehabilitated mine, solidified slimes dam, which has developed cracks, and surrounded by trees



Figure 3-9: Bantjies dump mine, re-mining is taking place (brick making)



Figure 3-10: Princess un-rehabilitated abandoned mine

3.4.4. Climate

The Witwatersrand area is typical Highveld climate, and is characterized by warm summer and cool winters. Repeat measurements were taken at different seasons for each study area. The summary of a study areas climate calendar is shown in **table 3-2**.

Table 3-2: Calendar for the measurements taken at the study areas

3.5. SAMPLE COLLECTION

Months	Autumn	Winter	Spring	Summer	Date
March					01/03/2014
April					
May					31/05/2014
June					01/06/2014
July					
August					31/08/2014
September					01/09/2014
October					
November					30/11/2014
December					01/12/2014
January					
February					28/02/2015

168 samples were collected from selected mines (study area) to ensure that the exposure levels are clearly identified and quantified.

3.5.1. ENVIRONMENTAL CONDITIONS

Daily ground based meteorology observation was obtained from the South African weather service Lanseria station. Meteorological parameters include pressure, precipitation, temperature, relative humidity, wind direction and wind speed. Microsoft excel was used to draw wind rose diagrams. Multiple regressions were used to determine the correlation between meteorological data and fine particulate matter concentration. The hourly actual measurements were recoded table 3-3.

Table 3-3: Detailed environmental conditions of the study areas

Date	Sample No.	Name of the mine	Season of the year	Wind Speed (m/s)	wind Direction	Temperature (°C)	Relative Humidity (%)
06/03/2014	D1, D2,D3,D4,D5, D6& B1	SS1	Autumn	2.7	125 (ESE)	17.8	40
28/03/2014	F1, F2,F3,F4,F5, F6& B2	SS2	Autumn	2.8	65 (ENE)	16.5	32.7
02/04/2014	P1, P2,P3,P4,P5, P6& B3	SS3	Autumn	2.5	107.5 (ESE)	14.4	36.6
17/04/2014	L1, L2,L3,L4,L5, L6& B4	SS4	Autumn	3.4	67.5 (ENE)	17.3	32.7
09/05/2014	R1, R2,R3,R4,R5, R6& B5	SS5	Autumn	3.3	183.7 (SSW)	20.3	24.2
23/05/2014	V1, V2,V3,V4,V5, V6& B6	SS6	Autumn	3.9	165 (SSE)	20.8	20.7
12/06/2014	D7, D8,D9,D10,D11, D12& B7	SS1	Winter	6.1	103.7 (ESE)	13.1	52.8
2506/2014	F7, F8,F9,F10,F11, F12& B8	SS2	Winter	6.3	20 (NNE)	11.2	68.5
17/07/2014	P7, P8,P9,P10,P11, P12& B9	SS3	Winter	3.6	70 (ENE)	16.2	58.6
31/07/2014	L7, L8,L9,L10,L11, L12 & B10	SS4	Winter	5.01	140 (SSE)	17.7	60.2
12/08/2014	R7, R8,R9,R10,R11, R12 & B11	SS5	Winter	4.2	265 (WSW)	16.8	55.3
22/08/2014	V7, V8,V9,V10,V11, V12 & B12	SS6	Winter	6.6	251.2(WSW)	15.5	65.1
12/09/2014	D13, D14,D15,D16,D17, D18 & B13	SS1	Spring	5.2	178.7 (SSE)	15.7	10.3
16/09/2014	F13, F14,F15,F16,F17, F18 & B15	SS2	Spring	6.3	33.7 (NNE)	16.1	11.2
15/10/2014	P13, P14,P15,P16,P17, P18 & B16	SS3	Spring	3.5	178.7 (SSE)	18.1	18
20/10/2014	L13, L14,L15,L16,L17, L18 & B17	SS4	Spring	5.6	162.5 (SSE)	19.3	20.5
04/11/2014	R13, 14,R15,R16,R17, R18 & B18	SS5	Spring	4.2	173.7 (SSE)	16.4	16.6
19/11/2014	V13, V14,V15,V16,V17, V18 & B19	SS6	Spring	6.6	156.2 (SSE)	18.6	18.8
02/12/2014	D19, D20, D21, D22, D23, D24, &B20	SS1	Summer	5.4	255 (WSW)	23.7	20.6
12/12/2014	F19, F20, F21, F22, F23, F24 & B21	SS2	Summer	6.3	261.2(WSW)	24.9	45
26/01/2015	P19, P20, P21, P22, P23, P24 &B22	SS3	Summer	7.1	296.2(WNW)	26.2	35.8
28/01/2015	L19, L20, L21, L22, L23, L24 &B23	SS4	Summer	11.2	23.7 (NNE)	24.3	32.8
04/02/2015	R19, R20, R21, R22, R23, R24 &B24	SS5	Summer	7.6	182.5 (SSW)	25.9	35.6
16/02/2015	V19, V20, V21, V22, V23, V24 &B25	SS6	Summer	1.7	212.5(SSW)	24.7	24.6

3.6. MATERIAL USED FOR THE STUDY

The method of United States environmental protection agency, 1994 was used to select the sampling materials. The materials that were used for sampling includes cassette with base, 25mm diameter PVC filters, forceps, stainless steel, blunt tipped, blue protective caps for filters (before sampling), red protective caps for filter cassettes (after sampling), yellow protective hose covers for field blank cassettes (blank), 47mm petri dishes, zip lock two quart plastic bags, sampling pumps, belt and tube pipe. Site and sampling date stickers for sampling cassette labelling, sampling sheets, and environmental conditions sampling sheets.

3.7. CALIBRATION OF SAMPLING PUMPS

Sampling pumps were calibrated and operated properly to draw a constant flow (Knight, 1971). To ensure this, the sampling pump were sufficiently charged, properly maintained, and calibrated with appropriate airflow meter instrumentation. The sampling pumps were calibrated before sampling and after sampling. The calibration tubing was inspected for leaks, deformed tubing, and cracked rubber **Fig** 3-6.

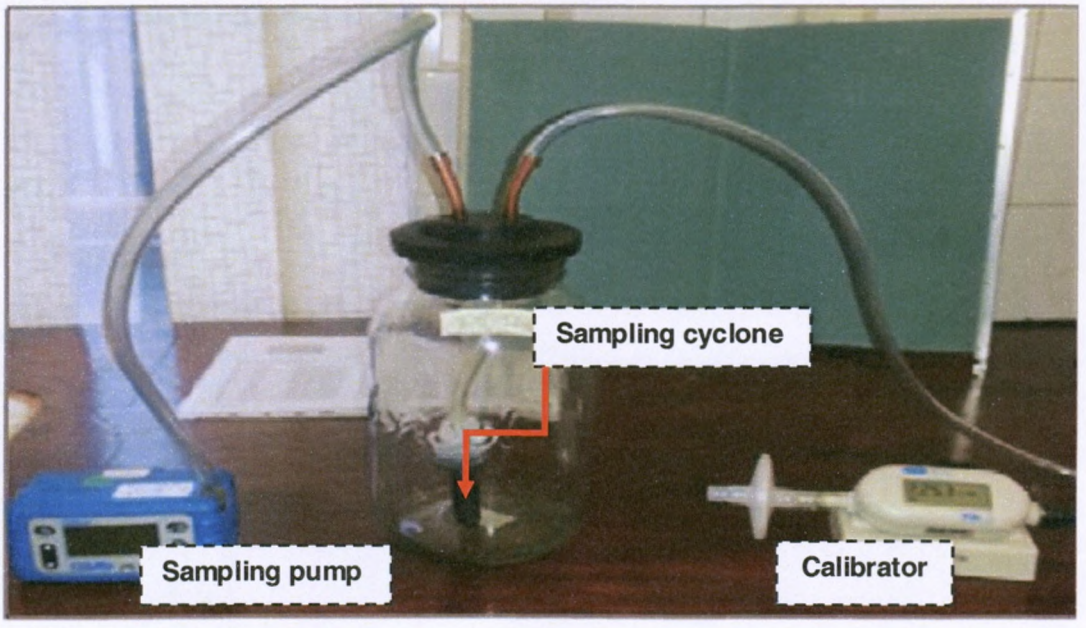

Figure 3-11: Calibration setup

3.8. ASSEMBLING THE SAMPLING EQUIPMENTS IN THE STERILE AREA (LAMINAR DOWN FLOW)

Forceps were used to place the filter support pad in the top tier of the cassette. The plug was removed from the outlet of the cassette; the end was attached to cassette using tygon tubing. The filter was placed on top of the support pad in the top tier of the cassette and the middle tier was added and closed at the both ends of the cassettes with a protective cap. The cellulose shrink band was placed around the filter cassette and allowed to dry.

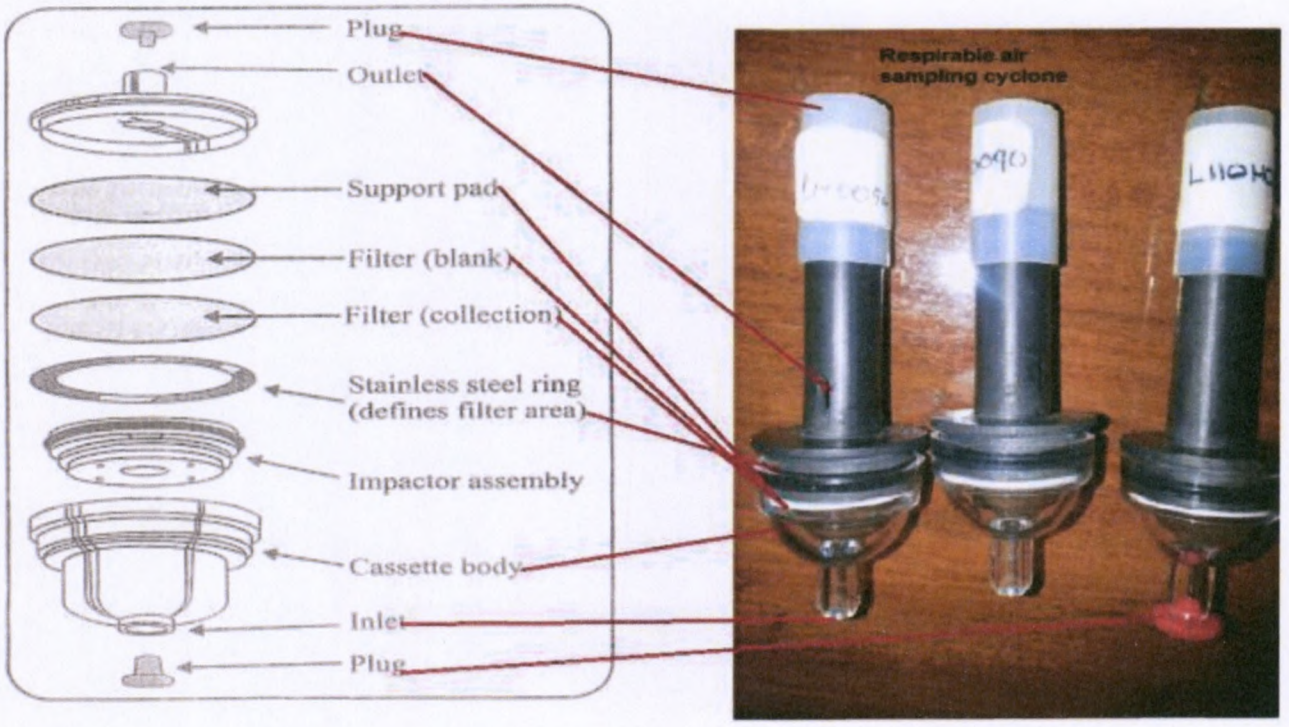

Figure 3-12: Setting up the air sampling train

The sampler was labelled with the unique code given to the filter and filter was connected to the head (filter cassette with a filter on a cyclone) to pump using the short flexible connecting tube **Fig 3-7.**

3.9. SAMPLING PLAN

Four stationery sampling stations were selected in each abandoned mine seasonally. In each sampling station, 2 x air sample was collected on 25 mm diameter, 5.0 µm pore size PVC, silicon-free filters, dorr-oliver cyclone sampling device to Used to define respirable particle sampling criteria at 2.2 l/min for sampling time of eight hours using low volume sampling pumps in all abandoned mines. The sampling plans are summarized at figures below.

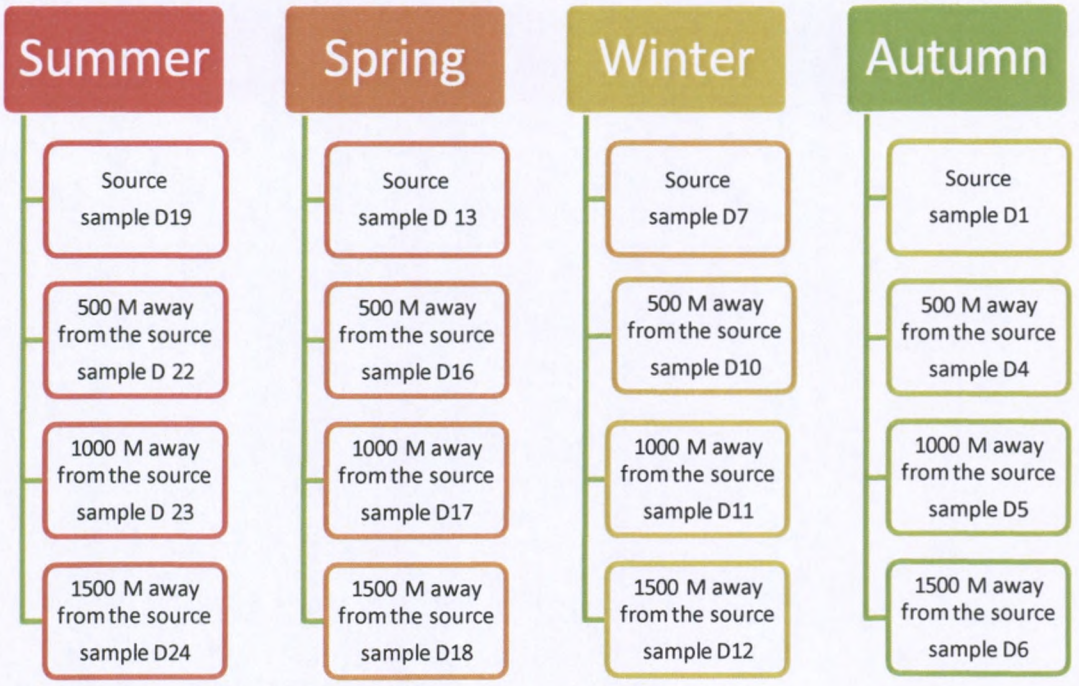

Figure 3-13: Sampling plan for Durban deep mine

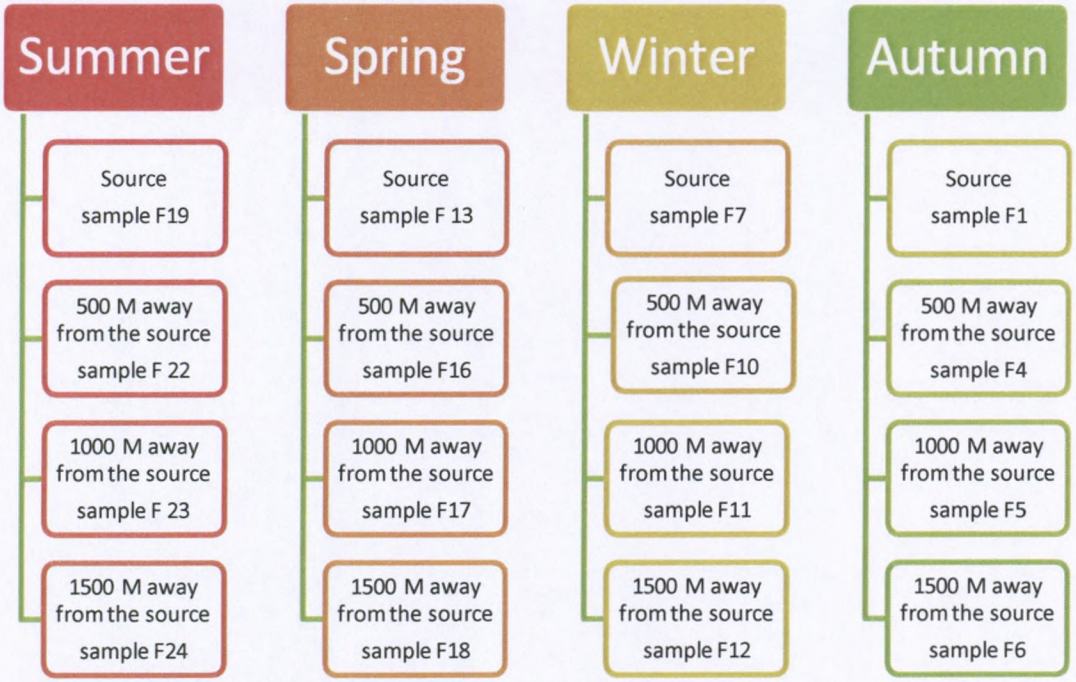

Figure 3-14: Sampling plan for Bentjies mine

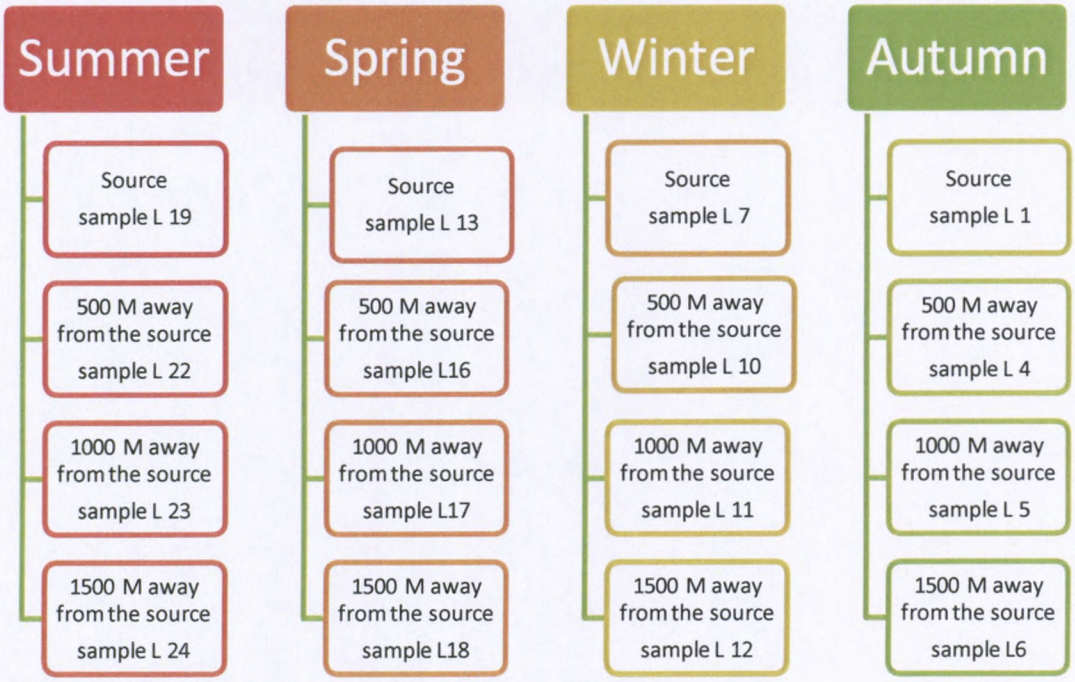

Figure 3-15: Sampling plan for East champ D'Or mine

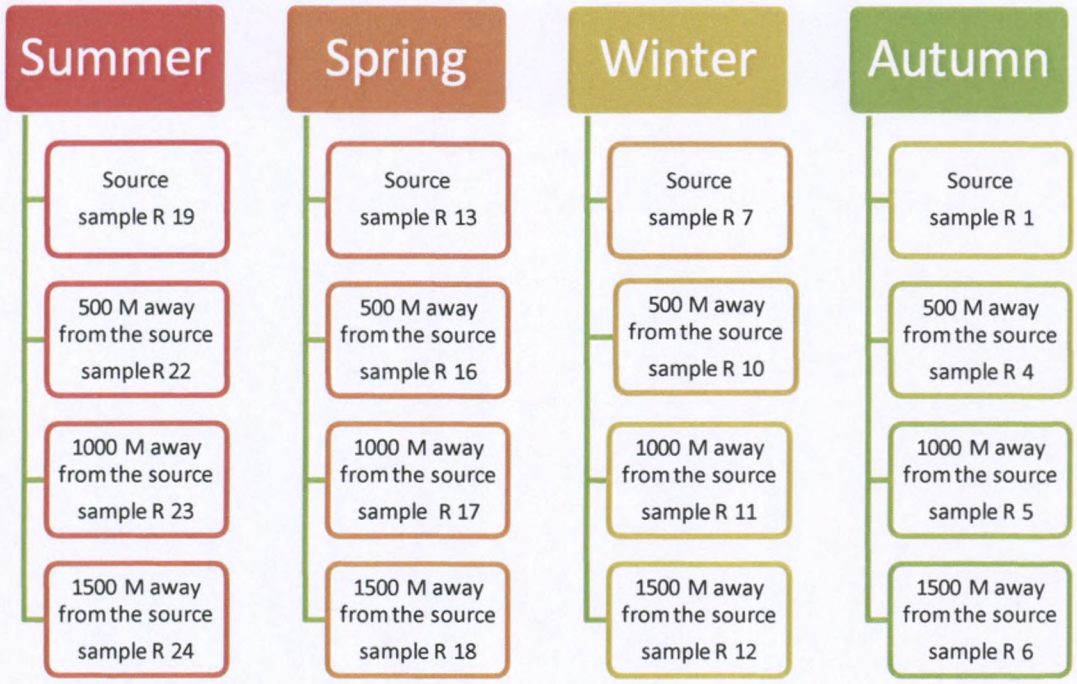

Figure 3-16: Sampling plan for Crown mines

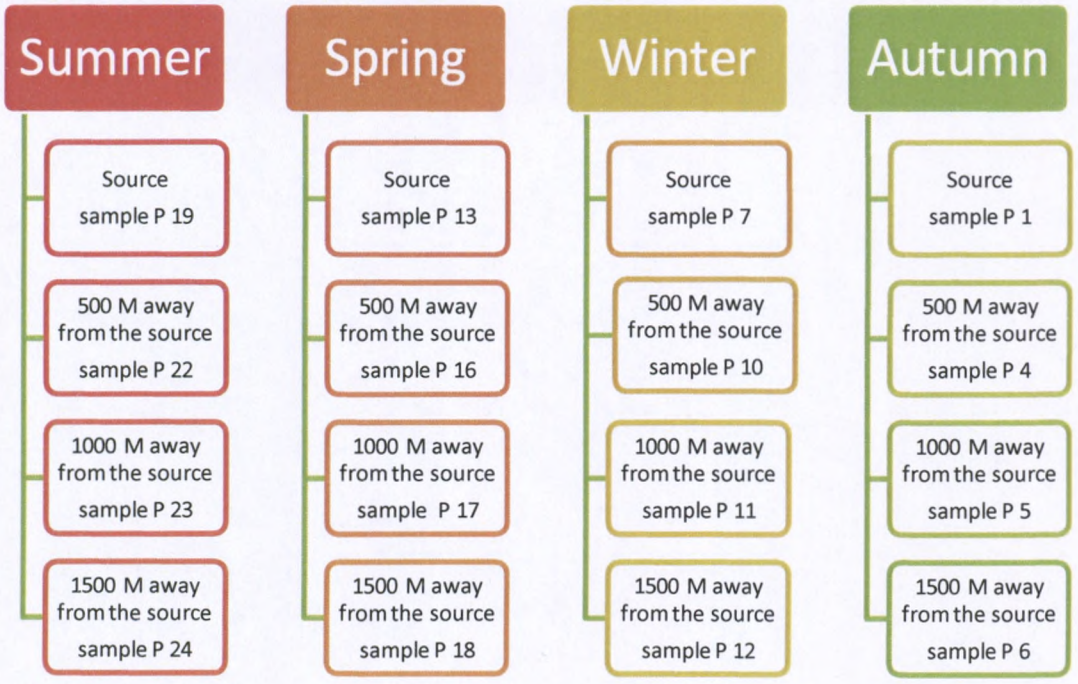

Figure 3-17: Sampling plan for Princess mine

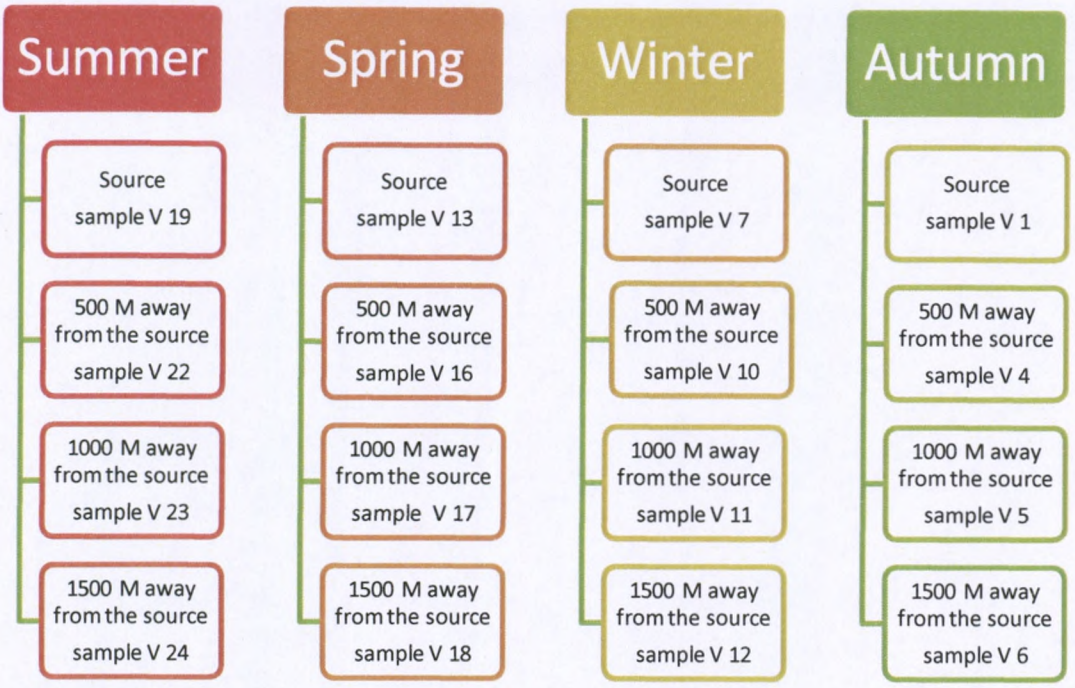

Figure 3-18: Sampling plan for Randfontein estates mine

3.10. SAMPLING STRATEGY

A total numbers of 96 air samples were collected in spring, summer, autumn and winter for all study areas. 2 x soil samples were collected from 6 abandoned mines and placed in the containers. All the containers that carried samples were sealed to prevent any release of particles in to the environment. The containers were labelled indicating the type of material mass. 48 soil samples were collected directly from the sampling points using shovel and placed in the containers **Fig** 3-19.

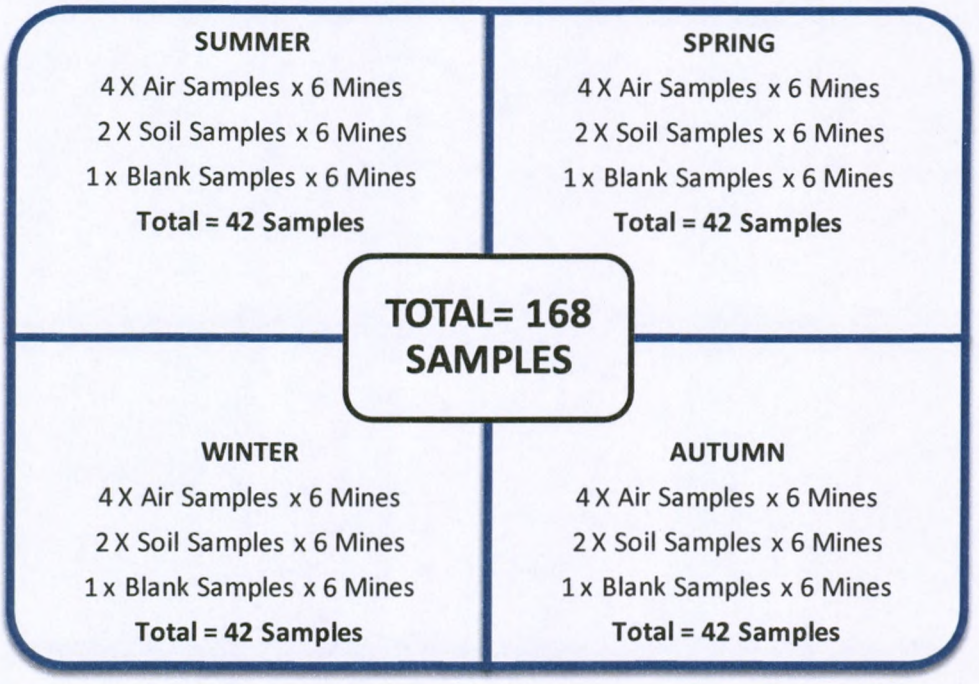

Figure 3-19: Sampling strategy

3.11. TRANSPORTATION OF SAMPLES INTO THE LABORATORY

3.11.1. Air samples

The cassettes were placed upside down and covered with a red cap to show that sampling has been completed. The box was closed, locked securely packed in the upright position within purpose designed special cases designated for transporting equipment and transported to the laboratory together with sampling sheets **fig 3-20**



Figure 3-20: Air samples inside the sample transportation box

The condition of the samples was checked well. After receipt, the cassettes holders were opened and filter papers were taken out using a forceps and placed in the labelled filter holder **Fig 3-21**.

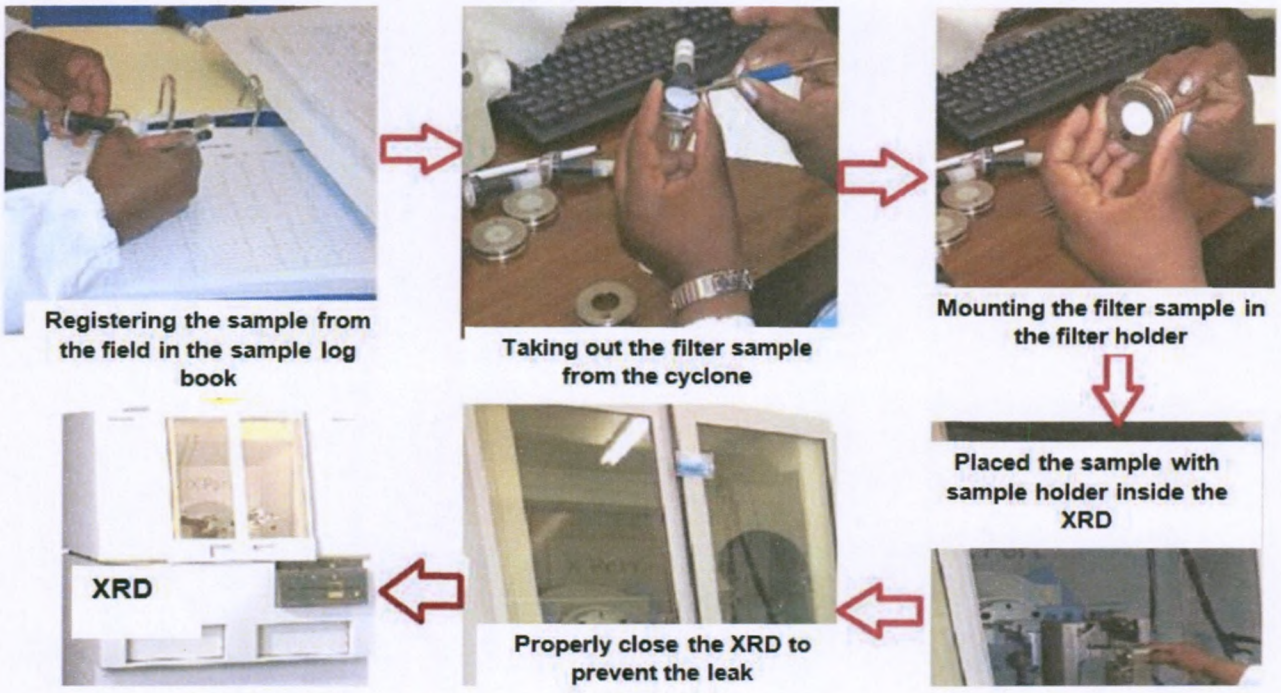

Figure 3-21: Air samples analysis preparation

3.16.2. Soil samples

Soil samples were collected at the depth from 0-6 cms and placed into the containers, properly sealed and then transported into the laboratory the same day of the survey. The depth of the soil samples were determined by measuring tape. The surface were remove by spade to prevent the organic material on the top surface **Fig 3-22**



Figure 3-22: Measuring soil depth

It was important to follow a drying method in the preparation of bulk sample analysis. The soil samples were received from the field in good condition, logged in the log book (checking name of the sender, received date and condition of the samples) **fig 3-23**.



Figure 3-23: A & B= Soil samples collected in the study areas; C=Soil samples being prepared for analysis

After logging the samples were weighed with sample holder in the same day of collection to determine the weight of soil and moisture. The weight was determined by using four decimal places Mettler Toledo mass balance **figure 3-24.**

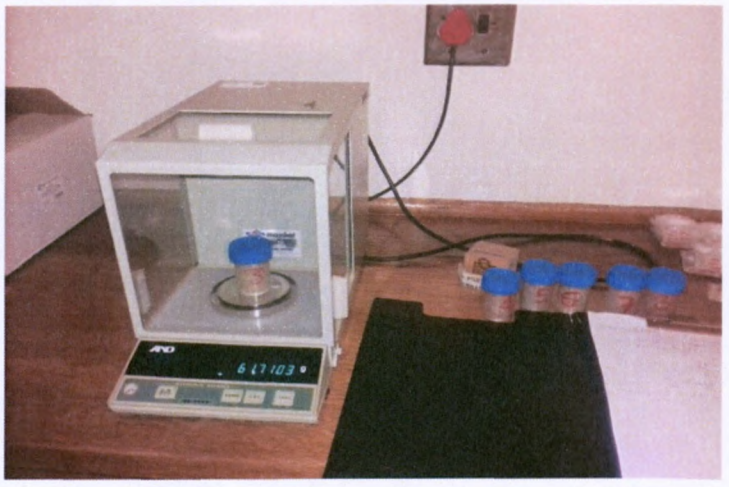

Figure 3-24: Mettle Toledo weighing balance

After weighing, the samples were taken out the holders and dried out for 120 hours (five days) in temperature of 25°. (Olivers and Bennet, 1992) **figure 3-25**.

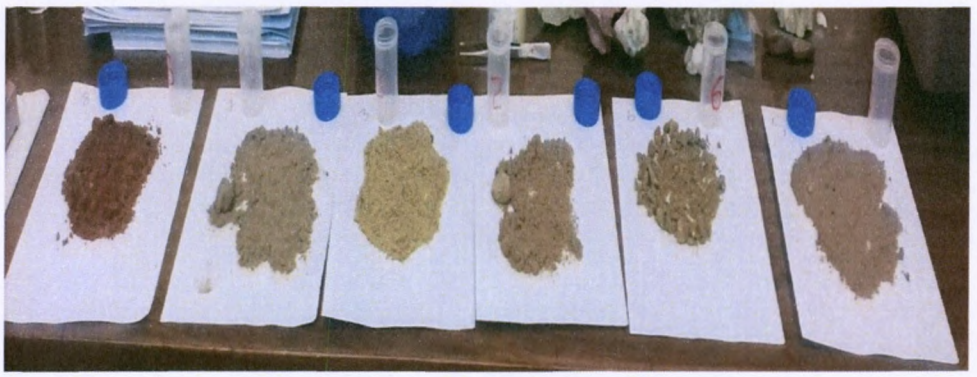

Figure 3-25: Drying out the soil samples for 120 hours

The moisture content of the soil was calculated using the following equation:

$$\%W = \frac{Weight\ A - Weight\ B}{Weight B} \times 100$$

Where:

%W= Percentage of moisture in the sample

A=Weight of wet sample (grams), and

B= Weight of dry sample (gram)

The samples were then sieved to 0.02mm (20 micrometer) to be ready for XRD analysis. Sieving was carried out in small batches to prevent soil loss. The sieve was gently shaken to allow the soil to pass through. The ≥0.02 mm fraction passing through the sieve was collected and set aside and weighed to record the mass. The samples were then prepared for analysis by XRD **Fig.3-26**

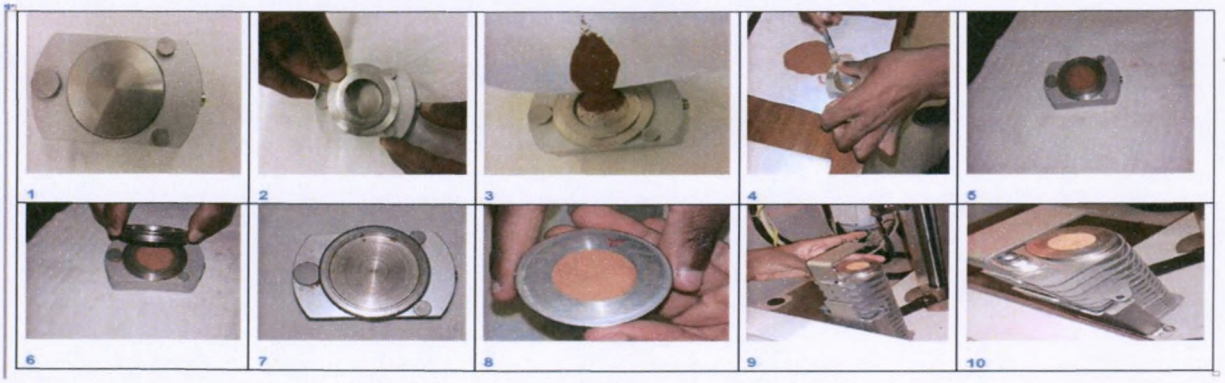

Figure 3-26: Soil sample preparation for XRD analysis

Sample preparation procedure as per fig 3-26:

1. Sample preparation kit to prepare the sample
2. Soil samples were placed in the holder ring and heaped up into a conical shape inside the holder ring
3. Powder press block is used to press soil sample inside the sample holder ring. During pressing some powder flows out of the holder ring.
4. The knife blade was used to scrape the powder back into the holder ring.
5. The surplus soil was cleaned using dusting brush
6. The bottom plate of sample holder was placed onto the holder ring and clamped into it
7. The completed sample was removed from the preparation table
8. The handles gently pulled out the sample from sample holder
9. The completed samples were then mounted in the a sample holder composed of 15 Exchanger units inside the XRD

3.12. OVERVIEW OF THE ANALYSIS LABORATORY

The soil and filter samples were analysed at the X-ray Diffraction Laboratory (Occupational Hygiene Section) of the National Institute for Occupational Health, Johannesburg. NIOH is using PANalytical X' Pert Pro Powder diffractometer with X'celerator detector and divergence and receiving slits. The XRD laboratory is a dust-analysis laboratory equipped with sophisticated instruments and staffed by highly competent technicians' and scientists. To ensure high quality of the results, the laboratory participates in national and international proficiency testing schemes for reliable quality controlled analytical performance, accuracy and traceability of all methods and measurements.

3.13. EQUIPMENT USED IN THE LABORATORY TO ANALYSE THE SAMPLES

3.13.1. Weighing balance

Seven decimal RADWAG weighing balance was used to weigh the air sample and four decimal Mettle Toledo weighing balance was used to weigh the soil samples before and after sampling **Fig.3-27.**

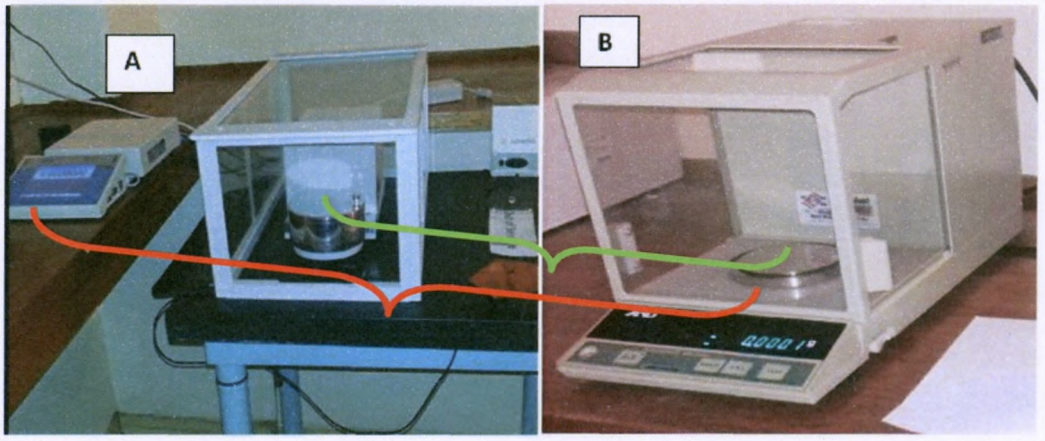

Figure 3-27: A= RADWAG weighing balance to weigh the air samples **B=** Mettle Toledo weighing balance to weigh the soil samples; green represents weighing dish and red represents display screen.

The weighing balances are installed in optimized working conditions to obtain the results that are within a specified tolerance of sample weight variation, accuracy of technological processes and others. The operation principle of the weighing balance is movement of the weighing dish assembly in an electromagnetic field. When the samples is placed on the weighing dish, the change in position of the weighing dish changes the electronic characteristics of those magnetic fields in proportion to the mass. The translated mass value is displayed on the balance. The weighing determines the mass of particulates that are collected on samples during air sampling and soil collection **fig 3-27**. The samples weighed before sampling and after sampling to determine the weight gain or loss of the air samples during air sampling and to determine the moisture percentage content in the soil samples.

To test for the accuracy of the balance a known weight of 1000µg, 2000µg or 5000µg was placed on the balance. This was done before weighing of air samples and recorded

in a weighing sheet. The workstation was located far away from air conditioning devices being a source of air drafts **figure 3-28**.

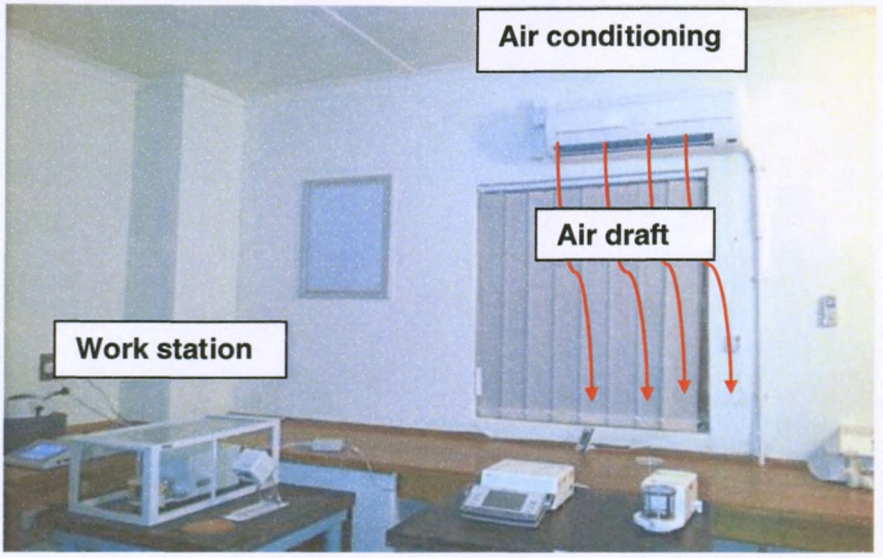

Figure 3-28: Position of a weighing balance workstation

The samples were acclimatized overnight before weighing within a balance room temperature and humidity to obtain the precise weighing results on the next day. The filter holders were half open for 24 hours to dry out the moisture in the samples **fig 3-29**.



Figure 3-29: Acclimatization of air samples in a stable environmental condition at weighing balance room where temperature range is 20°c-25°c and Humidity range of 45%-75%.

The samples were ready for gravimetric analysis. The analysis was done using following steps.

Mass 1: The weighed mass of sample filters before sampling **(Eq. 3.1)**

Example: *1935.4µg*

Mass 2: The weighed mass of sample filters after sampling **(Eq. 3.2)**

Example: *1936.7µg*

Mass 3: mass 2 –mass 1 **(Eq. 3.3)**

Example: 1936.7µg-1935.4µg

=1.3 µg

The volume of air passing through the sampler was calculated by multiplying the average volumetric flow rate in litres per minute by sampling time in minutes. Example:

$$\text{Sample volume } (m^3) = \frac{\text{Average pump flow rate in } l.m^{-1} \text{ x Sample time in minutes}}{1000} \quad \textbf{(Eq. 3.4)}$$

$$= \frac{2.2\ l.m^{-1} \text{ x } 480\ \text{min}}{1000}$$

$$= \frac{960L}{1000}$$

$$= 0.96m^3$$

The net weight/ mass correction gain (has been converted into mg by multiplying by 1000) of the samples and divided by air sampled (m^3) to give the average dust concentration in milligram per cubic meter of air (mg/m^3).

Example:

$$\text{Dust concentration} = \frac{\text{Mass correction (mg)}}{\text{Volume of air sampled } (m^3)} \quad \textbf{(Eq. 3.5)}$$

$$= \frac{1.3\ \mu g}{0.96m^3} \text{ x } 1000$$

$$= \frac{0.3\ mg/m^3}{0.96m^3}$$

$$= 1.35mg/m^3$$

3.12.2. X-ray Fluorescence (XRF)

The portable handled X-ray fluorescence (XRF) DP 6000 was used to determine the chemical composition of the sample. X-ray fluorescence radiation was emitted from the sample to receiver where the element started to be analysed. The analyses was done based on United State –Environmental Protection Agency 6200 this is the method of determination for element in the soil using XRF (revision 2007) **fig 3-30**.



Figure 3-30: IN-SITU analysis of soil in the abandoned mines by X-rays Fluorescence

The analysis took place when the rays from the sample source strike an inner shell electron in the sample and remove it from the atom **fig 3-31**. As the atom consists of a nucleus (protons and neutrons) and electrons, the electrons spin in the shells at specific distances from the nucleus and separate energy in the inner shell where the electrons are bound more tightly and are harder to be removed from the atom **fig 3-32.**

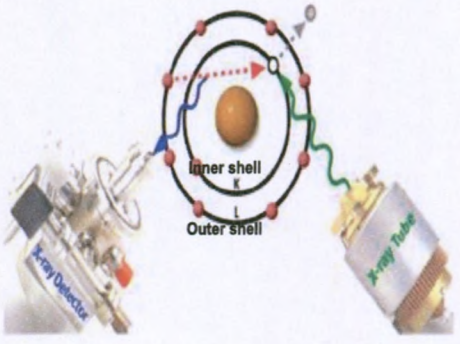

Figure 3-31: (Bohr, 2003)

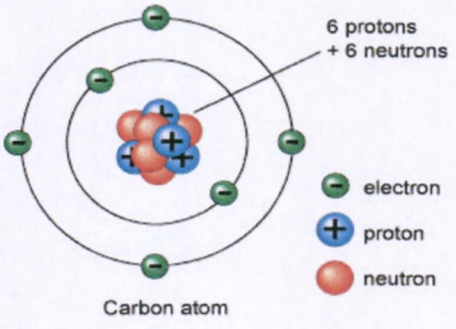

Figure 3-32 : Atomic structure after Georg Siegbahn, 1924

The enough energy of 20 keV was used to remove atom from the inner shell (K) to outer shell (N). The electrons were then start move through the gas and create a current, which raises some electrons in other atoms to higher energy levels, this level is x-ray emission lines for a heavy elements including Au and Pb (Bohr, 2003). Once the energy level increases, the electrons turn back in the atoms and release electromagnetic radiation (light). The amount of light released at different wavelengths, called the emission spectrum to detect a light elements (such as Mg, Al, Si, Ca) or medium elements (such as Cr, Fe, Cu, Ag) which are located at 1st energy level (Petrucci, 2007).

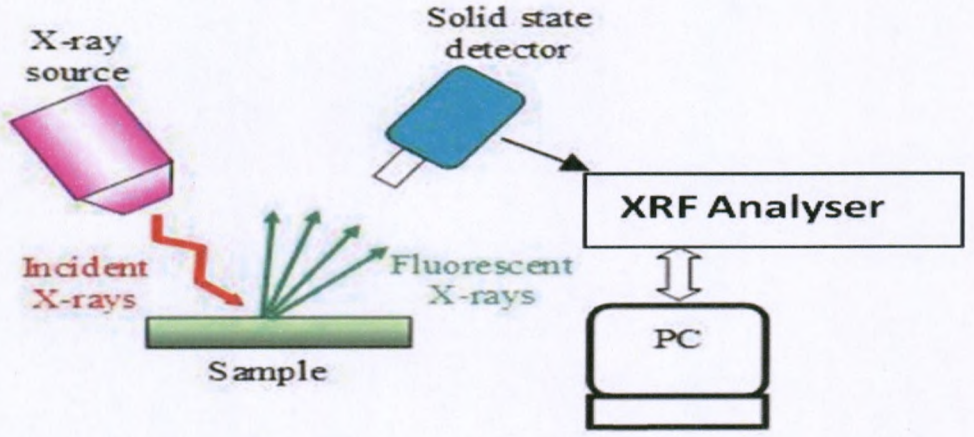

Figure 3-33: How does light affect molecules and atoms (D.C Harris, 2007)

In **figure 3-33**, detailed how the samples are analysed. The source X-rays irradiates the sample, and the sample detector measures the X-ray fluorescence radiation emitted from the sample. To stimulate the emission of characteristic X-rays from a specimen, a high-energy beam of charged particles such as electrons or protons were determined into the sample. The X-rays were emitted from a specimen and measured by an energy-dispersive spectrometer and produce photoelectric effect in a XRF spectrum form.

3.13.3. X-ray diffraction

The PANalytical X'Pert PRO diffractometer equipment was used to analyse the air and soil samples. X-ray powder diffraction (XRD) is a versatile, non destructive analytical technique for identification and quantitative determination of a various crystalline forms.

The analysis was based on "method for determination of Hazardous substance" by Health and safety Laboratory in United Kingdom(101, 2005) and (7500, 1989).



Figure 3-34: XRD equipment

The equipment was set before samples analysis. The generator PW 3040 (MPPC) is set on the tension of 45kV and current of 45mA. This energy was enough to knock out the electrons in the target from normal position, and to emit the photoelectron and kinetic energy to generate the x-rays. The radiation beam diffracted by the sample was collected by a proportional detector, and there was the formation of electrical pulses sent to a computer for processing and data storage. Scans of samples were performed in a time step of the tube-detector system of 0.5 seconds and the angle step size equal to 0.02° 2θ, which generated analyses that lasted 27 minutes each test.

The High Score plus 2.0 (software from PANalytical) was used to characterization the samples. These was done by comparing the generated diffraction patterns with reference standards organized into sheets available in the database PDF2 of the ICDD - International Centre for Diffraction Data to maintain the crystallographic information including interplanar distances. In this procedure, the software performed a search for three to ten most intense peaks of each crystalline compound which was kept in the database and compared them with the peaks of the sample diffractogram. After the

process of searching and comparison being done, the results values were expressed in increasing order of rank. The major proximity of values led to the identification of the mineral.

The single-crystal measurements of the samples were mounted on a goniometer (powder scan) to position the crystal at selected orientations of 26.6° for both qualitative and quantitative phase analysis (Little, 1976). The angle between incident beam and sample was equal to the angle between the sample and diffracted beam (ITT, 1983). In the measurements, only crystallites planes parallel to the surface participated to diffracted signal. X-ray powder diffraction is composed of crystallites which are randomly orientated to one another. When the sample is placed in the monochromatic X-ray beam, diffraction occurs from the planes in those crystallites that are oriented at the correct angle (2θ) to fulfil the Bragg condition $n \lambda = 2dsin\theta$.

Where: d = is the spacing between diffracting planes

θ=is the incident angle

n =is any integer

λ= is the wavelength of the beam.

The bragg law relates the wavelength of electromagnetic radiation to the diffraction angle and the lattice spacing in a crystalline sample. The X-rays were directed at the sample, and the diffracted rays were collected in the angle between incident and diffracted rays. The planes giving rise to the smallest Bragg angle will have the largest d-spacing.

The RIETVELD XRD method was used to refine a crystal structure and to determine the quantities of crystalline and amorphous components in multiphase mixtures (Little, 1976). RIETVELD analysis is a technique that has been developed for solving/refining crystal structures from powder diffraction data. It involves an interpretation of the peak positions and intensities (McKee C., 1990). The measured match intensity was compared with the alpha quartz peak intensity against pure respirable alpha quartz

standard NIST 1878a (93.9% of quartz). NIST1878a pure silica standard is used to allow the chemical and crystallographic purity to be known

LIMITATION OF THE STUDY

Due to the mandate of and the time available for the study:

Qualitative analysis was achieved by IN-SITU measurement that were taken directly on a heap of soil at the source of each mine, this method was limited to the identification of the atomic and other elements species. Not all elements from periodic table were detected.

The confirmatory of the results was not achieved for this study; this involves the determination of samples with specified thickness and morphology (grain size, texture, surface) and the use of standards of known concentration. This may be achieved taking one confirmatory sample for every 10 samples collected. The confirmatory samples are collected from the same sample material that is analyzed on site, but are sent to an off-site laboratory for formal analysis. The purpose of a confirmatory sample is to judge the accuracy of the data obtained by analysis on site and to allow corrections, if necessary. It is always recommended that analyst compare prepared-sample results to laboratory results.

Policy recommendations and measures for control of mining impacts in the areas studied are limited to the minimization and mitigation of wind-blown dust.

Particle size distribution and characterization of mine dust have not been investigated in addition to impact of dust all aspects of the environment.

Particle sizes of crystalline silica were not determined from the source to the 1.5km away from the source.

CHAPTER FOUR

4. RESULTS

4-1. Temperature

Autumn had a minimum temperature of 14°C and maximum temperature of 21°C. In winter, the minimum temperature was 11°C and the maximum temperature was 16°C. Spring experienced a minimum temperature of 13°C and maximum temperature of 21°C. Generally the minimum temperature for all study areas in summer was 20°C and the maximum temperature was 26 °C Fig. 4-1.

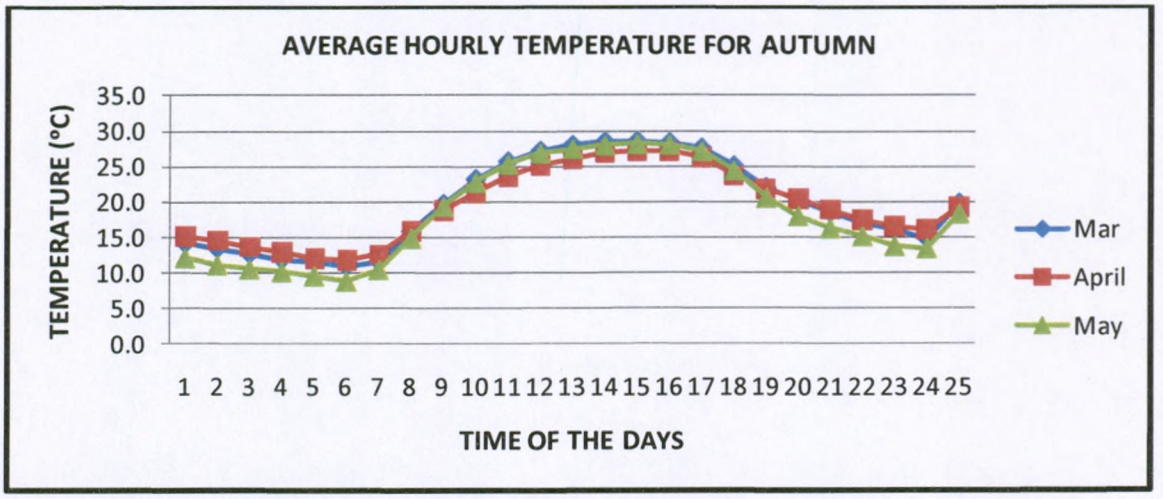

Figure 4-1: Average hourly autumn temperature

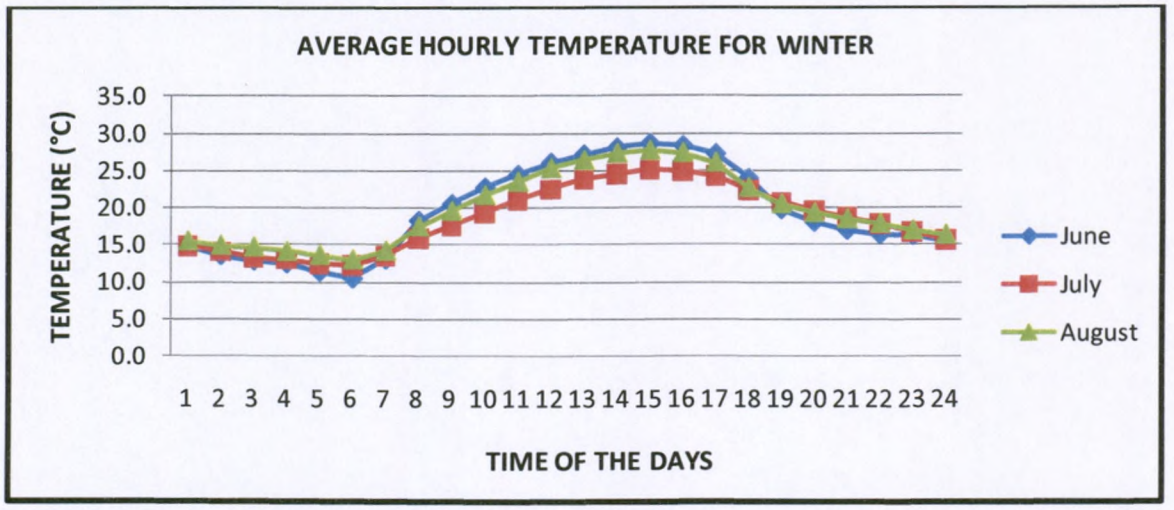

Figure 4-2: Average hourly winter temperature

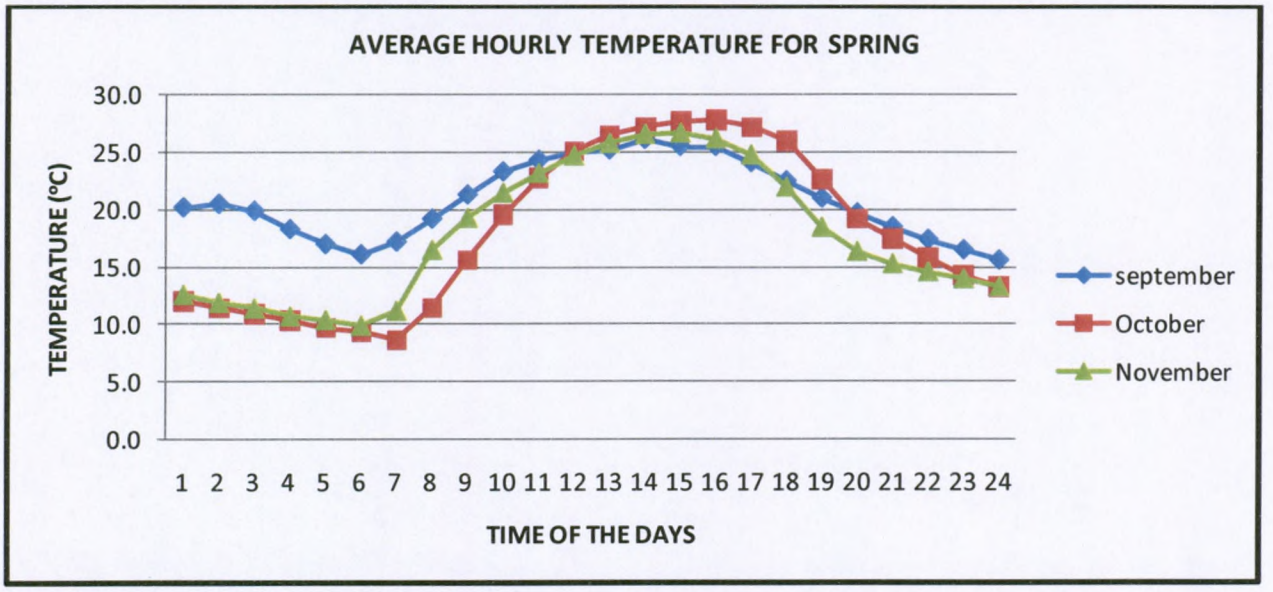

Figure 4-3: Average hourly spring temperature

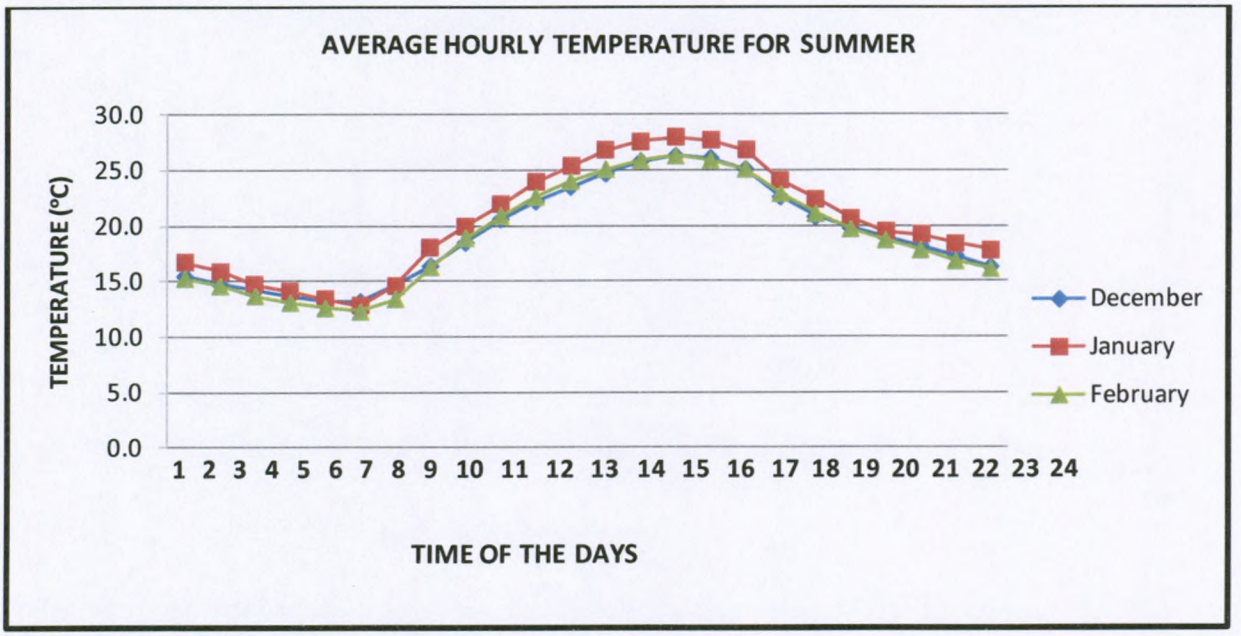

Figure 4-4: Average hourly summer temperature

4-2. Wind speed

The study areas experienced a minimum average wind speed of 2.2 m/s and average maximum wind speed of 3.9 m/s in autumn. Winter had a minimum average wind speed of 3.6 m/s and maximum average wind speed of 6.6 m/s. In spring, the study areas were exposed to a minimum average wind speed of 2.9 m/s and maximum average wind speed of 7.9 m/s and average minimum wind speed of 5.4 m/s in summer and average maximum wind speed of 11.5 m/s **Fig. 4.5-4.8**.

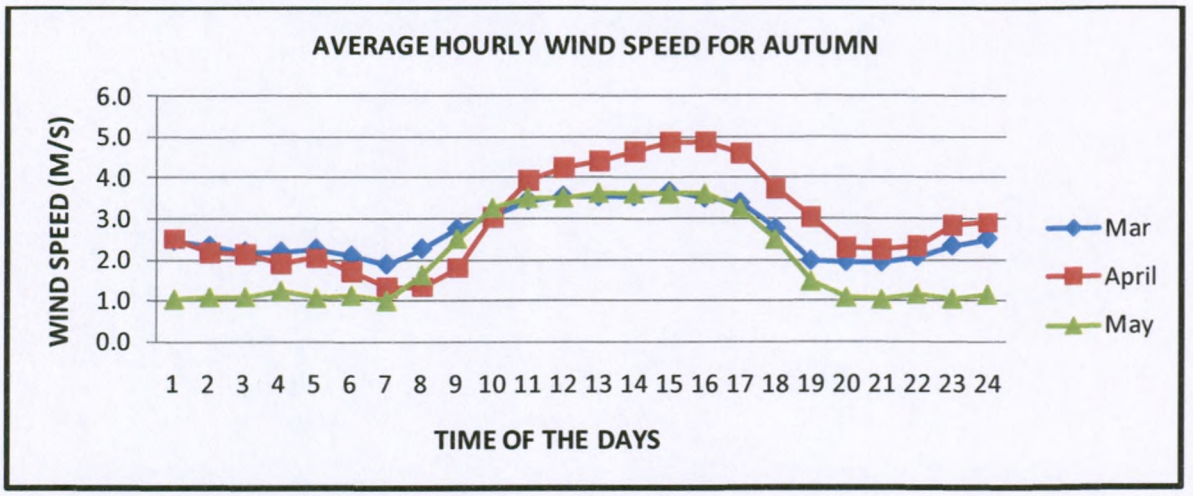

Figure 4-5: Average daily autumn wind speed

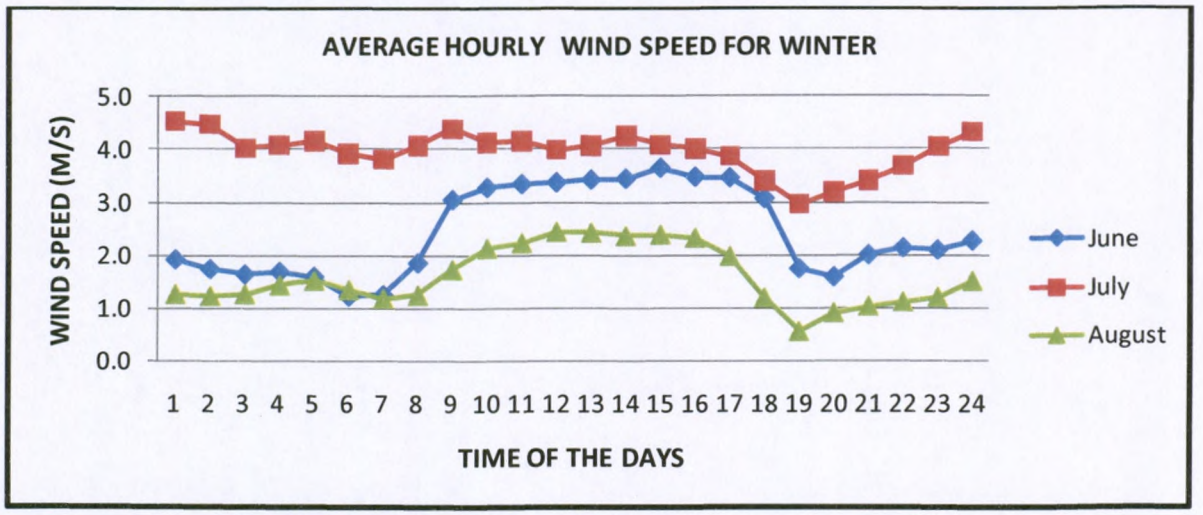

Figure 4-6: Average daily winter wind speed

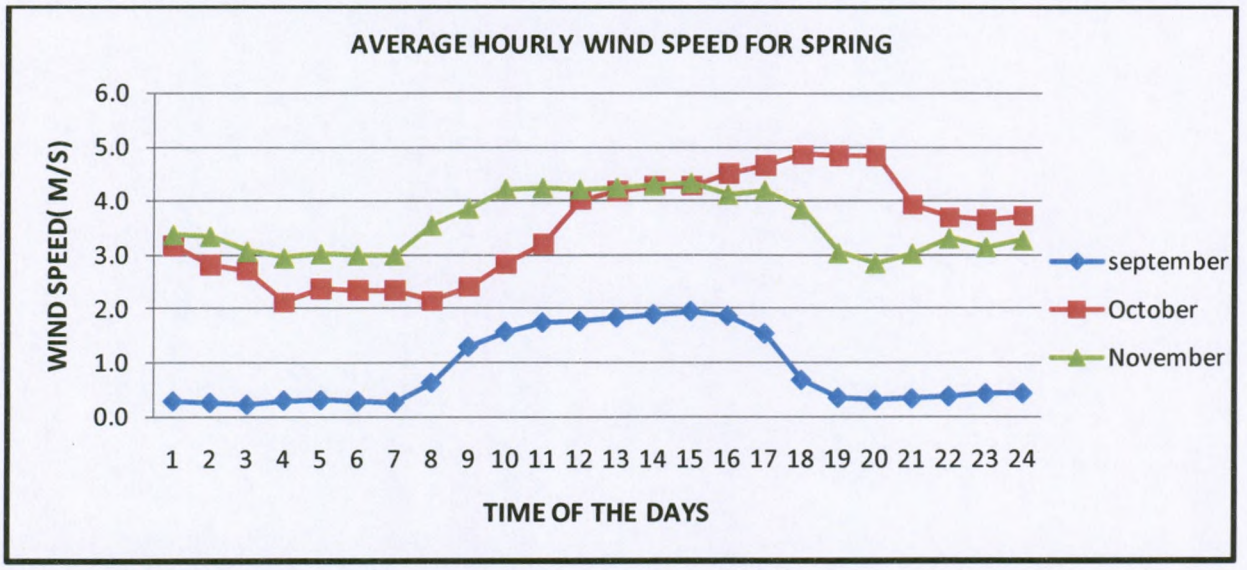

Figure 4-7: Average daily spring wind speed

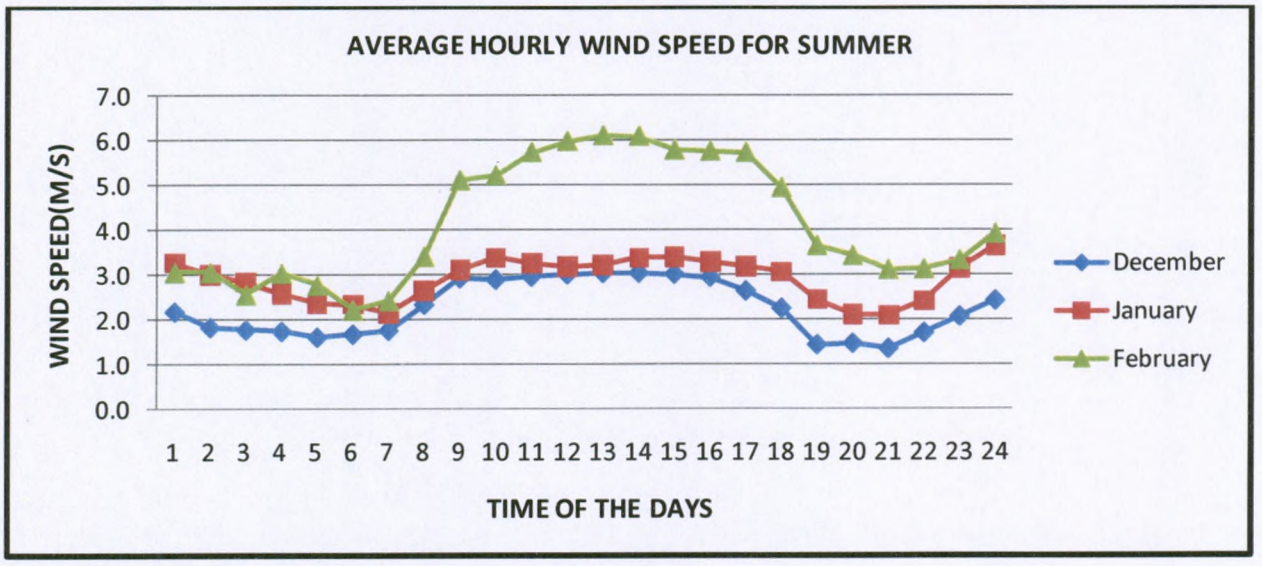

Figure 4-8: Average daily summer wind speed

4-3. Wind direction

Wind direction was monitored for 24 hours. the study areas experienced north west, South West and South East wind direction in autumn **Fig. 4-9 to 4-12.**

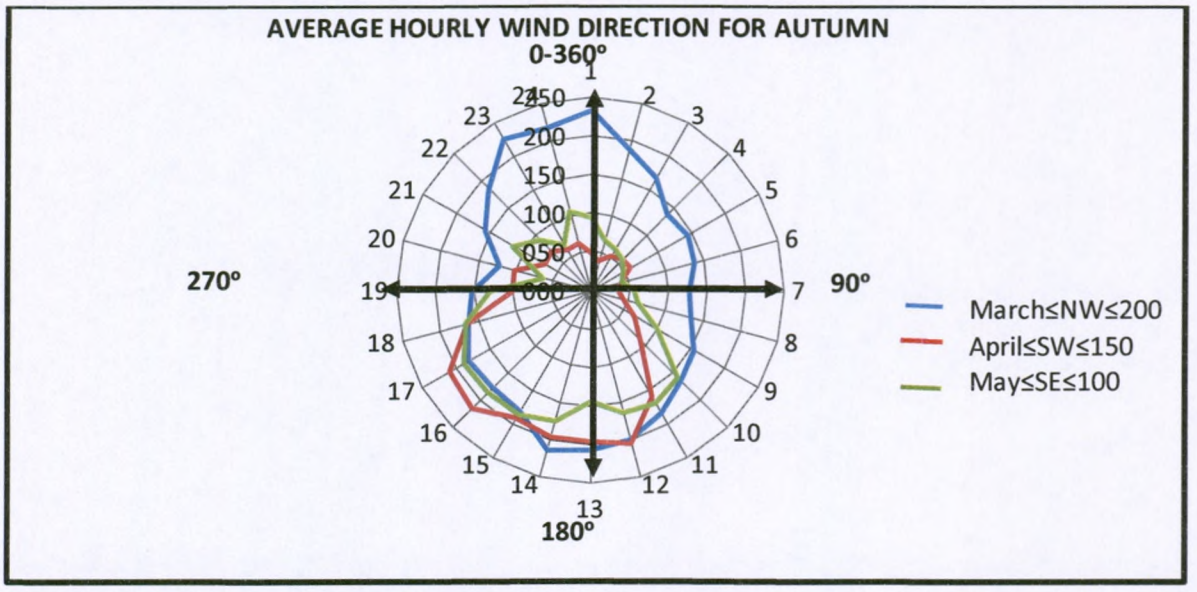

Figure 4-9: Average hourly wind direction for autumn

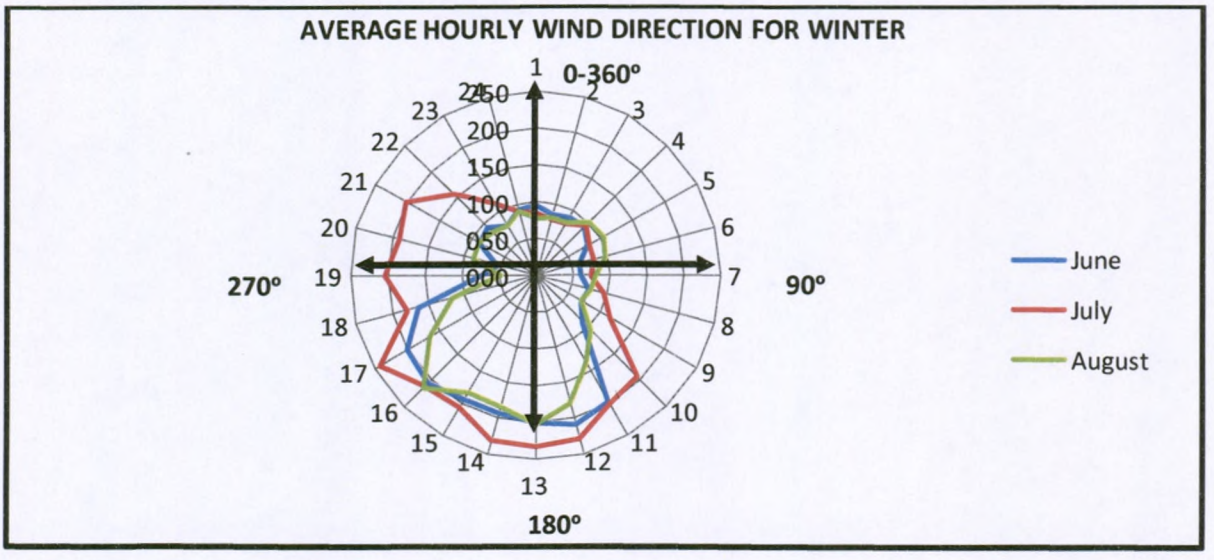

Figure 4-10: Average hourly wind direction for winter, showing that the study areas experienced North West wind direction at 200 mb and south wind direction at 50

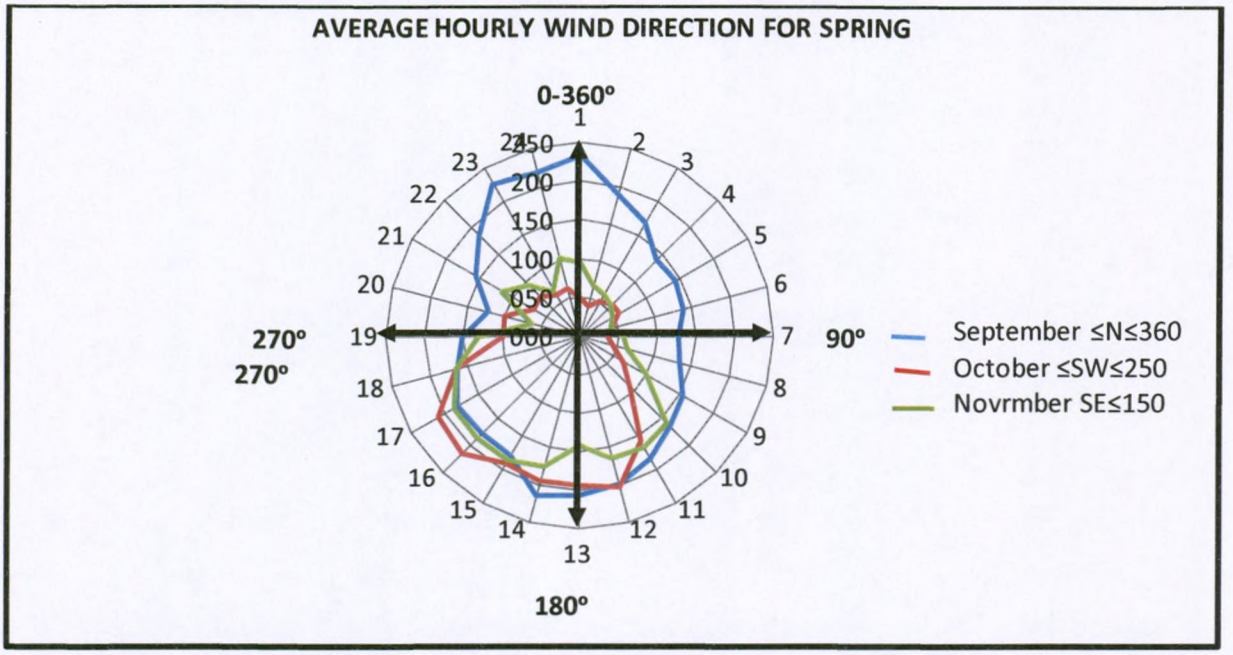

Figure 4-11: Average hourly wind direction for spring, showing that the study areas experienced North, South West and South East wind direction.

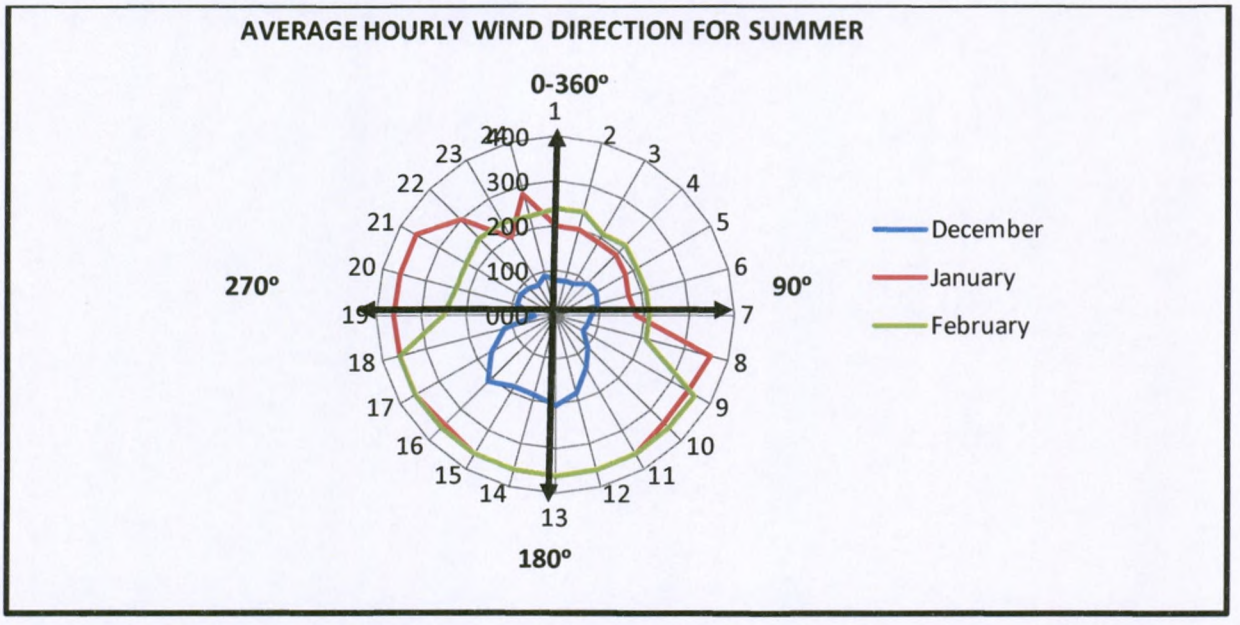

Figure 4-12: Average hourly wind direction for summer, the study areas experienced south westerly wind direction at 100, southwards wind direction at 250.

4-4. Humidity

Witwatersrand experienced a minimum humidity of 20% and maximum humidity of 40% in autumn. In winter, minimum humidity was 50% and the maximum humidity was 70% and minimum humidity of 11% and maximum humidity of 21% in spring. The minimum humidity was 20% and maximum humidity for all study areas in summer was 45% **Fig. 4-13 to 4-16**

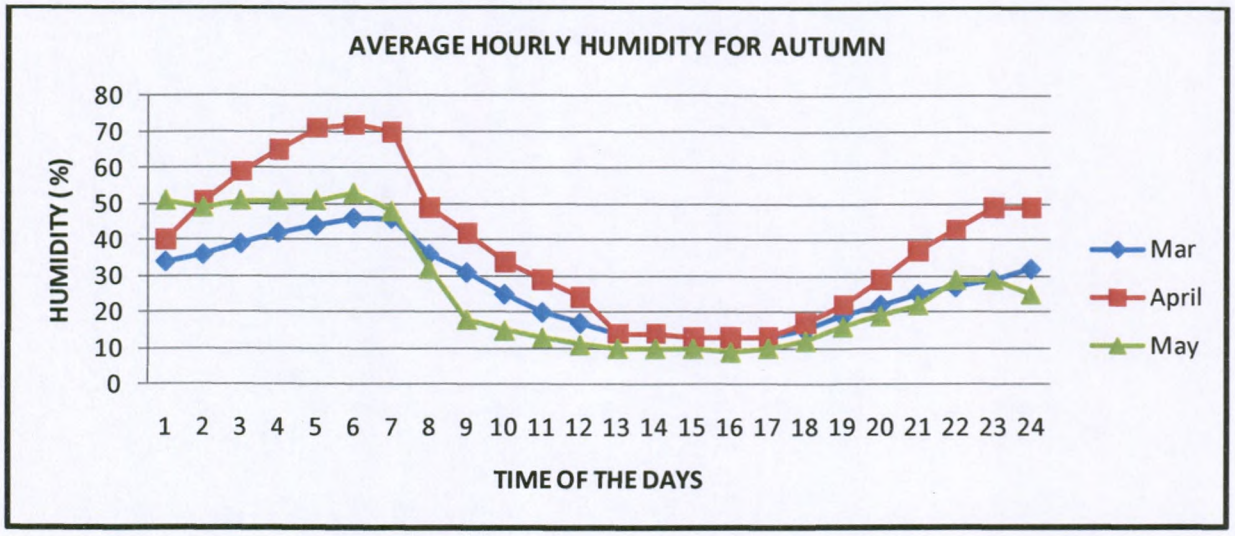

Figure 4-13: Average hourly autumn humidity

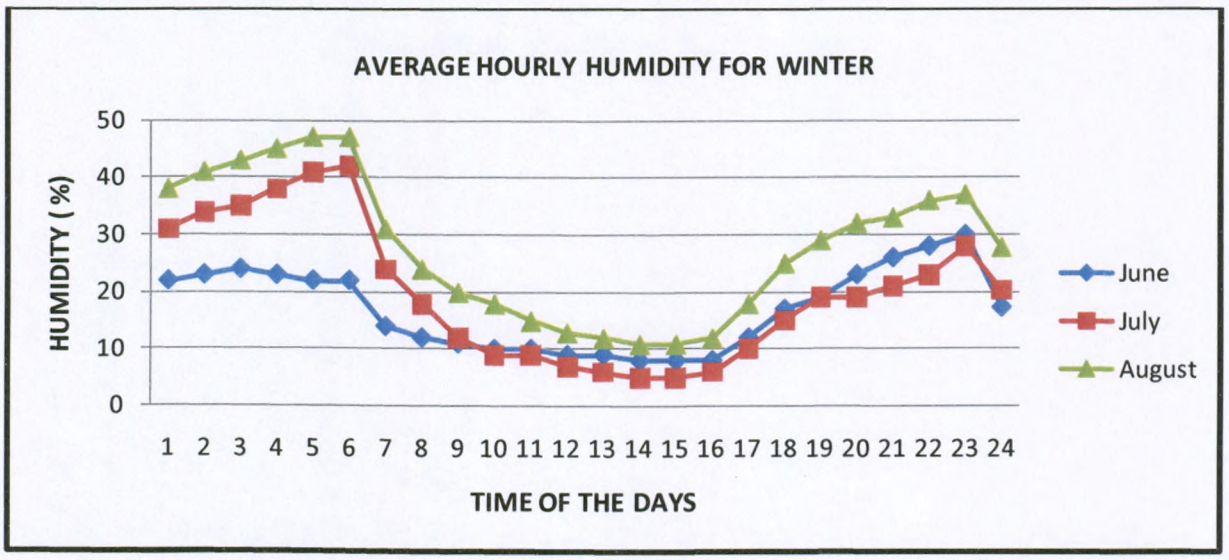

Figure 4-13: Average hourly winter humidity

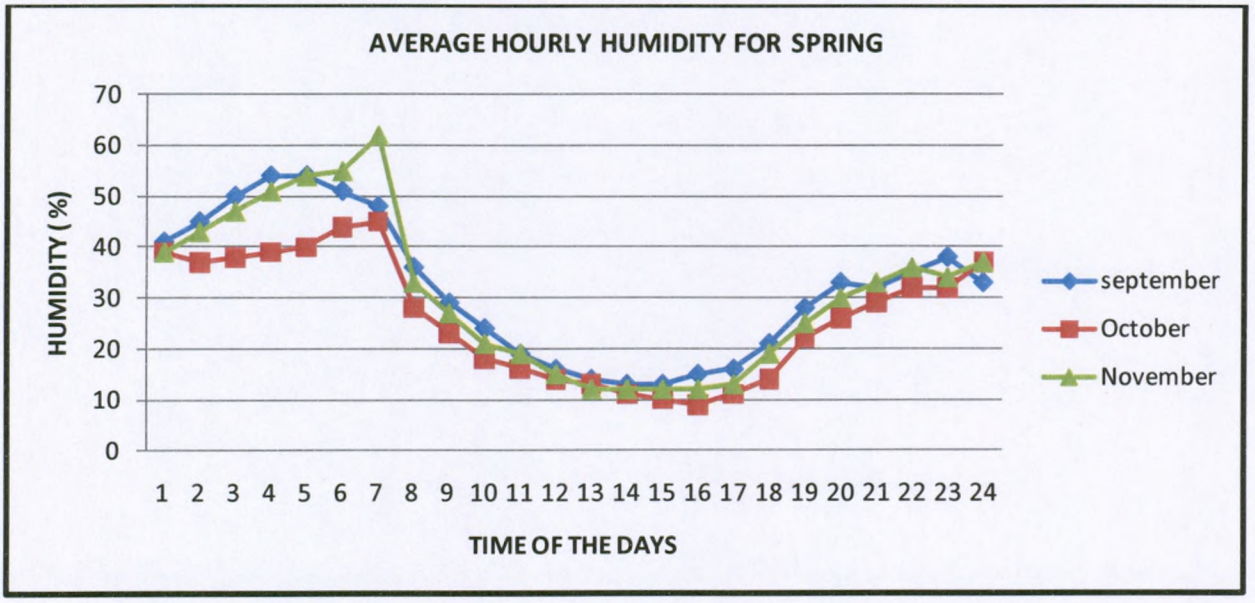

Figure 4-15: Average hourly spring humidity

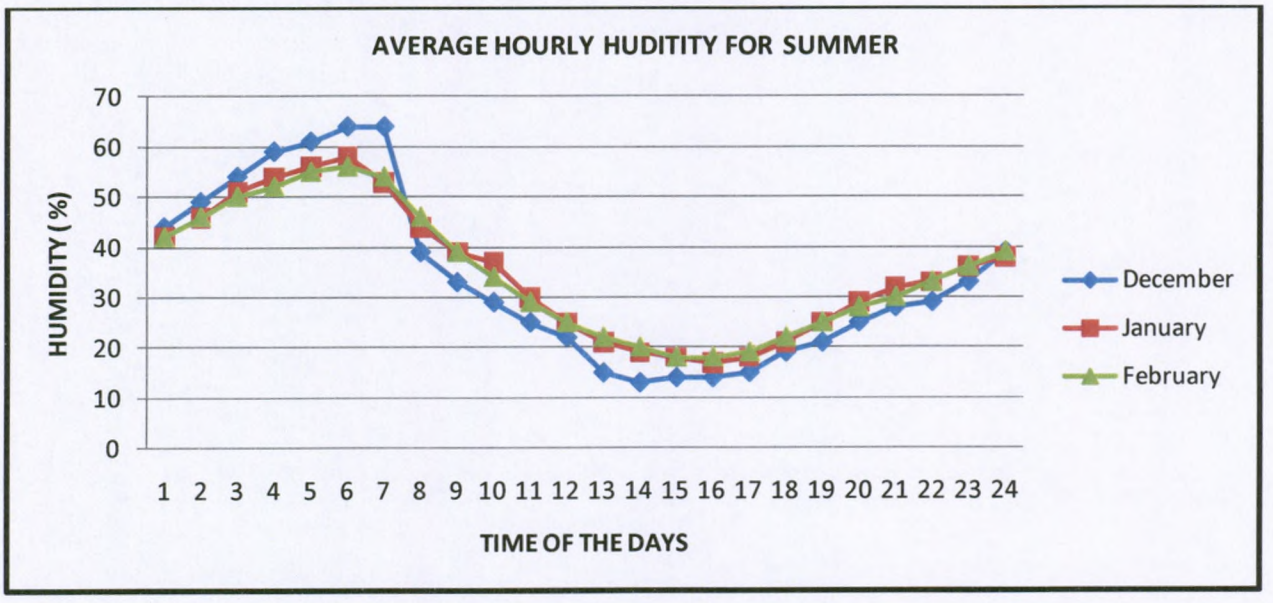

Figure 4-16: Average hourly summer humidity

4.2. AIR SAMPLE RESULTS

Table 4-1: Durban deep mine

Season	Distance from Source	Sample Number	Co ordinates		Filter Mass Before	Filter mass after	Difference	Flow rate	Sample time	Volume	Dust concentration in air	XRD Results	Silica concentration in air
			Latitude	Longitude	µg	µg	µg	l.min^{-1}	minutes	m^3	µg.m^{-3}	% silica in sample	µg.m^{-3}
Environmental Exposure Limit of respirable crystalline silica													3
Spring	0	D13	26°10'28.74"S	27°51'35.39" E	5277	5287	10	2	480	0.96	10.42	58.90%	6.14
	500	D16	26°10'24.69"S	27°51'34.30" E	5526	5529	3	2	480	0.96	3.13	38.40%	1.20
	1000	D17	26°10'22.90"S	27°51'32.19" E	5286	5287	1	2	480	0.96	1.04	44.00%	0.46
	1500	D18	26°10'30.02"S	27°51'30.07" E	5367	5369	2	2	480	0.96	2.08	54.00%	1.13
Summer	0	D19	26°10'28.74"S	27°51'35.39" E	5336	5339	3	2	480	0.96	3.13	37.00%	1.16
	500	D22	26°10'24.69"S	27°51'34.30" E	5531	5541	10	2	480	0.96	10.42	9.30%	0.97
	1000	D23	26°10'22.90"S	27°51'32.19" E	5936	5937	1	2	480	0.96	1.04	22.00%	0.23
	1500	D24	26°10'30.02"S	27°51'30.07" E	5427	5429	2	2	480	0.96	2.08	15.50%	0.32
Autumn	0	D1	26°10'28.74"S	27°51'35.39" E	5379	5389	10	2	480	0.96	10.42	8.60%	0.90
	500	D4	26°10'24.69"S	27°51'34.30" E	5413	5433	20	2	480	0.96	20.83	58.00%	12.08
	1000	D5	26°10'22.90"S	27°51'32.19" E	5304	5305	1	2	480	0.96	1.04	82.00%	0.85
	1500	D6	26°10'30.02"S	27°51'30.07" E	5367	5377	10	2	480	0.96	10.42	13.00%	1.35
Winter	0	D7	26°10'28.74"S	27°51'35.39" E	5467	5469	2	2	480	0.96	2.08	18.30%	0.38
	500	D10	26°10'24.69"S	27°51'34.30" E	5226	5230	4	2	480	0.96	4.17	30.80%	1.28
	1000	D11	26°10'22.90"S	27°51'32.19" E	6038	6048	10	2	480	0.96	10.42	15.00%	1.56
	1500	D12	26°10'30.02"S	27°51'30.07" E	5239	5241	2	2	480	0.96	2.08	10.00%	0.21

Table 4-2: Bantjies Mine

Season	Distance from Source	Sample Number	Co ordinates		Filter Mass Before	Filter mass after	Difference	Flow rate	Sample time	Volume	Dust conc air	XRD Results	Silica conc air
			Latitude	Longitude	µg	µg	µg	l.min^{-1}	minutes	m^3	µg.m^{-3}	% silica in sample	µg.m^{-3}
Environmental Exposure Limit of respirable crystalline silica													3
Spring	0	F13	26°11'6.48"S	27°54'35.93"E	5944	5945	1	2	480	0.96	1.04	30.00%	0.31
	500	F16	26°11'9.55"S	27°54'38.38"E	5283	5285	2	2	480	0.96	2.08	70.20%	1.46
	1000	F17	26°11'18.20"S	27°54'35.28"E	6057	6059	2	2	480	0.96	2.08	54.00%	1.13
	1500	F18	26°11'14.86"S	27°54'38.09"E	5487	5497	10	2	480	0.96	10.42	65.00%	6.77
Summer	0	F19	26°11'6.48"S	27°54'35.93"E	5794	5797	3	2	480	0.96	3.13	10.00%	0.31
	500	F22	26°11'9.55"S	27°54'38.38"E	5821	5831	10	2	480	0.96	10.42	10.20%	1.06
	1000	F23	26°11'18.20"S	27°54'35.28"E	5619	5620	1	2	480	0.96	1.04	13.20%	0.14
	1500	F24	26°11'14.86"S	27°54'38.09"E	5062	5066	4	2	480	0.96	4.17	10.00%	0.42
Autumn	0	F1	26°11'6.48"S	27°54'35.93"E	5006	5016	10	2	480	0.96	10.42	50.70%	5.28
	500	F4	26°11'9.55"S	27°54'38.38"E	4989	4999	10	2	480	0.96	10.42	10.90%	1.14
	1000	F5	26°11'18.20"S	27°54'35.28"E	5094	5098	4	2	480	0.96	4.17	35.00%	1.46
	1500	F6	26°11'14.86"S	27°54'38.09"E	5944	5945	1	2	480	0.96	1.04	50.70%	0.53
Winter	0	F7	26°11'6.48"S	27°54'35.93"E	5283	5286	3	2	480	0.96	3.13	63.10%	1.97
	500	F10	26°11'9.55"S	27°54'38.38"E	6067	6068	1	2	480	0.96	1.04	50.00%	0.52
	1000	F11	26°11'18.20"S	27°54'35.28"E	5487	5497	10	2	480	0.96	10.42	43.50%	4.53
	1500	F12	26°11'14.86"S	27°54'38.09"E	5569	5571	2	2	480	0.96	2.08	26.30%	0.55

Table 4-3: East champ D'Or Mine

Season	Distance from Source	Sample Number	Co ordinates		Filter Mass Before	Filter mass after	Difference	Flow rate	Sample time	Volume	Dust concentration in air	XRD Results	Silica concentration in air
			Latitude	Longitude	µg	µg	µg	l.min^{-1}	minutes	m^3	µg.m^{-3}	% silica in sample	µg.m^{-3}
Environmental Exposure Limit of respirable crystalline silica													3
Spring	0	L13	26°07'53.84" S	27°49'25.54" E	7737	7738	1	2	480	0.96	1.04	22.00%	0.23
	500	L16	26°07'58.30" S	27°49'28.32" E	7692	7699	7	2	480	0.96	7.29	10.20%	0.74
	1000	L17	26°08'01.29" S	27°49'33.48" E	7746	7747	1	2	480	0.96	1.04	15.00%	0.16
	1500	L18	26°08'05.29" S	27°49'35.48" E	7803	7823	20	2	480	0.96	20.83	11.90%	2.48
Summer	0	L19	26°07'53.84" S	27°49'25.54" E	7718	7729	11	2	480	0.96	11.46	45.70%	5.24
	500	L22	26°07'58.30" S	27°49'28.32" E	7741	7776	35	2	480	0.96	36.46	29.30%	10.68
	1000	L23	26°08'01.29" S	27°49'33.48" E	7768	7798	30	2	480	0.96	31.25	22.80%	7.13
	1500	L24	26°08'05.29" S	27°49'35.48" E	7774	7984	210	2	480	0.96	18.75	36.00%	7.75
Autumn	0	L1	26°07'53.84" S	27°49'25.54" E	7739	7749	10	2	480	0.96	10.42	55.20%	5.75
	500	L4	26°07'58.30" S	27°49'28.32" E	7935	7945	10	2	480	0.96	10.42	54.90%	5.72
	1000	L5	26°08'01.29" S	27°49'33.48" E	7715	7716	1	2	480	0.96	1.04	76.00%	0.79
	1500	L6	26°08'05.29" S	27°49'35.48" E	7689	7699	10	2	480	0.96	10.42	83.00%	8.65
Winter	0	L7	26°07'53.84" S	27°49'25.54" E	7883	7913	30	2	480	0.96	31.25	55.16%	7.24
	500	L10	26°07'58.30" S	27°49'28.32" E	7745	7805	60	2	480	0.96	62.50	50.20%	3.38
	1000	L11	26°08'01.29" S	27°49'33.48" E	7799	7812	13	2	480	0.96	13.54	43.30%	5.86
	1500	L12	26°08'05.29" S	27°49'35.48" E	7719	7720	1	2	480	0.96	1.04	40.21%	0.42

Table 4-4: Crown mines

Season	Distance from Source	Sample Number	Co- ordinates		Filter Mass Before	Filter mass after	Difference	Flow rate	Sample time	Volume	Dust concentration in air	XRD Results	Silica concentration in air
			Latitude	longitude	µg	µg	µg	l.min^{-1}	minutes	m^3	µg.m^{-3}	% silica in sample	µg.m^{-3}
Environmental Exposure Limit of respirable crystalline silica													3
Spring	0	R13	26°22'5.93"S	27°45'30.70"E	7756	7779	23	2	480	0.96	23.96	15.90%	3.81
	500	R16	26°22'8.07"S	27°27'31.17"E	7741	7745	4	2	480	0.96	4.17	10.90%	0.45
	1000	R17	26°22'10.4"S	27°27'31.72"E	7739	7749	10	2	480	0.96	10.42	10.63%	1.11
	1500	R18	26°22'12.97"S	27°27'32.2"E	7905	7909	4	2	480	0.96	4.17	9.47%	0.39
Summer	0	R19	26°22'5.93"S	27°45'30.70"E	7715	7719	4	2	480	0.96	4.17	47.10%	1.96
	500	R22	26°22'8.07"S	27°27'31.17"E	7689	7699	10	2	480	0.96	10.42	34.30%	3.57
	1000	R23	26°22'10.4"S	27°27'31.72"E	7803	7813	10	2	480	0.96	10.42	33.50%	3.49
	1500	R24	26°22'12.97"S	27°27'32.2"E	7745	7747	2	2	480	0.96	2.08	26.60%	0.55
Autumn	0	R1	26°22'5.93"S	27°45'30.70"E	7769	7779	10	2	480	0.96	10.42	55.90%	5.82
	500	R4	26°22'8.07"S	27°27'31.17"E	7719	7720	1	2	480	0.96	1.04	57.30%	0.60
	1000	R5	26°22'10.4"S	27°27'31.72"E	7739	7749	10	2	480	0.96	10.42	39.00%	4.06
	1500	R6	26°22'12.97"S	27°27'32.2"E	7736	7737	1	2	480	0.96	1.04	87.00%	0.91
Winter	0	R7	26°22'5.93"S	27°45'30.70"E	7786	7789	3	2	480	0.96	3.13	52.30%	1.63
	500	R10	26°22'8.07"S	27°27'31.17"E	7896	7899	3	2	480	0.96	3.13	44.70%	1.40
	1000	R11	26°22'10.4"S	27°27'31.72"E	7795	7797	2	2	480	0.96	2.08	52.80%	1.10
	1500	R12	26°22'12.97"S	27°27'32.2"E	7749	7779	30	2	480	0.96	31.25	40.00%	12.50

Table 4-5: Princess Mine

seasons	Distance from Source	Sample Number	Co ordinates		Filter Mass Before	Filter mass after	Difference	Flow rate	Sample time	Volume	Dust concentration in air	XRD Results (silica in sample)	Silica concentration in air
			Latitude	longitude	µg	µg	µg	$l.min^{-1}$	minutes	m^3	$µg.m^{-3}$	%	$µg.m^{-3}$
Environmental Exposure Limit of respirable crystalline silica													3
Spring	0	P13	26°07'53.84" S	27°49'25.54" E	7736	7756	20	2	480	0.96	20.83	55.60%	11.58
	500	P16	26°07'58.30" S	27°49'28.32" E	7741	7743	2	2	480	0.96	2.08	53.30%	1.11
	1000	P17	26°08'01.29" S	27°49'33.48" E	7739	7749	10	2	480	0.96	10.42	45.00%	4.69
	1500	P18	26°08'05.29" S	27°49'35.48" E	7905	7955	50	2	480	0.96	52.08	38.00%	19.79
Summer	0	P19	26°07'53.84" S	27°49'25.54" E	7715	7725	10	2	480	0.96	10.42	32.70%	3.41
	500	P22	26°07'58.30" S	27°49'28.32" E	7689	7690	1	2	480	0.96	1.04	12.20%	0.13
	1000	P23	26°08'01.29" S	27°49'33.48" E	7803	7823	20	2	480	0.96	20.83	10.50%	2.19
	1500	P24	26°08'05.29" S	27°49'35.48" E	7745	7747	2	2	480	0.96	2.08	8.94%	0.19
Autumn	0	P1	26°07'53.84" S	27°49'25.54" E	7769	7772	3	2	480	0.96	3.13	66.10%	2.07
	500	P4	26°07'58.30" S	27°49'28.32" E	7719	7720	1	2	480	0.96	1.04	45.70%	0.48
	1000	P5	26°08'01.29" S	27°49'33.48" E	77385	77395	10	2	480	0.96	10.42	46.00%	4.79
	1500	P6	26°08'05.29" S	27°49'35.48" E	7736	7738	2	2	480	0.96	2.08	35.00%	0.73
Winter	0	P7	26°07'53.84" S	27°49'25.54" E	7736	7739	3	2	480	0.96	3.13	50.90%	1.59
	500	P10	26°07'58.30" S	27°49'28.32" E	7898	7908	10	2	480	0.96	10.42	45.50%	4.74
	1000	P11	26°08'01.29" S	27°49'33.48" E	7745	7747	2	2	480	0.96	2.08	43.70%	0.91
	1500	P12	26°08'05.29" S	27°49'35.48" E	7740	7749	9	2	480	0.96	9.38	33.20%	3.11

Table 4-6: Randfontein estate Mine

Season	Distance from Source	Sample Number	Co ordinates		Filter Mass Before	Filter mass after	Difference	Flow rate	Sample time	Volume	Dust concentration in air	XRD Results	Silica concentration in air
			Latitude	Longitude	µg	µg	µg	l.min^{-1}	minutes	m^3	µg.m^{-3}	%	µg.m^{-3}
Environmental Exposure Limit of respirable crystalline silica													3
Spring	0	V13	26°22'1.00" S	27°49'54.58" E	7747	7757	10	2	480	0.96	10.42	42.00%	4.38
	500	V16	26°22'1.00" S	27°49'54.58" E	7692	7696	4	2	480	0.96	4.17	13.60%	0.57
	1000	V17	26°11'50.55' 'S	27°49'41.40" E	7747	7759	12	2	480	0.96	12.50	26.00%	3.25
	1500	V18	26°11'52.37' 'S	27°49'37.25" E	7893	7897	4	2	480	0.96	4.17	12.00%	0.50
Summer	0	V19	26°22'1.00" S	27°49'54.58" E	7791	7796	5	2	480	0.96	5.21	62.00%	3.23
	500	V22	26°22'1.00" S	27°49'54.58" E	7795	7796	1	2	480	0.96	1.04	55.30%	0.58
	1000	V23	26°11'50.55' 'S	27°49'41.40" E	7757	7759	2	2	480	0.96	2.08	65.00%	1.35
	1500	V24	26°11'52.37' 'S	27°49'37.25" E	7738	7739	1	2	480	0.96	1.04	45.00%	0.47
Autumn	0	V1	26°22'1.00" S	27°49'54.58" E	7729	7739	10	2	480	0.96	10.42	20.00%	2.08
	500	V4	26°22'1.00" S	27°49'54.58" E	7986	7987	1	2	480	0.96	1.04	15.00%	0.16
	1000	V5	26°11'50.55' 'S	27°49'41.40" E	7728	7729	1	2	480	0.96	1.04	18.00%	0.19
	1500	V6	26°11'52.37' 'S	27°49'37.25" E	7636	7639	3	2	480	0.96	3.13	12.00%	0.38
Winter	0	V7	26°22'1.00" S	27°49'54.58" E	7864	7867	3	2	480	0.96	3.13	13.20%	0.41
	500	V10	26°22'1.00" S	27°49'54.58" E	7787	7789	2	2	480	0.96	2.08	50.00%	1.04
	1000	V11	26°11'50.55' 'S	27°49'41.40" E	7764	7767	3	2	480	0.96	3.13	50.30%	1.57
	1500	V12	26°11'52.37' 'S	27°49'37.25" E	7799	7800	1	2	480	0.96	1.04	10.65%	0.11

4.3. MINERAL IDENTIFICATION USING XRD

Table 4-7: Mineralogical Identification results for the samples taken in all the study areas.

Mine	Distance from Source	Sample Number	CO-Ordinates		Quartz	kaolinite	Calcite	dolomite	Muscovite/ Illite/ nimisite	Rutile/ Anatase	Pyrite	Gypsum	Hematite	Clinochlore/ Anorthosite
			Latitude	Longitude										
Durban Deep	0	D2	26°10'28.74" S	27°51'35.39" E	P	P	A	A	A	P	A	A	A	A
		D3	26°10'28.74" S	27°51'35.39" E	P	A	A	A	A	P	A	A	P	A
	500	F2	26°10'24.69" S	27°51'34.30" E	P	A		A	A	A	A	A	A	A
		F3	26°10'24.69" S	27°51'34.30" E	P	A	A	P	A	A	A	A	A	A
	1000	P2	26°10'22.90" S	27°51'32.19" E	P	P	A	A	A	P	A	P	A	A
		P3	26°10'22.90" S	27°51'32.19" E	P	A	A	A	A	A	A	A	A	A
	1500	L2	26°10'30.02" S	27°51'30.07" E	P	A	P	A	A	A	A	P	A	A
		L3	26°10'30.02" S	27°51'30.07" E	P	A	A	A	A	A	A	A	A	A
Bentjies	0	R 2	26°11'6.48" S	27°54'35.93" E	P	A	A	A	A	A	P	A	A	A
		R 3	26°11'6.48" S	27°54'35.93" E	P	A	A	P	A	A	A	A	A	A
	500	V2	26°11'9.55" S	27°54'38.38" E	P	A	A	P	A	A	A	A	A	A
		V3	26°11'9.55" S	27°54'38.38" E	P	A	A	P	A	A	A	A	A	A
	1000	D8	26°11'18.20" S	27°54'35.28" E	P	A	A	A	A	A	A	A	A	P
		D9	26°11'18.20" S	27°54'35.28" E	P	A	A	A	A	A	A	A	A	P
	1500	F8	26°11'14.86" S	27°54'38.09" E	P	P	p	P	P	P	A	A	A	A
		F9	26°11'14.86" S	27°54'38.09" E	P	A	A	A	P	A	A	P	A	A

P=present minerals within the sample, A=absent mineral within the sample

Mine	Distance from Source	Sample Number	CO-Ordinates		Quartz	kaolnite	Calcite	dolomite	Muscovite/ Illite/ nimisite	Rutile/ Anatase	Pyrite	Gypsum	Hematite	Clinochlore/ Anorthosite
			Latitude	Longitude										
Princess	0	P8	26°07'53.84" S	27°49'25.54" E	P	P	A	P	P	A	A	A	P	A
		P9	26°07'53.84" S	27°49'25.54" E	P	P	A	A	P	A	P	A	A	P
	500	L8	26°07'58.30" S	27°49'28.32" E	P	A	A	P	P	P	A	A		P
		L9	26°07'58.30" S	27°49'28.32" E	P	P	A	A	P	A	P	A	A	P
	1000	R 8	26°08'01.29" S	27°49'33.48" E	P	A	P	A	P	A	A	A	A	A
		R 9	26°08'01.29" S	27°49'33.48" E	p	P	A	P	p	P	A	P	p	p
	1500	V8	26°08'05.29" S	27°49'35.48" E	P	A	A	A	A	A	A	P	A	A
		V9	26°08'05.29" S	27°49'35.48" E	P	A	P	A	A	A	A	A	A	A
	0	D14	26°07'39.09" S	27°45'24.04" E	P	P	A	P	P	A	A	A	P	A
		D15	26°07'39.09" S	27°45'24.04" E	P	A	A	A	P	A	P	A	A	A
	500	F14	26°07'35.45" S	27°45'16.20" E	P	A	P	p	P	A	P	p	p	A
		F15	26°07'35.45" S	27°45'16.20" E	P	A	A	A	A	P	A	P	A	A
	1000	P14	26°07'30.59" S	27°45'09.50" E	P	A	P	P	A	A	A	A	A	A
		P15	26°07'30.59" S	27°45'09.50" E	P	A	P	p	P	A	P	p	p	A
	1500	L14	26°07'24.62" S	27°45'02.30" E	P	P	p	P	P	A	P	P	A	A
		L15	26°07'24.62" S	27°45'02.30" E	p	P	A	P	p	P	A	P	p	p

P=present minerals within the sample, A=absent mineral within the sample

Mine	Distance from Source	Sample Number	CO-Ordinates		Quartz	kaolnite	Calcite	dolomite	Muscovite/ Illite/ nimisite	Rutile/ Anatase	Pyrite	Gypsum	Hematite	Clinochlore/ Anorthosite
			Latitude	Longitude										
Crown mines	0	R 14	26°22'5.93" S	27°45'30.70" E	P	A	A	P	A	A	P	A	P	A
		R 15	26°22'5.93" S	27°45'30.70" E	P	A	A	P	A	A	P	P	A	A
	500	V14	26°22'8.07" S	27°27'31.17" E	P	A	A	P	P	A	A	A	A	A
		V15	26°22'8.07" S	27°27'31.17" E	P	A	A	A	A	A	P	P	A	A
	1000	D20	26°22'10.43" S	27°27'31.72" E	P	P	p	P	A	P	p	P	A	P
		D21	26°22'10.43" S	27°27'31.72" E	P	A	A	P	P	A	A	P	A	A
	1500	F20	26°22'12.97" S	27°27'32.2"E	P	A	A	A	P	A	A	A	P	P
		F21	26°22'12.97" S	27°27'32.2"E	P	A	A	P	A	A	P	P	A	A
Randfontein estates	0	P20	26°22'1.00" S	27°49'54.58" E	P	A	P	P	P	A	A	A	P	A
		P21	26°22'1.00" S	27°49'54.58" E	P	A	A	A	A	P	A	P	A	A
	500	L20	26°11'54.57" S	27°49'45.48" E	P	A	A	P	A	A	P	P	A	A
		L21	26°11'54.57" S	27°49'45.48" E	P	A	A	P	A	A	P	P	A	A
	1000	R 20	26°11'50.55" S	27°49'41.40" E	P	A	A	A	P	A	A	A	A	P
		R 21	26°11'50.55" S	27°49'41.40" E	P	P	P	P	A	A	A	A	A	A
	1500	V20	26°11'52.37" S	27°49'37.25" E	P	A	P	P	A	P	P	A	A	P
		V21	26°11'52.37" S	27°49'37.25" E	P	P	A	A	A	A	A	A	A	A

P=present minerals within the sample, A=absent mineral within the sample

4-8: GEOCHEMICAL ANALYSIS RESULTS

Table 4-10: Element determination results for *in-situ* analysis done at Durban deep mine using XRF

Element	LoD	O distance (m)		500 distance (m)		1000 distance (m)		1500 distance (m)	
		Co-ordinates		Co-ordinates		Co-ordinates		Co-ordinates	
		Latitude	Longitude	Latitude	Longitude	Latitude	Longitude	Latitude	Longitude
		26°10'28.74"S	27°51'35.39"E	26°10'24.69"S	27°51'34.30"E	26°10'22.90"S	27°51'32.19"E	26°10'30.02"S	27°51'30.07"E
Hg		30.6%		37.6%		39.6%		30.6%	
S_i		1.76%		1.76%		1.76%		1.76%	
Cu		<LoD		<LoD		<LoD		<LoD	
Fe		75.00%		75.00%		75.00%		75.00%	
W		7.5%		7.5%		7.5%		7.5%	
Al		39%		39%		39%		39%	
Sb		<LoD		<LoD		<LoD		<LoD	
Sn		4%		4%		4%		4%	
Cd		<LoD		<LoD		<LoD		<LoD	
Ag		<LoD		<LoD		<LoD		<LoD	
Pb		3%		3%		3%		3%	
Zn		24.83		24.83		24.83		24.83	
As		1.23%		1.23%		1.23%		1.23%	

%= Results above detection limit, <LoD=Less than limit of detection

Table 4-9: Element determination results for *in-situ* analysis done at Bentjies mine using XRF

Element	O distance (m)		500 distance (m)		1000 distance (m)		1500 distance (m)	
	Co-ordinates		Co-ordinates		Co-ordinates		Co-ordinates	
	Latitude	Longitude	Latitude	Longitude	Latitude	Longitude	Latitude	Longitude
	26°10'28.74"S	27°51'35.39"E	26°10'24.69"S	27°51'34.30"E	26°10'22.90"S	27°51'32.19"E	26°10'30.02"S	27°51'30.07"E
Hg	42.6%		52.6%		62.6%		47.6%	
S_i	1.90%		1.60%		1.00%		1.50%	
Cu	<LoD		<LoD		<LoD		<LoD	
Fe	55.55%		50.55%		45.55%		45.55%	
Al	33.12%		35.12%		33.15%		37.12%	
Sb	<LoD		<LoD		<LoD		<LoD	
Sn	3.10%		4.10%		3.70%		5.10%	
Cd	<LoD		<LoD		<LoD		<LoD	
Ag	<LoD		<LoD		<LoD		<LoD	
Pb	2.70%		2.90%		2.80%		2.50%	
Zn	19.11%		39.11%		29.11%		19.13%	
As	1.11%		1.15%		1.01%		1.61%	
Sr	1.23%		1.43%		1.26%		1.43%	

%= Results above detection limit, <LoD=Less than limit of detection

Table 4-10: Element determination results for *in-situ* analysis done at Princess mine using XRF

Element	O distance (m)		500 distance (m)		1000 distance (m)		1500 distance (m)	
	Co-ordinates		Co-ordinates		Co-ordinates		Co-ordinates	
	Latitude	Longitude	Latitude	Longitude	Latitude	Longitude	Latitude	Longitude
	26°10'28.74"S	27°51'35.39"E	26°10'24.69"S	27°51'34.30"E	26°10'22.90"S	27°51'32.19"E	26°10'30.02"S	27°51'30.07"E
Hg	50.0%		51.0%		50.10%		50.04%	
S_i	2.69%		2.70%		2.79%		2.89%	
Cu	<LoD		<LoD		<LoD		<LoD	
Fe	68.46%		68.00%		68.50%		67.46%	
W	32.73%		25.73%		30.03%		32.00%	
Al	11.83%		11.00%		11.85%		12.00%	
Sb	<LoD		<LoD		<LoD		<LoD	
Sn	6.69%		6.00%		5.69%		6.99%	
Cd	<LoD		<LoD		<LoD		<LoD	
Ag	<LoD		<LoD		<LoD		<LoD	
Pb	0.32%		0.30%		0.42%		0.12%	
Zn	14.75%		14.75%		17.70%		10.70%	
As	1.25%		1.35%		1.45%		1.00%	
Sr	1.32%		1.30%		1.35%		1.42%	

%= Results above detection limit, <LoD=Less than limit of detection

Table 4-13: Element determination results for *in-situ* analysis done at Crown mines using XRF

Element	O distance (m)		500 distance (m)		1000 distance (m)		1500 distance (m)	
	Co-ordinates		Co-ordinates		Co-ordinates		Co-ordinates	
	Latitude	Longitude	Latitude	Longitude	Latitude	Longitude	Latitude	Longitude
	26°10'28.74"S	27°51'35.39"E	26°10'24.69"S	27°51'34.30"E	26°10'22.90"S	27°51'32.19"E	26°10'30.02"S	27°51'30.07"E
Hg	49.2%		29.2%		19.2%		40.0%	
S_i	1.89%		3.89%		1.80%		2.89%	
Cu	<LoD		<LoD		<LoD		<LoD	
Fe	75.23%		75.23%		65.23%		75.23%	
W	22.73%		22.73%		22.73%		22.73%	
Al	21.83		20.03		21.00		20.00	
Sb	<LoD		<LoD		<LoD		<LoD	
Sn	11.86%		13.06%		13.86%		11.86%	
Cd	<LoD		<LoD		<LoD		<LoD	
Pb	1.00%		1.20%		1.20%		1.00%	
Zn	4.75%		2.05%		2.75%		1.75%	
As	1.25%		2.25%		1.25%		1.05%	
Sr	1.35%		1.75%		1.35%		1.35%	

%= Results above detection limit, <LoD=Less than limit of detection

Table 4-14: Element determination results for *in-situ* analysis done at East chamo D'Or mine using XRF

Element	O distance (m)		500 distance (m)		1000 distance (m)		1500 distance (m)	
	Co-ordinates		Co-ordinates		Co-ordinates		Co-ordinates	
	Latitude	Longitude	Latitude	Longitude	Latitude	Longitude	Latitude	Longitude
	26°10'28.74"S	27°51'35.39"E	26°10'24.69"S	27°51'34.30"E	26°10'22.90"S	27°51'32.19"E	26°10'30.02"S	27°51'30.07"E
Hg	46.2%		36.2%		23.2%		16.2%	
S_i	2.07%		2.17%		2.07%		2.07%	
W	34.73%		44.73%		34.73%		38.73%	
Al	31.83%		37.83%		36.83%		51.83%	
Sb	<LoD		26.3%		345ppm		<LoD	
Sn	13.80%		33.80%		13.80%		16.80%	
Cd	<LoD		123ppm		123ppm		423ppm	
Ag	<LoD		352ppm		624ppm		456ppm	
Pb	1.30%		1.30%		1.60%		3.30%	
Zn	17.75%		15.75%		14.75%		16.75%	
As	1.35%		2.35%		3.35%		2.35%	
Sr	1.72%		1.62%		1.32%		2.72%	

%= Results above detection limit, <LoD=Less than limit of detection

Table 4-15: Element determination results for *in-situ* analysis done at Randfontein estates mine using XRF

Element	O distance (m)		500 distance (m)		1000 distance (m)		1500 distance (m)	
	Co-ordinates		Co-ordinates		Co-ordinates		Co-ordinates	
	Latitude	Longitude	Latitude	Longitude	Latitude	Longitude	Latitude	Longitude
	26°10'28.74"S	27°51'35.39"E	26°10'24.69"S	27°51'34.30"E	26°10'22.90"S	27°51'32.19"E	26°10'30.02"S	27°51'30.07"E
Hg	53.7%		40.0%		46.2%		29.2%	
S_i	2.30%		2.89%		2.07%		3.89%	
Cu	<LoD		<LoD		<LoD		<LoD	
Fe	55.23%		75.23%		65.23%		75.23%	
W	30.73%		22.73%		34.73%		22.73%	
Al	34.83%		20.00		31.83%		20.03	
Sb	<LoD		<LoD		<LoD		<LoD	
Sn	10.80%		11.86%		13.80%		13.06%	
Cd	<LoD		<LoD		<LoD		<LoD	
Ag	<LoD		<LoD		<LoD		<LoD	
Pb	2.03%		1.00%		1.30%		1.20%	
Zn	20.75%		1.75%		17.75%		2.05%	
As	1.37%		1.05%		1.35%		2.25%	

%= Results above detection limit, <LoD=Less than limit of detection

CHAPTER FIVE

5. INTERPRETATION AND DISCUSSION

5.1. INTRODUCTION

This is the first study looking at characterization of respirable crystalline silica dust in the abandoned mines around Roodepoort in South Africa. This study adopted the American limit of 3µg/m^3 (OEHHA, 2005). The hypothesis of the current study is "*Environmental exposure concentration to respirable crystalline silica around abandoned mines in Roodepoort is greater than a concentration of 3µg/m^3*". The concentration of respirable crystalline silica was determined in the dust and reported using tables, charts and graphs presentations. The correlation analysis was employed to investigate the relationship between meteorological parameters and crystalline silica exposure at each of the monitoring sites.

5.2. CRYSTALLINE SILICA CONCENTRATION

The crystalline silica concentration was generally low in autumn and summer, high concentration in spring and winter. The concentration of crystalline silica in summer for sample number V19 (Randfontein estates); DR 22 &DR 23 (Crown mines); L19, L22, L23, L24 (East Champ D' Or) and P19 (Princess Mine) was higher than the health exposure limit. P19 was positioned at the source so it accumulated more dust than the samples that were positioned away from the source at this study area. In autumn, the concentrations were low except high concentration levels that were observed in sample D4 (Durban deep Mine); F4 (Bentjies Mine dump); DR1 & DR5 (Crown mines); L1, L4 & L6 (East Champ D' Or) and P1 & P5 (Princess Mine).

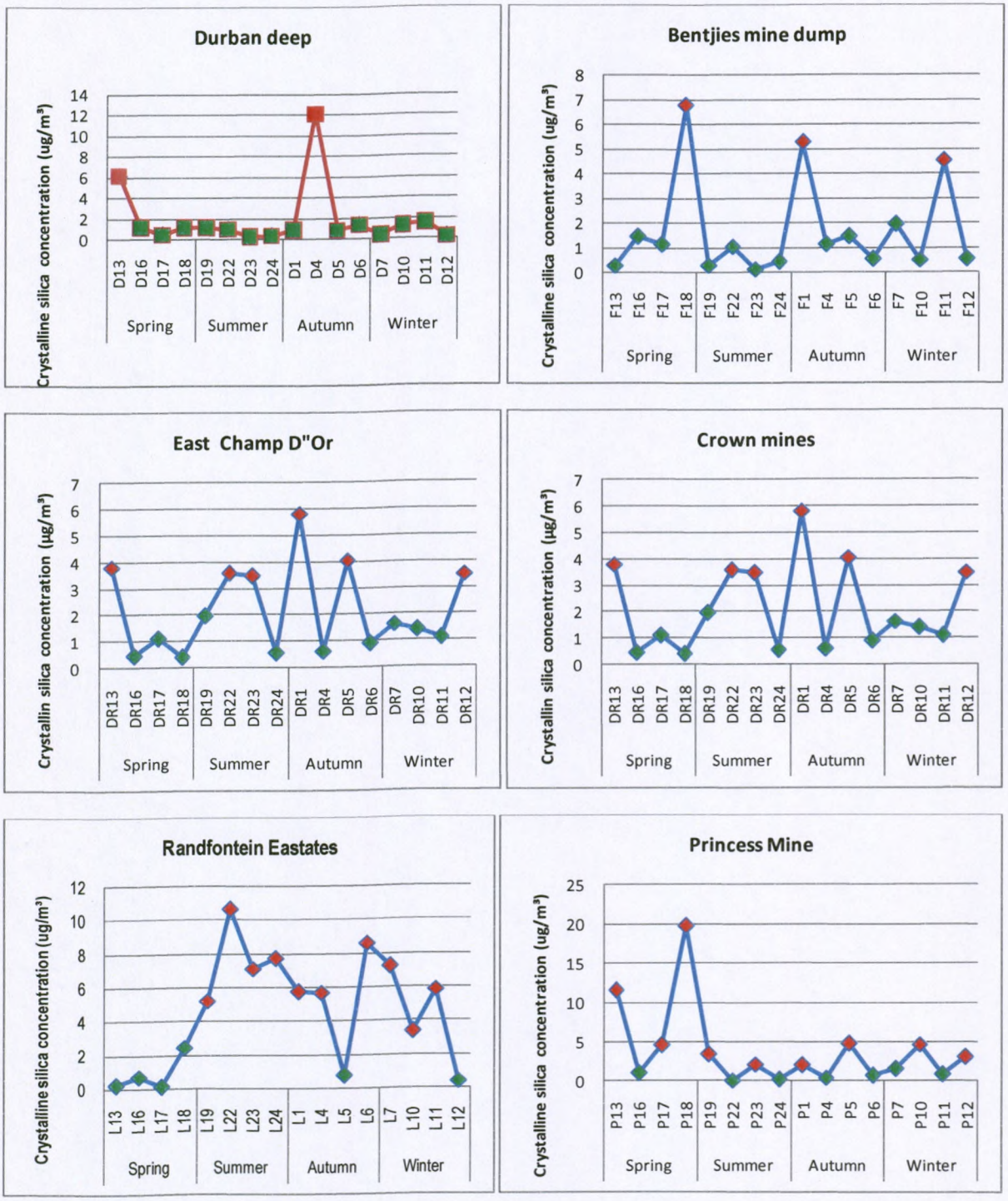

Figure 5-1: Seasonal crystalline silica concentration. Red colour indicates the samples that have crystalline silica concentration of above environmental health limit of 3µg/m³. The green colour represents the samples that have crystalline silica exposure concentration of below environmental health limit of 3µg/m³.

Winter experienced a high concentration of respirable crystalline silica in sample F11 (Bentjies Mine dump); DR 12 (Crown mines); L7, L10 &L11 (Randfontein estates) and P10 & P12 (Princess Mine) was recorded. About 90% of crystalline silica dust is from abandoned mines (EPA, 1996a). In winter, there is huge amount of dry eroded materials that may be preventing the dust to emit in to the atmosphere and increase the crystalline silica concentration (Petrucci, 2007). High concentration was also recorded in spring. it was confirmed that a high wind speed and high dust emission in Witwatersrand happens in spring (H. J. Annegarn and S. J. Sithole, 2002) and (K.Naddafi., 2006). The abandoned mines are associated with waste dumping and resulted to dirty rotten materials such as papers, boxes, leaves, tins and etc; all these may result in high dust emission during high wind speed. High wind speed resulted from dust erosion, slope imbalances and seasonal conditions (Bowen G.G. Dussek C. Hamilton R.M. Mather J, 1998). Erosion of dust contains sand led to infiltration of the heavy minerals between the pebbles and resulting in the quartz pebble reef (Smith, 1997).

Respirable crystalline silica concentration was also computed for location of the study area and seasons. Pearson correlation coefficient for linear relationship between the dependent variable and predicator variables was established **table 5-1**.

Table 5-1: Average summary of silica concentration by location and season

Location of mines	**Mean(µg/m3)**	**(SD)**
Crown mines	2.4	±2.3
Durban Deep	1.9	±3.1
Bentjies mine dump	1.7	±2.0
East Champ D Or	6.6	±8.0
Princess	3.8	±5.1
Randfontein setates	1.3	±1.3
Season		
Autumn	2.8	±3.1
Spring	3.1	±2.2
Summer	2.2	±2.6
Winter	3.8	±7.0
SD: Standard deviation		

Table 5-1 shows summary of respirable crystalline silica concentration according to location of mines and season. The highest average concentration of respirable crystalline silica was almost 7 µg/m^3 with standard deviation of ±8.0 has been found in East Champ D' Or, followed by nearly 4 µg/m3 carried standard deviation of ±5.1 in Princess, and the lowest respirable crystalline silica concentration was observed in Randfontein Eastates. Much of the respirable crystalline silica concentration was obtained during spring and winter season in all study areas. The average concentration during winter was about 4 µg/m3 while in spring was 3.1 µg/m^3. During summer, average respirable crystalline silica concentration was low 2.2 µg/m^3 and standard deviation of ±2.6.

To assess association between variables and respirable crystalline silica concentration, linear regression modelling was conducted for unadjusted analysis. This model was based on the calculation of mean, minimum and maximum and standard deviation values of each variable. Five variables were assessed (study locations, seasons, humidity, wind speed and distance). The outcome variable respirable crystalline silica concentration was log transformed before the analysis **table 5-2.**

Table 5-2: Relationship between study characteristics and silica concentration

Study characteristics	**Coefficients**	**P values**
Location of mines	0.0522	0.6134
Season	0.0554	0.5920
Humidity	-0.0938	0.3631
Wind Speed	0.0704	0.4954
Distance	-0.1073	0.2983

Table 5-2 indicates measure of the strength of the linear relationship between the explanatory factors and the outcome variables. All the variables showed non-significantly weak correlation with silica concentration. The location of mines, season and wind speed showed a positive correlation, that is to say the concentration of silica increases as location was moved towards Valkfontein, as season is approaching winter and as the wind speed increases. The silica concentration decreased as humidity and distance increases (negative correlation) **table 5-3.**

Table 5-3: Association between study variables and silica concentration

Variables	**Coefficients**	**P values**	**95% Confidence Intervals**	
Season		0.853*		
Autumn	Ref (0)	-	-	-
Spring	-0.059		-0.795	0.677
Summer	-0.316		-1.052	0.420
Winter	0.013		-0.723	0.750
Location of mines		0.712*		
Crown mines	Ref (0)	-	-	-
Durban Deep	-0.381		-1.236	0.472
Bentjies mine dump	-0.178		-1.134	0.777
East Champ D' Or	0.728		-0.156	1.614
Princess	0.029		-0.833	0.893
Randfontein Eastates	-0.818		-1.672	0.035
Distance	-0.0005	0.050	-0.00091	-3.06^{-7}
Wind Speed	0.140	0.069	-0.011	0.293
Humidity	-0.002	0.834	-0.021	0.017
*Overall p value				

In table 5-3, the unadjusted analysis for the association between study factors and silica concentrated is shown in table 1. The overall p value for season showed statistically non-significant association with log transformed average silica concentration (p=0.853). The summer season showed 6% decrease in silica average concentration compared to autumn but not with statistically significant differences, similar result was observed with spring season. The winter season had a 1.3% increase in average concentration compared to autumn. The location of the mine also showed non-significant association with silica concentration. Moving from

Crown mines to Durban Deep, Bentjies mine dump and Randfontein Eastates, there was decrease in average concentration of silica with statistically non-significant differences, while East Champ D' Or and Princess showed an increase in average silica concentration than Crown mines. For a 1 metre increase in distance, the average concentration of silica decreased by 0.05% with marginally significant differences (Coefficient: -0.0005; 95% CI: -0.00091 -3.06-7; P= 0.050). As the wind speed increased by every 1 m/s2, the mean of concentration silica increased by 14% while every 1% increase in humidity showed a 0.2% decrease in average silica concentration.

5.3. IMPACTS ON THE ENVIRONMENT

Dust is the particulate matter, according to (Zhang, 2013a) particulate matter affects our environment in terms of air quality, visibility, direct and indirect radiative forcing, climate effects and ecosystem. Particulate matter plays an important role in formation of acid rain (Zunckei, 2008). The potential of particulate matter to absorb and scatter solar radiation and serving as a cloud condensation nuclei affects the global climate and hydrological cycle (Zhang, 2013b). Deposition of particulate matter may also block stomata thus decreasing the rate of transpiration and reduce the amount of light reaching the chloroplasts, thereby decreasing the rate of photosynthesis (Perrino, 2011), and affect plant growth, heavy metals present in particulate matter exert their toxic effect on plants (Matooane, 2008). Particulate matter damages materials through soiling of painted surfaces, fabrics, electronics, and works of art and corrosion of metals and other building materials by acid aerosols and salts (Eiseman, 1998).

5.3. MINERALOGY AND GEOCHEMISTRY

Durban deep is characterised by quartz, pyrite, Hematite and gypsum whereas, Bentjies mine dump composed of quartz, and Hematite. Princess has the sediments of quartz, cristoballite, tridymite, pyrite and gypsum. Clinochlore, gypsum quartz, cristoballite, tridymite and clay minerals has been determined in crown mines. East Champ D' Or has a massive of clay minerals, gypsum quartz, cristoballite, tridymite and hematite. Furthermore Randfontein estates is characterised by Clinochlore, quartz, cristoballite, tridymite and pyrite.

The presence of these minerals in the samples collected from the study areas confirms that the Witwatersrand is overlain by felsic igneous rocks such as rhyolites, trachytes, obsidian and andesite which were formed at temperature of above 1470°c and also exposed to the sedimentation of alluvial fan. The availability of quartz-pebble reef facies in the abandoned mines tells us that these abandoned mines are of gold because gold is concentrated in the upper (top) portion of the reef (DA, 1975).

CHAPTER SIX

6. CONCLUSIONS AND RECOMMENDATIONS

Public concerns regarding dust emitted from abandoned mines around Roodepoort necessitate a need to characterize its non-occupational or ambient crystalline silica exposure, mainly to communities residing nearby these mines. The ambient respirable crystalline silica concentration in the study areas is lower than the American health limit of 3µg/m³ in some study areas and above in other study areas. The study confirmed that there is respirable crystalline silica at a distance of 1.500m from the source which is within the residential areas of some study areas like Bentjies mine dump, Princess and Durban Deep. The close proximity of communities to the mines may pose potential health risk effects to the residents.

In 1996 EPA also confirm low levels of ambient respirable crystalline silica of 0.8 to 5.0 µg/m^{3}, whereas current study determines 0.2 to 7.0 µg/m^{3}. High concentration of respirable crystalline silica was determined in spring and winter. The relationship between distance and respirable crystalline silica is inversely proportional, as the concentration decreases as the distance increases.

Alpha Quartz was determined in the samples collected from the study areas.. Furthermore, clay minerals, carbonates, sulphides oxides minerals, trace elements and heavy metals were identified in the samples collected from the study areas. These findings confirm that the study areas are exposed to different forms of toxic materials.

CHAPTER SEVEN

7. REFERENCES

101, M. 2005. Method for determination hazadous substances.

7500, N. M. 1989. Measurement of Respirable Crystalline Silica Using X-ray Powder Diffraction.

ABELL M. T., D. D. D., PALASSIS J 1984. NIOSH Method 7500. *Measurement of Respirable Crystalline Silica Using X-ray Powder Diffraction. Manual of Analytical Methods,* 84- 100.

AFFAIRS, D. O. E. 2009. State of Air Report 2005. A report on the state of air in South Africa. *Department of Environmental Affairs,* Pretoria.

BEACH, A., SMITH, R., 2007. Structural geometry and development of the Witwatersrand Basin, South Africa. In: Ries, A.C., Butler, R.W.H., Graham, R.H. (Eds.), Deformation

of the Continental Crust:. *The Legacy of Mike Coward: Geological Society, London, Special Publications,* 272**,** 533-542.

BOHR, N. 2003. Physicist and Humanitarian. *Enslow Publishers.*

BOWEN G.G. DUSSEK C. HAMILTON R.M. MATHER J, B. D., DUMPLETON S, FERMOR M, EDITORS. 1998. Pollution resulting from abandonment and subsequent flooding of Wheal Jane Mine in Cornwall, UK. In. *London Geological Society,* vol. 28. **,** 93-9.

BRANDL, G. & DE WIT, M. 1997. The Kaapvaal Craton, South Africa. *Oxford Monographs on Geology and Geophysics,* 35**,** 581-607.

CASTRANOVA V, V. V., RAMSEY D.M., MCLAURIN J.L., PACK D., LEONARD S., BARGER M.W., DALAL N.S., TEASS A. 1997. Augmentation of pulmonary reactions to quartz inhalation by trace amounts of iron-containing particles. *Environmental health perspectives,* 105 1319-1324.

DA, P. 1975. The depositional environment of the WWR goldfields: a chronological review of speculation and observations. *Minerals Science and Engineering,* 7:18-47.

DA, P. 1982. The source of Witwatersrand gold: conjecture of the unknown In Forster RP (Editor). Gold '82: The Geology, Geochemistry and Genesis of Gold Deposits *Geological Society of Zimbabwe, Balkema, Rotterdam, Netherlands. ,* Special Publication 1**,** p. 219.

EISEMAN, E. 1998. Monitoring for fine particulate matter. *Rand critical technologies institute,* Washington, DC.

EPA, U. 1996a. Ambient levels and noncancer health effects of inhaled crystalline and amorphous silica: health issue assessment. *US Environmental Protection Agency, Office of Research and Development.*

EPA, U. S. 1996b. "Ambient Levels and non-cancer health effects of inhaled crystalline and amorphous silica.". *U.S. Environmental Protection Agency, Office of Research and Development, National Center For Environmental Assessment, Research Triangle Park Office, Research Triangle Park,* NC, EPA/600/R-95.

FREEMAN, C. & GROSSMAN, E. 1995. Silica exposures in the United States between 1980 and 1992. *Scandinavian journal of work, environment and health,* 21**,** 47-49.

FRIMMEL, H. E., MINTER, W.E.L., 2002. Recent developments concerning the geological history of the Witwatersrand gold deposits, South Africa. In: Goldfarb, R., Nielsen, R.L. (Eds.), Global Exploration 2002 - Integrated Methods for Discovery. . *Society of Economic Geologists, Littleton,* 9**,** 17-45.

FUBINI, B. 1998). Surface chemistry and quartz hazard. *Annals of occupational hygiene,* 42**,** 521-530.

GILES, P. & CEE, R. 1987. "OSHA Laboratory Quartz Detection Limit Study.". *Occupational Safety and Health Administration, Salt Lake City Analytical Laboratory.*

H. J. ANNEGARN AND S. J. SITHOLE, , FEBRUARY. 2002. "Dust monitoring and mitigation on gold tailings reclamation," *in Proceedings of the Mine Ventilation Society Symposium*, pp. 1–13.

H. Z. MASSOUD, J. D. P., AND E. A. IRENE. 1985. Thermal oxidation of silicon in dry oxygen: Growth - rate enhancement in the thin regime II. Physical mechanisms. *Journal of The Electrochemical Society,*, 132(11):2693-2700.

HARDY, T. S. E. A. 1995. "Crystalline Silica: Risks and Policy. *Environmental Health Perspectives,* 103,152.

HNIZDO, E. & CREMER, G. 1991. Silica exposure, silicosis, and lung cancer: a mortality study of South African gold miners. *British journal of industrial medicine,* 48, 53-60.

HNIZDO, E. & CREMER, G. 1993. Risk of silicosis in a cohort of white South African gold miners. *American journal of industrial medicine,* 24, 447-457.

HNIZDO, E. & MURRAY, J. 1998. Risk of pulmonary tuberculosis relative to silicosis and exposure to silica dust in South African gold miners. *Occupational and environmental medicine,* 55, 496-502.

IARC 1987a. Silica and Some Silicates. *IARC Monographs on the Evaluation of the Carcinogenic Risk of Chemicals to Humans,,* 42, 1-144.

IARC 1987b. Silica and some silicates. *Lyon, France, International Agency for Research on Cancer,* Vol. 42, pp. 33-143.

IARC , V., . (TOXICOLOGY) 1987. "Silica and Some Silicates" *IARC Monographs on the Evaluation of the Carcinogenic Risk of Chemicals to Humans,,* 42, 1-144.

ITT 1983. Preliminary Evaluation of Direct Free Silica Analysis on PVC Membranes by X-ray Diffraction. *Illinois Institute of Technology Research Institute,* Final Report, Task 8 Phase 2, Prepared for NIOSH, , 210-81-7108.

K.NADDAFI., R. N., Z. SOLTANIANZADEH., AND M.H.EHRAMPOOSH 2006. "Evaluation of dust-fall in arid air of Yazd," *Journal of Environmental Health Science Engineering,* vol. 3, pp. 161- 168.

KAMPA, M. A. C., E. 2008. Human health effects of air pollution. *environmental pollution,* 151, 362-367.

KOSITCIN, N., KRAPEŽ, B., 2004. Relationship between detrital zircon age-spectra and the tectonic evolution of the Late Archaean Witwatersrand Basin, South Africa. Precambrian

Research 129, 141-168.

LITTLE 1976. Evaluation of the NIOSH X-ray Diffraction Method for the Determination of Free Silica in Respirable Dust. *A. D. Little*.

MATOOANE, M. A. D., R. 2008. hy we need to manage air quality, department of environmental affairs, environmental quality and protection, chief directorate: . *wair quality management and climate change,* Publication series A, Book 4.

MCKEE C., R. J. 1990. Quantitative Analysis of Quartz in Perlite by X-ray Diffraction. *Society of Mining Engineering Meeting, Salt Lake City, New Mexico Bureau of Mines and Natural Resources, Socorro, NM 87801*.

MINTER, W. E. L. 1982. The Golden Proterozoic. (Chapter 4) In: Tankard, A.J., Jackson, M.P.A., Eriksson, K.A., Hobday, D.H., Hunter, D.R., Minter, W.E.L. (Eds.), Crustal Evolution of Southern Africa: 3.8 Billion Years of Earth History. *Springer-Verlag, New*

York, Heidelberg and Berlin, 115-150.

MMSD 2002. Research on Mine Closure Policy, including a section on Economic and Financial Considerations, prepared by the Mining, Minerals and Sustainable Development. January,.

MUHLE H., T. S., MOHR U., DASENBROCK C., MERMELSTEIN R., 1989. Lung tumor induction upon long term low level inhalation of crystalline silica. *American journal of industrial medicine,* 15(3), 343-346.

NEVADA 2003. Mining Bonding Task Force Report. Hosted on the Mining Life-Cycle Center website.

PERRINO, C. T., S. CATRAMBONE, M. TORRE, S.D. RANTICA, E. CANEPARI, S. 2011. chemical characterixation of atmospheric PM in Delhi, India, during different periods of the year including Diwali festival. . *Atmospheric pollution researc,* 2, 418-427.

PETRUCCI, R. H., WILLIAM S., HARWOOD., GEOFFERY F., HERRING., AND J.D. MADURA 2007. General Chemistry. *New Jersey: Pearsin Prentice Hall,* 9th ed.

SCHMITZ, M. D., BOWRING, S.A., DE WIT, M.J., GARTZ, V., 2004. Subduction and terrane collision stabilize the western Kaapvaal craton tectosphere 2.9 billion years ago. *Earth and Planetary Science Letters* 222**,** 363-376.

SETA J.A, S. D. A., PEDERSEN D.H 1988. National occupational exposure survey field guidelines. . *Cincinnati, OH, US Department of Health and Human Services, Public Health Service, Centers for Disease Control, National Institute for Occupational Safety and Health, Division of Surveillance, Hazard Evaluations, and Field Studies (DHHS (NIOSH)* 1**,** 88-106.

SMITH, D. K. 1997. Evaluation of the detectability and quantification of respirable crystalline silica by X-ray powder diffraction methods. *Powder Diffraction,* 12**,** 200-227.

ZHANG, R. J., J. TAO, J. HSU, S.C. WANG, G. ZAO, J. LEE C.S.L. ZHU, L. CHEN, Z. ZHAO, Y. SHEN, Z. 2013a. chemical characterization and source apportionment of PM2.5 in Beijing. *seasonal perspective, atmospheric chemistry,* 13.

ZHANG, R. J., J. TAO, J. HSU, S.C. WANG, G. ZAO, J. LEE C.S.L. ZHU, L. CHEN, Z. ZHAO, Y. SHEN, Z. () C: 2013b. hemical characterization and source apportionment of PM2.5 in Beijing. seasonal perspective, atmospheric chemistry, 13.

ZUNCKEI, M. D., R. AND MOGESH, N. 2008. Types and sources of air pollutants, Department of Environmental Affairs and Tourism, environmental quality and protection, chief directorate: . air quality management and climate change publication series A, Book 6.

CHAPTER EIGHT

8. APENDIX

1: Sample filter preparation sheet

NATIONAL HEALTH LABORATORY SERVICE
NATIONAL INSTITUTE FOR OCCUPATIONAL HEALTH

25 Hospital Street • PO Box 4788 Johannesburg 2000 South Africa • Tel: +27 11 712 6400 • Fax: +27 11 720 6405

SAMPLE FILTER PREPARATION SHEET

Filter batch number:				Date opened:			
ACCLIMITISATION CONDITIONS							
Date		Temp (0°)			Humidity (%Rh)		
	Before		After		Before		After
WEIGHING CONDITIONS							
Date		Temp(0°)			humidity(%rh)		
Control blank	1	2	3	Average(av)	Correction (?) value		comment
Calibration? Weights							
1000 µg		2000 µg	5000 µg			10 000µg	
Before	After	Before	After	Before	After	Before	After
Sample number	1	2	3	Average(av)	comments		
1							
2							
3							
4							
5							
6							
7							
8							
9							
10							

WORKING COPY

CONTROLLED DOCUMENT

NIOH OCC 0026

05/08/2011

2: Pumps calibration sheets

NIOH

Occupational Hygiene Department

SAMPLING PUMP CALIBRATION SHEET

Month: Calibration Done by: Survey no:

PRE CALIBRATION DATE	PUMP NO	TARGET FLOW RATE	UNIT	1	2	3	PRE CALIBRATION (AVE)	UNIT	POST CALIBRATION DATE	POST CALIBRATION	UNIT	DONE BY	COMMENTS
			l/m					l/m			l/m		
			l/m					l/m			l/m		
			l/m					l/m			l/m		
			l/m					l/m			l/m		
			l/m					l/m			l/m		
			l/m					l/m			l/m		
			l/m					l/m			l/m		
			l/m					l/m			l/m		
			l/m					l/m			l/m		
			l/m					l/m			l/m		
			l/m					l/m			l/m		
			l/m					l/m			l/m		
			l/m					l/m			l/m		
			l/m					l/m			l/m		
			l/m					l/m			l/m		

CONTROLLED DOCUMENT

WORKING COPY

3: Environmental condition work sheet

NIOH

Occupational Hygiene Department

ENVIRONMENTAL SAMPLING WORKSHEET

Sample Location: _____ Date: _____

Pump No:		Calibrated Before:		Calibrated After:	
Calibrated by:					
Start Time:		End Time:		Duration of Sample:	

Environmental Conditions: Good: ☐ Fair ☐ Poor ☐

Time	Wind Speed	Direction	Temp. °C	Comments

Comments	Drawing/Illustration

Sample Taken By: _____ Signature: _____

4: Sampling work sheet

NATIONAL HEALTH LABORATORY SERVICE
NATIONAL INSTITUTE FOR OCCUPATIONAL HEALTH

Occupational Hygiene Department
SAMPLING WORKSHEET

Plant: _____ Location: _____ Type of sampling: _____ Date: _____

Description of place:

_____

Pump no	Sample No/name	Workers Name	Worker Process	Starting Time	End Time	Sampling Time (min)	Notes

NIOH

CONTROLLED DOCUMENT

WORKING COPY

APPENDIX 5: MINERAL CHARACTERISATION

A full scan of sample D2

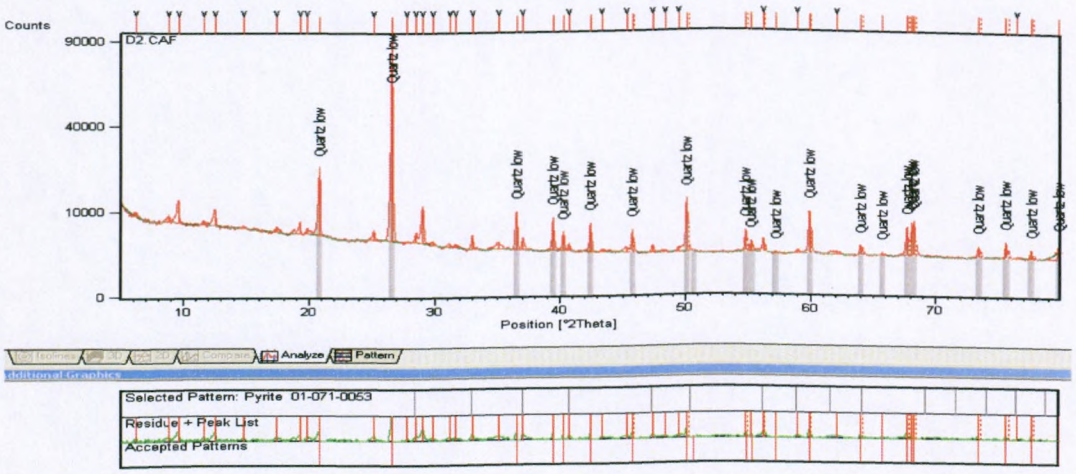

A full scan of sample D8

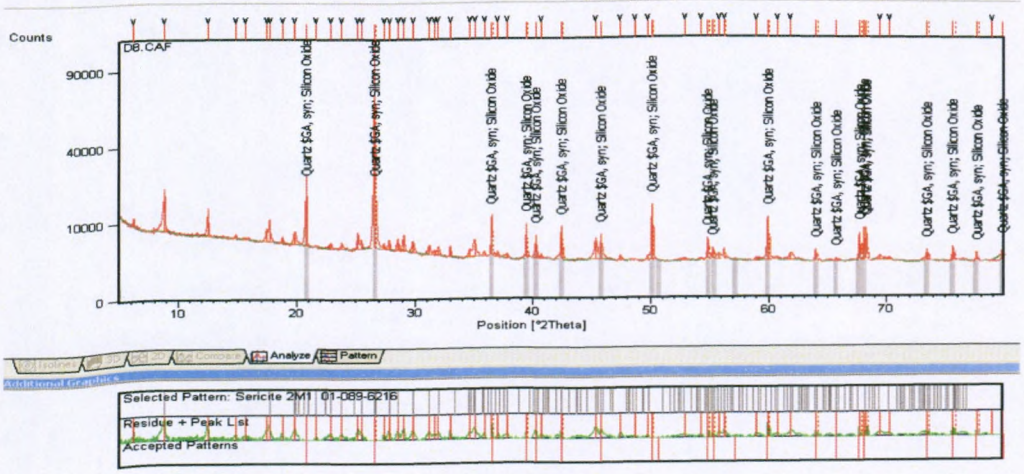

A full scan of sample D9

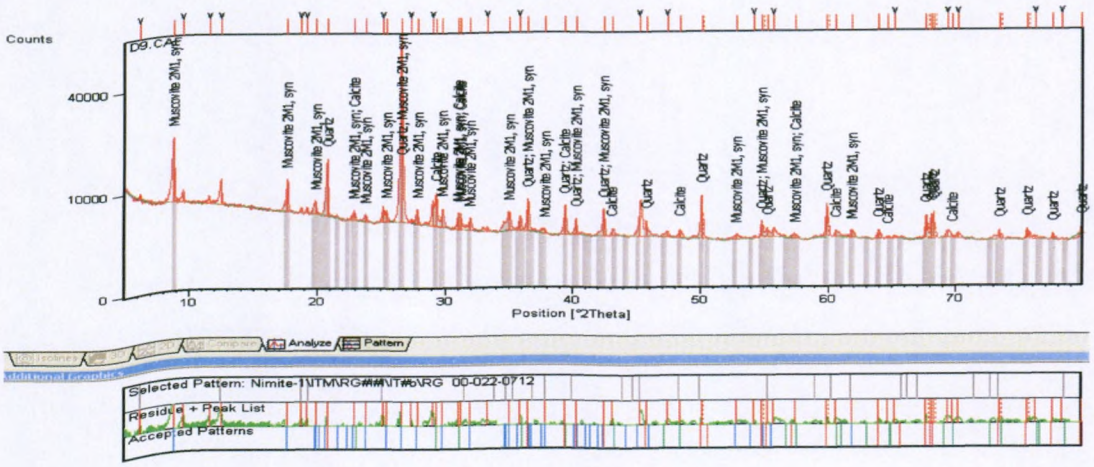

A full scan of sample D14

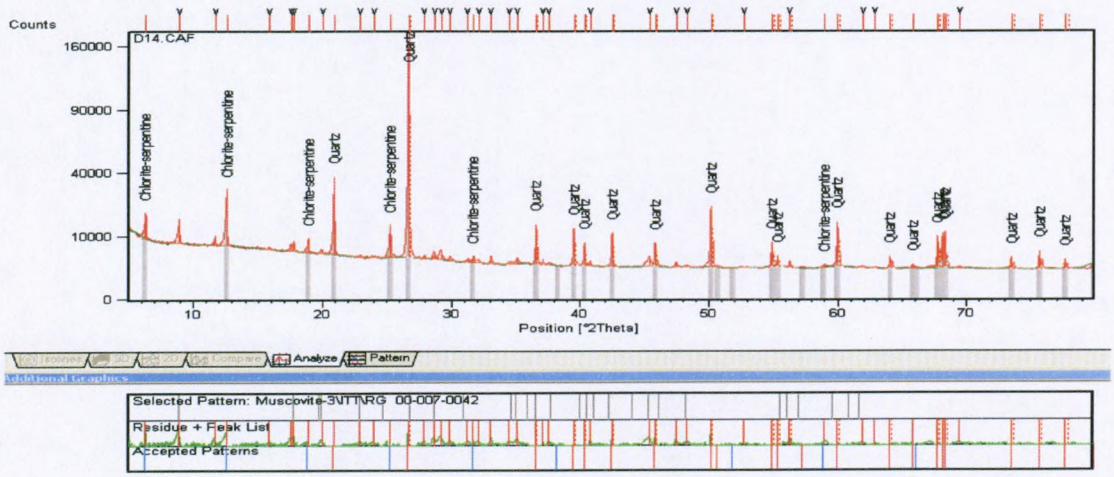

A full scan of sample D15

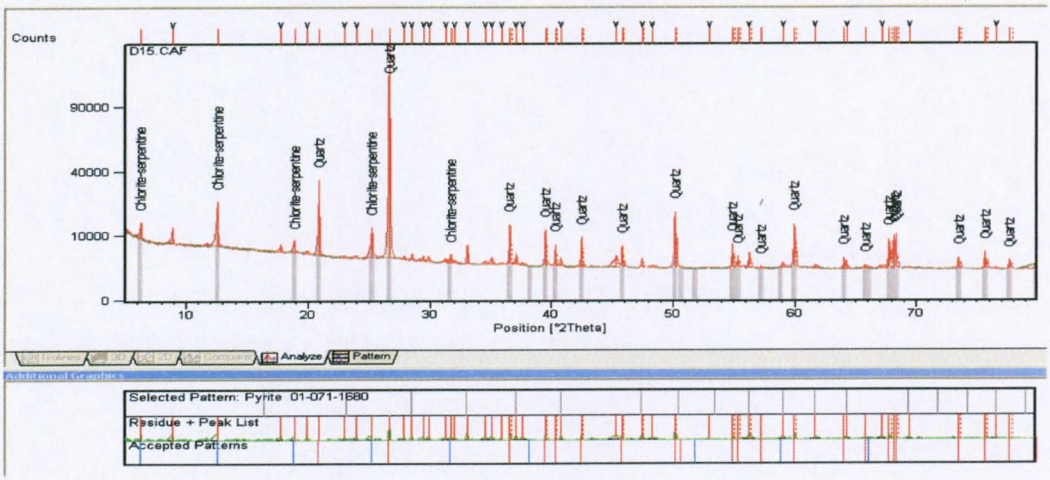

A full scan of sample F3

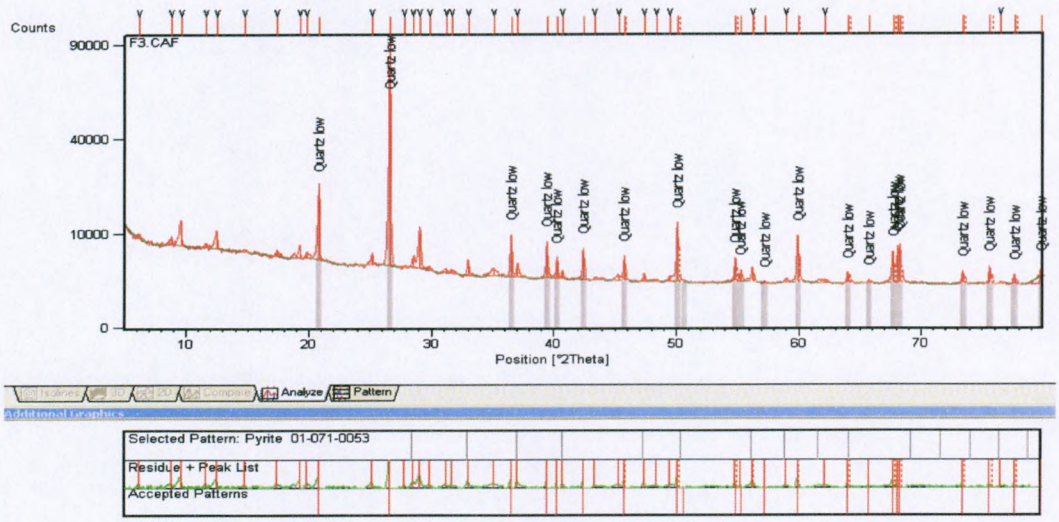

A full scan of sample F2

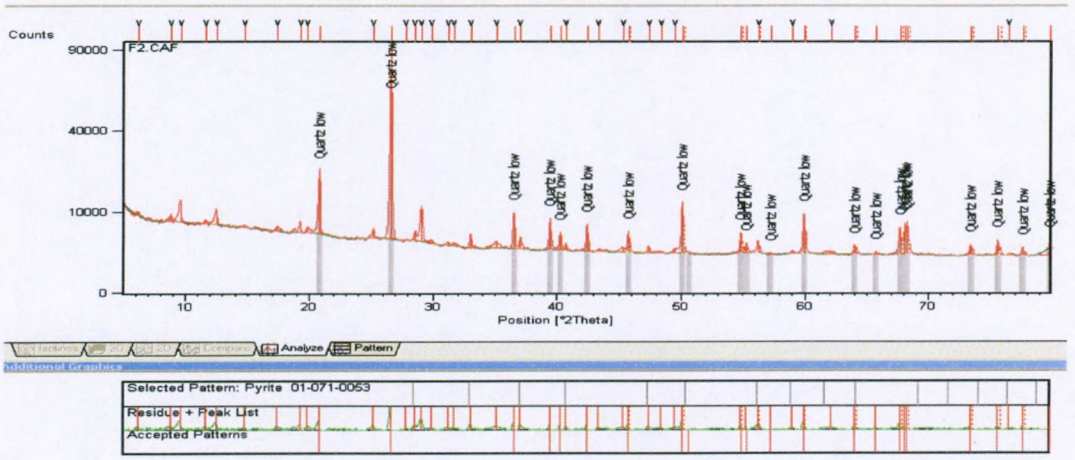

A full scan of sample F8

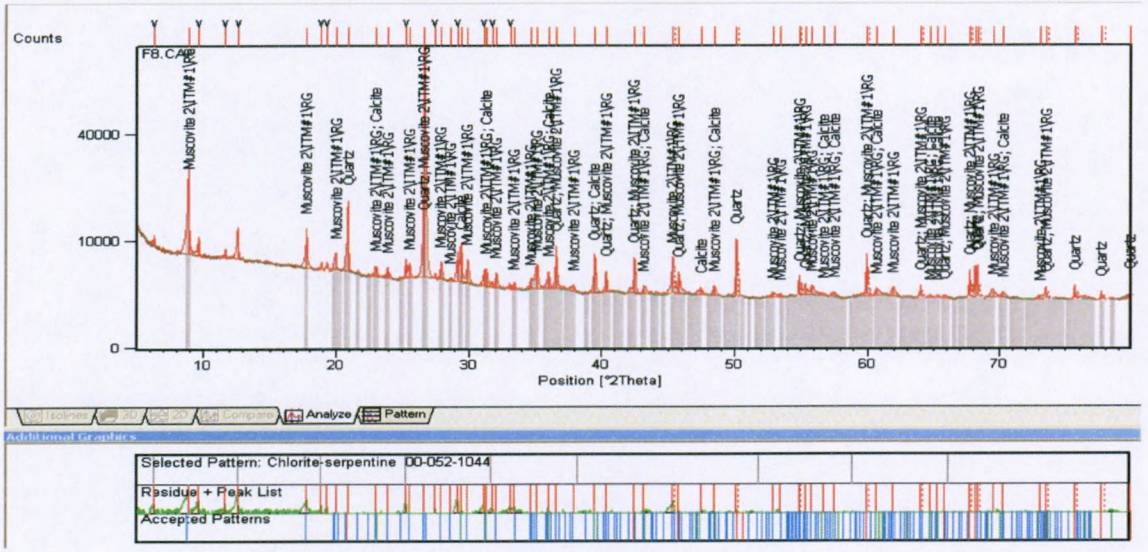

A full scan of sample F9

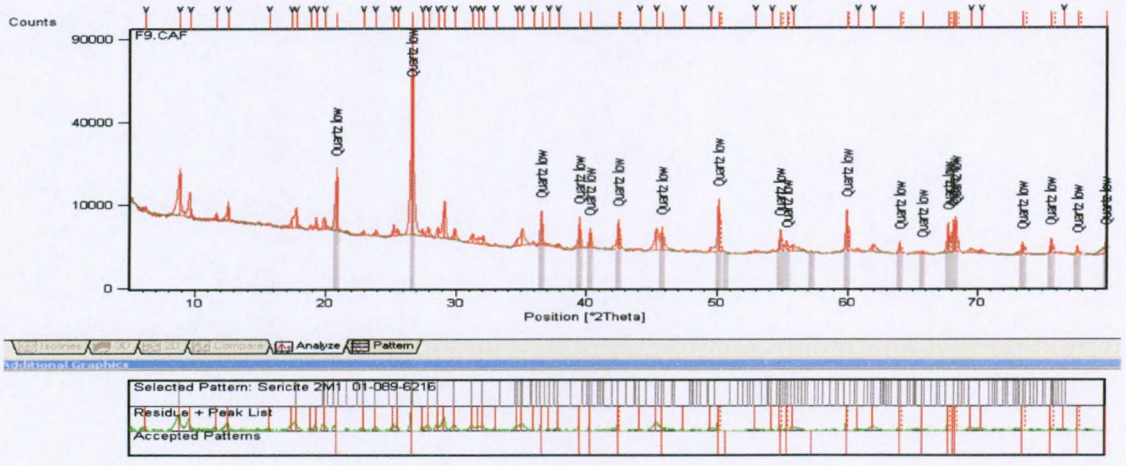

A full scan of sample F14

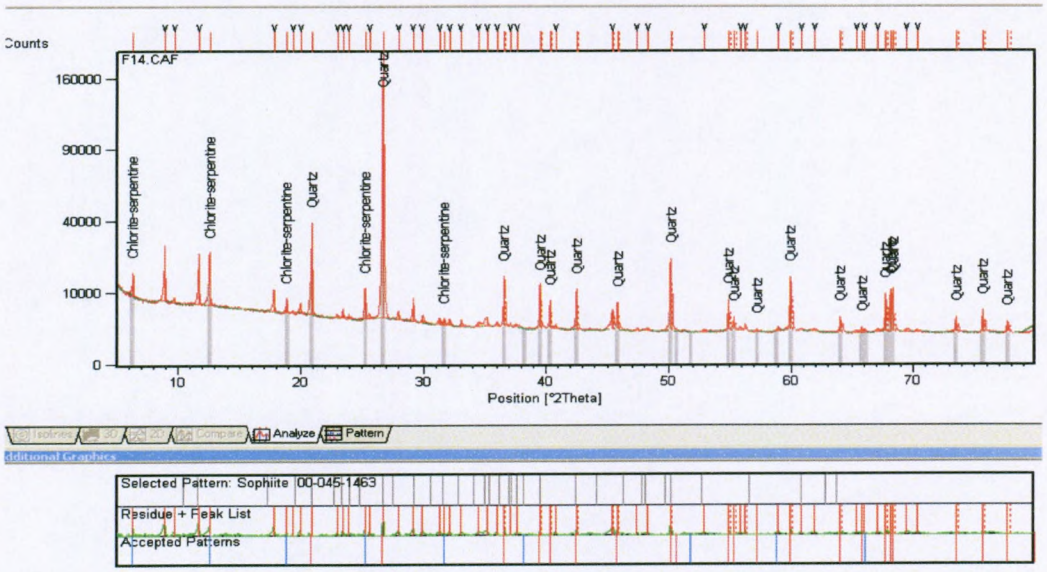

A full scan of sample F15

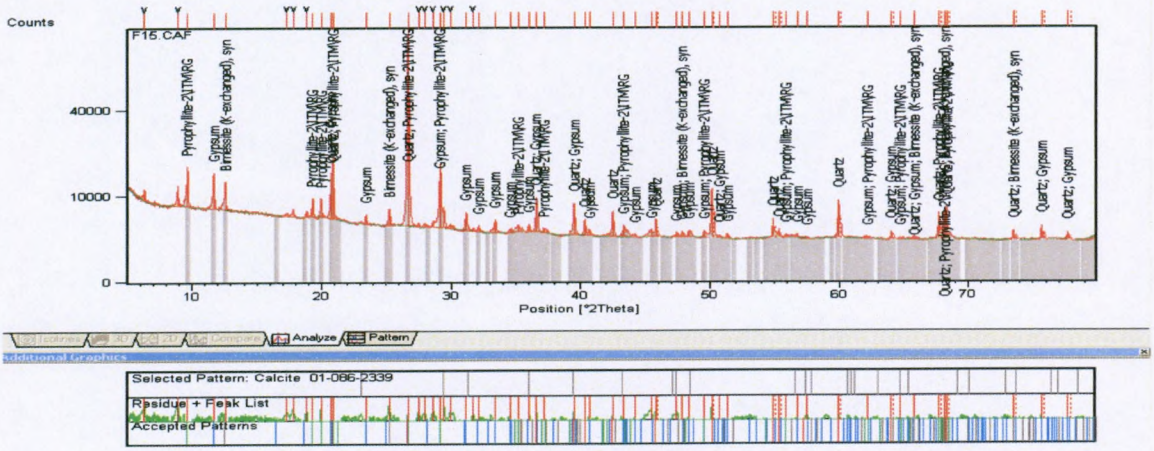

A full scan of sample L2

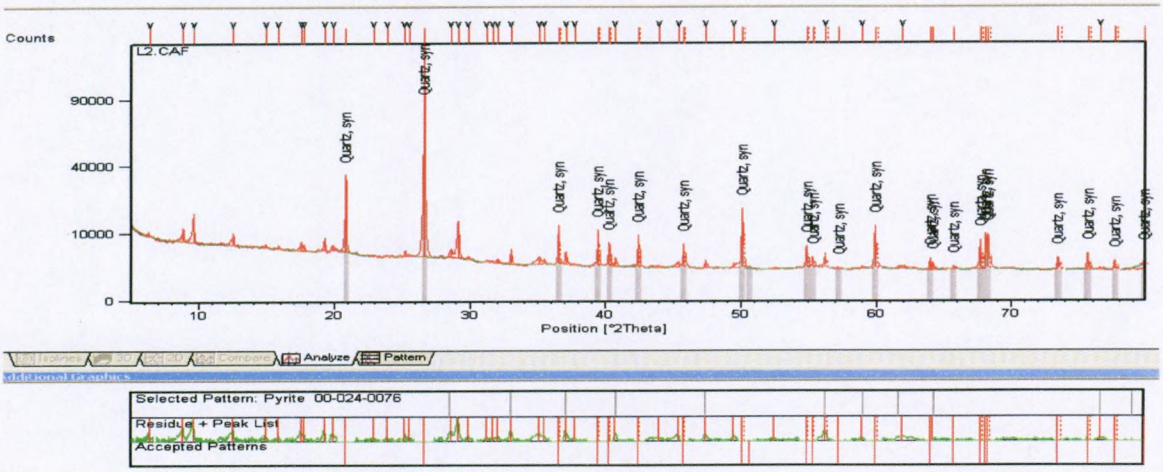

A full scan of sample L3

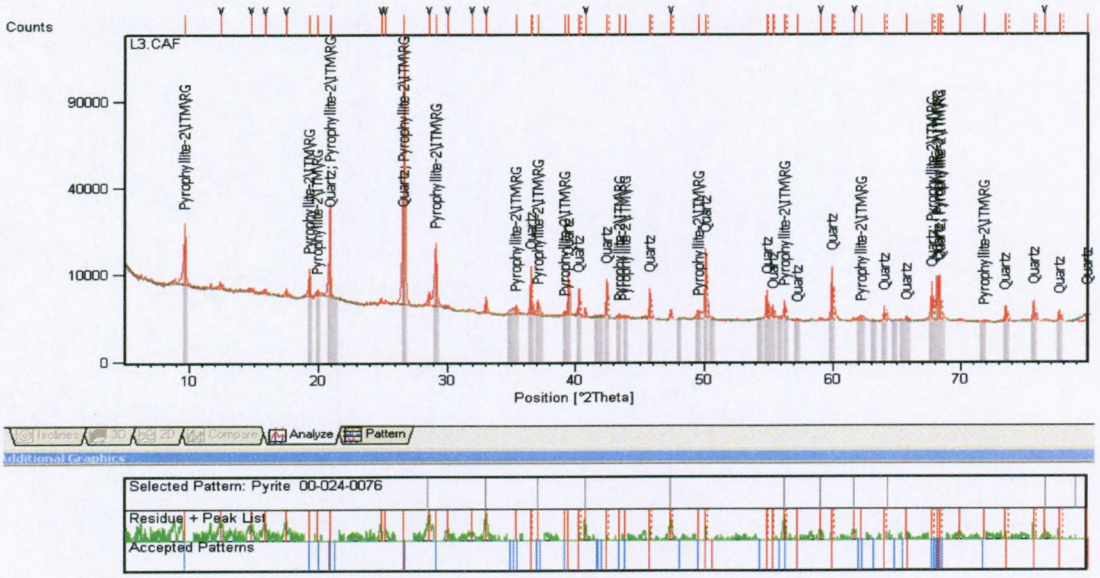

A full scan of sample L8

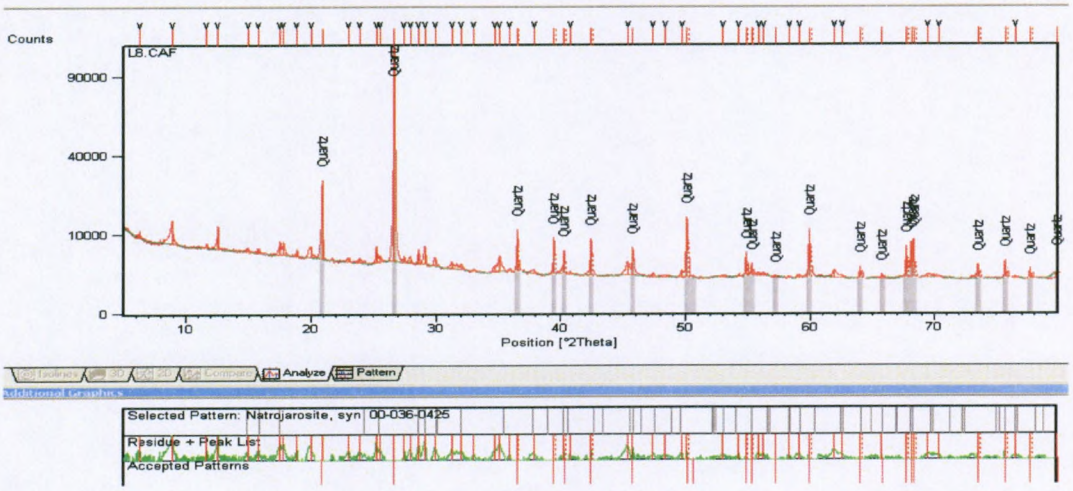

A full scan of sample L9

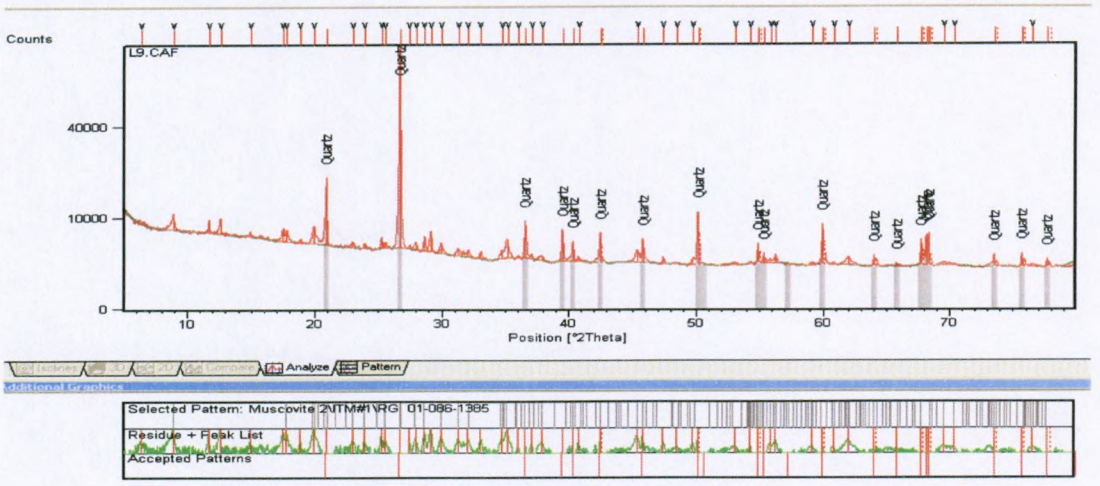

A full scan of sample P2

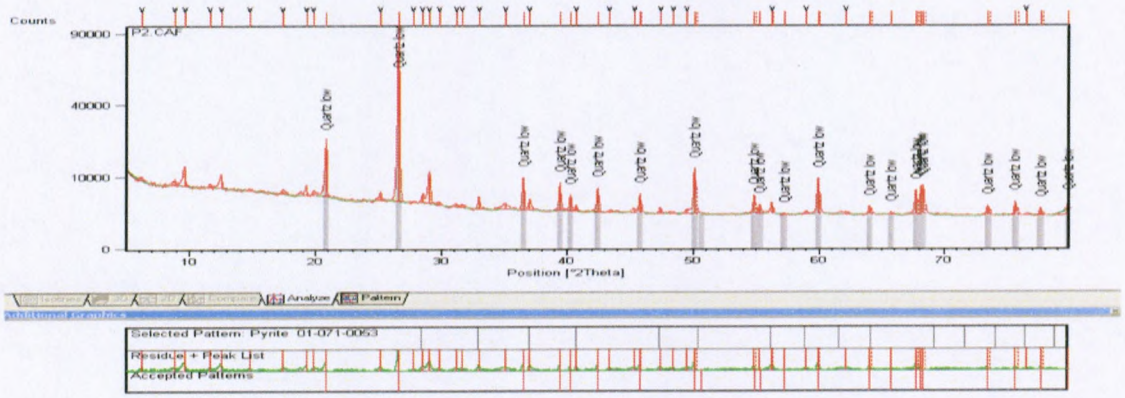

A full scan of sample R2

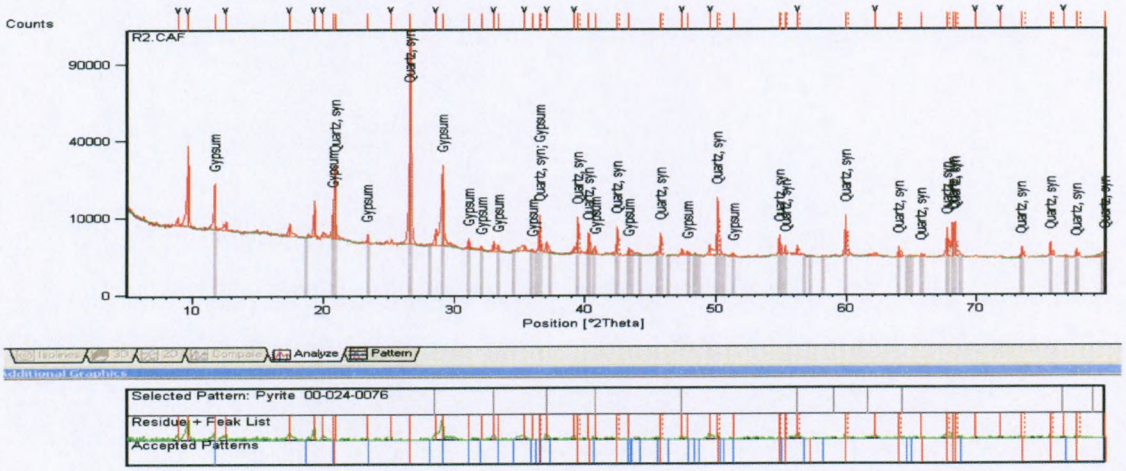

A full scan of sample R3

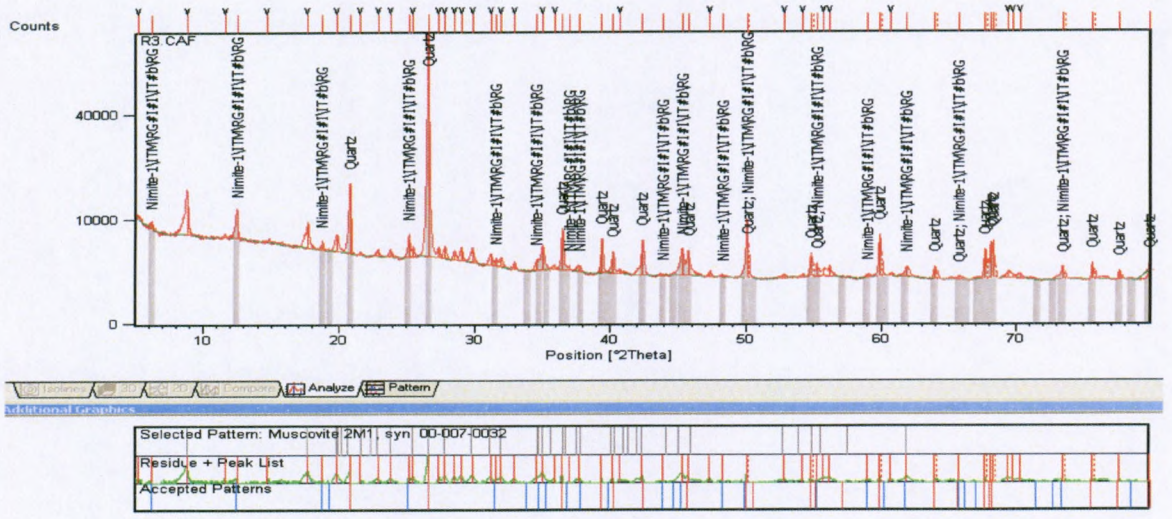

A full scan of sample V2

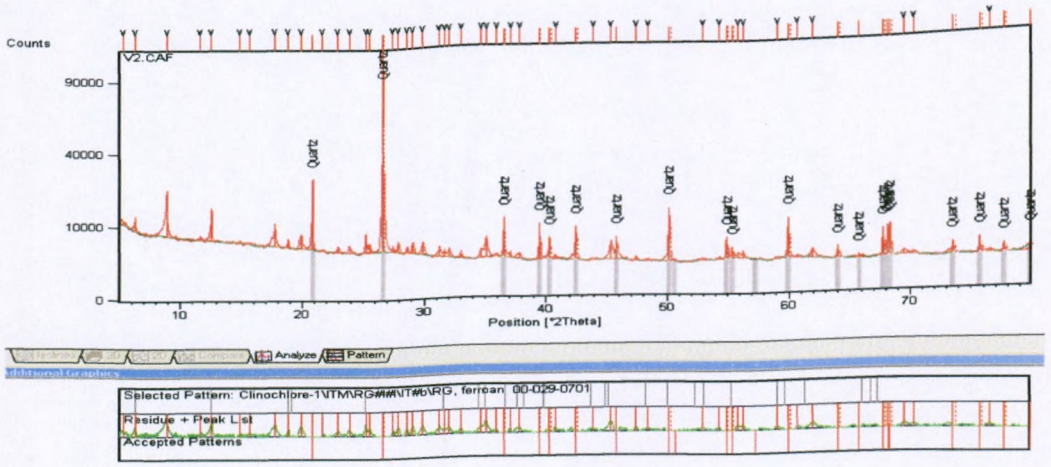

A full scan of sample V3

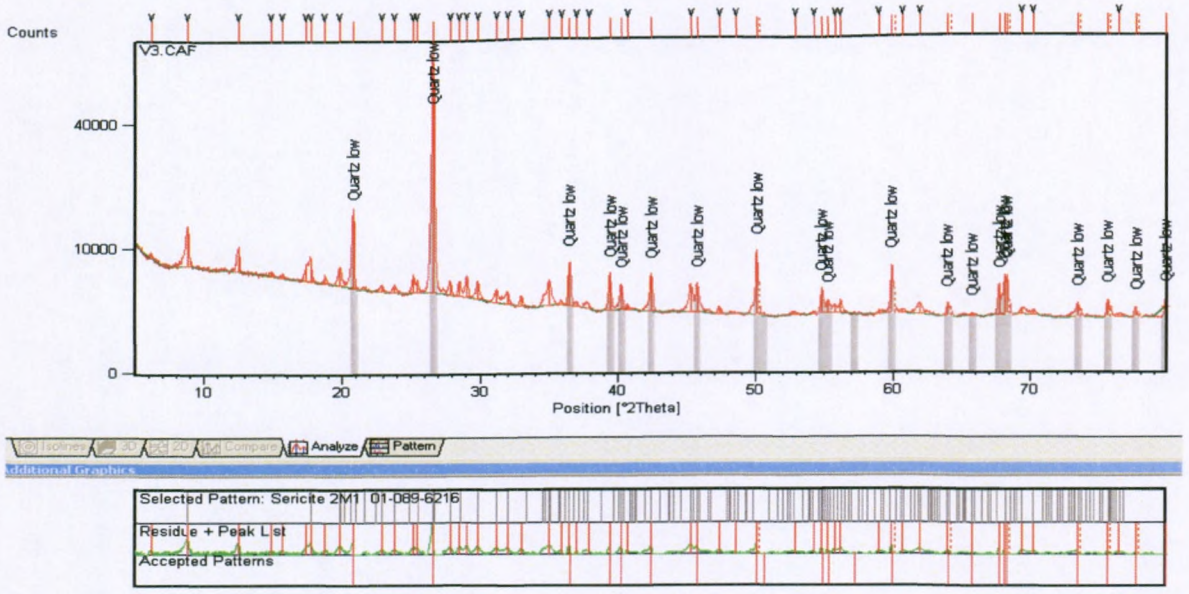

A full scan of sample V8

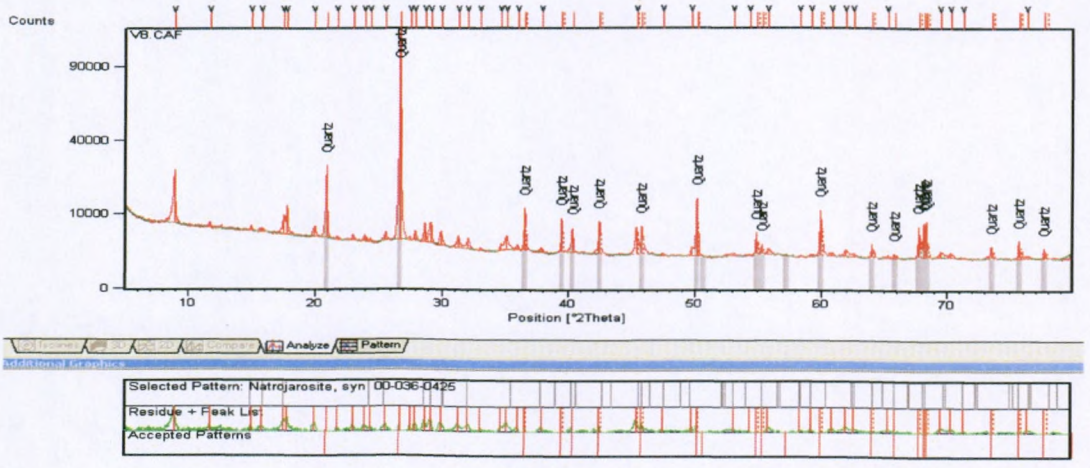

A full scan of sample V9

